A MITOCHONDRIAL TERMINOMICS TECHNIQUE TO STUDY HUMAN CELL DEATH DURING BACTERIAL INFECTION

by

Natalie Claire Marshall

B.Sc.H., The University of Guelph, 2012

A THESIS SUBMITTED IN PARTIAL FULFILLMENT OF

THE REQUIREMENTS FOR THE DEGREE OF

DOCTOR OF PHILOSOPHY

in

THE FACULTY OF GRADUATE AND POSTDOCTORAL STUDIES

(Microbiology & Immunology)

THE UNIVERSITY OF BRITISH COLUMBIA

(Vancouver)

May 2018

The following individuals certify that they have read, and recommend to the Faculty of Graduate and Postdoctoral Studies for acceptance, the dissertation entitled:

A mitochondrial terminomics technique to study human cell death during bacterial infection

submitted by Natalie Marshall in partial fulfilment of the requirements for

the degree of Doctor of Philosophy

in Microbiology & Immunology

Examining Committee:

B. Brett Finlay, Microbiology & Immunology
Supervisor

Christopher Overall, Biochemistry & Molecular Biology
Supervisory Committee Member

Thibault Mayor, Biochemistry & Molecular Biology
University Examiner

Vincent Duronio, Experimental Medicine
University Examiner

Additional Supervisory Committee Members:

Rachel Fernandez, Microbiology & Immunology
Supervisory Committee Member

Laura Sly, Experimental Medicine
Supervisory Committee Member

Abstract

Mitochondria are essential for human health. While mitochondria are primarily known for their essential role in generating cellular energy, these organelles play many vital roles in eukaryotic cells, including the cellular stress response, innate immunity, and the regulation of intrinsic apoptosis. Mitochondrial proteases are essential for mitochondrial function, including the import of 99% of the mitochondrial proteome, which often requires the proteolytic removal of a mitochondrial targeting sequence (MTS), creating a new protein amino terminus. However, little is known about how proteases regulate mitochondrial functions during health and disease because of the lack of tools able to examine global mitochondrial proteolysis and how it changes during mitochondrial processes. A novel terminomics workflow called 'MS-TAILS' was developed to address this gap by identifying changes in the mitochondrial terminal proteome, reflective of mitochondrial proteome-wide proteolysis. MS-TAILS identified the highest coverage of the human mitochondrial proteome and the most sites of import-associated MTS removal of any terminomics study to date, as well as 97 novel sites of mitochondrial proteolysis, demonstrating its utility to study mitochondrial proteolysis, proteases, and proteome import. MS-TAILS was applied to characterize mitochondrial changes during the induction of intrinsic apoptosis: a critical but poorly characterized mitochondrial process. MS-TAILS identified apoptosis-dependent changes in seven mitochondrial proteins not previously implicated in apoptosis, which may indicate conserved early apoptotic events. We examined the role of mitochondrial proteases in innate immunity by conducting the first terminomics study of microbial infection, identifying infection-specific mitochondrial changes during enteropathogenic *E.coli* (EPEC) infection: a pathogen that uses a type III secretion system (T3SS) to inject effectors into human cells and mitochondria to modulate apoptosis and

immunity. The majority of infection- and T3SS effector-dependent mitochondrial changes were unique from canonical apoptosis events, suggesting that EPEC T3SS effectors mediate an infection-associated mitochondrial apoptosis pathway. These findings were examined in a broader context to demonstrate the impact of this thesis work on the field. Overall, this work provides a novel approach to study global dynamics in mitochondrial proteolysis between conditions and therefore addresses a technical gap to characterize mitochondrial proteases, processes, and pathologies, including and beyond apoptosis.

Lay Summary

Mitochondria are cell components known as, “the powerhouse of the cell.” Mitochondria generate energy and regulate cell stress, immune defense, and cell death, making them essential for human health. Mitochondrial functions are regulated by enzymes that cleave proteins (‘proteases’), changing protein function. However, current tools cannot identify cleavage of >1,000 mitochondrial proteins to study how proteases affect mitochondrial functions. This thesis developed the first technique capable of identifying and quantifying changes in protein cleavage across mitochondrial proteins and applied it to profile mitochondrial changes during cell death and bacterial infection. When applied to study cell death, this work illuminated mitochondrial changes that may control this important but poorly-characterized process. When applied to bacterial infection, this work implicated an infection-specific pathway to control cell death. Overall, this thesis work addresses a technical gap to characterize important mitochondrial functions further, contributing to our understanding of mitochondrial proteases during cell death and infection.

Preface

This thesis is based on work conducted in collaboration between Natalie C. Marshall in Dr. B. Brett Finlay's lab and Dr. Theo Klein in Dr. Christopher M. Overall's lab. For the work presented in this thesis, I was responsible for designing all experiments, optimizing sample preparation (for cell culture, TAILS, and proteomics), conducting *in vitro* experiments, conducting TAILS experiments, and performing the data analysis.

Parts of Chapter 1 have been published. **Marshall NC** and Finlay BB. (2014) Targeting the type III secretion system to treat bacterial infections. *Expert Opinion on Therapeutic Targets*. 18(2): 137–152. I conducted and wrote this review of the literature.

Parts of Chapter 1 have been published. Deng W, **Marshall NC**, Rowland JL, McCoy JM, Worrall LJ, Santos AS, Strynadka NCJ, Finlay BB. (2017) Assembly, structure, function and regulation of type III secretion systems. *Nature Reviews Microbiology*. 15(6):323-337. I conducted a review of the literature and wrote parts of the 'Components and substructures of T3SSs' and 'Assembly of the core components of T3SSs' sections. I also designed, coordinated, and edited all of the figures.

A version of Chapters 2 and 3 has been submitted for publication. **Marshall NC**, Klein T, Thejoe M, von Krosigk N, Finlay BB, Overall CM. (*Submitted*) Profiling global mitochondrial proteolysis during intrinsic apoptosis initiation. I designed all experiments and the MS-TAILS workflow, optimized MS-TAILS sample preparation, conducted all *in vitro* experiments, designed and optimized models of early intrinsic apoptosis, conducted all MS-TAILS experiments, designed the two software programs (TAP and Center•Point), conducted all data analysis, and wrote the manuscript. Dr. Theo Klein provided training in the TAILS technique,

analyzed all MS-TAILS and preTAILS samples on a mass spectrometer, analyzed the raw mass spectrometry data, and provided guidance for subsequent MS-TAILS data analysis. Maichael Thejoe optimized the mitochondrial enrichment protocol within MS-TAILS. Niklas von Krosigk wrote the two software programs TAP and Center•Point for MS-TAILS data analysis. Drs. Christopher M. Overall and B. Brett Finlay provided supervision and funding for these experiments. I wrote the manuscript with assistance and editing from Maichael Thejoe, Dr. Klein, Dr. Finlay, Dr. Overall, and Dr. James M. McCoy.

A version of Chapter 4 is being prepared for publication. **Marshall NC**, Thejoe M, Klein T, Serapio-Palacios A, von Krosigk N, Stoynov N, Foster LJ, Overall CM, Finlay BB. (*In preparation*) Enteropathogenic *E. coli* type III secretion system effectors control the death of infected human cells by modulating global proteolysis in mitochondria and the whole cell. I designed all experiments, conducted all *in vitro* experiments, conducted all MS-TAILS experiments, and conducted all data analysis. Maichael Thejoe optimized the mitochondrial enrichment protocol, helped optimize infection conditions, and prepared the infected cell and mitochondrial samples for MS-TAILS. Dr. Theo Klein taught me the TAILS technique, analyzed the raw mass spectrometry data, and provided guidance for subsequent MS-TAILS data analysis. Dr. Antonio Serapio-Palacios optimized transfections and knockdowns (Figure 4.11) and performed the mitochondrial membrane potential experiments in Figure 4.12. Niklas von Krosigk wrote the two software programs TAP and Center•Point. Dr. Nick Stoynov analyzed all MS-TAILS samples on a mass spectrometer. Dr. Leonard J. Foster provided access to mass spectrometers so that data could be collected from these experiments. Drs. Christopher M. Overall and B. Brett Finlay provided supervision and funding for these experiments.

Parts of Chapters 5 and 1 have been published. **Marshall NC**, Finlay BB, Overall CM. (2017) Sharpening host defenses during infection: Proteases cut to the chase. *Molecular & Cellular Proteomics* 16: S161–S171. I wrote most of the manuscript, which was also written by Dr. Overall and edited by Dr. Finlay.

Table of Contents

Abstract ..... **iii**

Lay Summary ..... **v**

Preface ..... **vi**

Table of Contents ..... **ix**

List of Tables ..... **xiv**

List of Figures ..... **xv**

List of Supplementary Materials ..... **xviii**

List of Abbreviations ..... **xix**

Acknowledgements ..... **xxii**

Chapter 1: Introduction **1**

1.1 Mitochondria and apoptosis 1

1.1.1 Importance of mitochondria in cellular processes 2

1.1.2 Importance of mitochondria in human health 3

1.1.3 The mitochondrial proteome 5

1.1.4 Mitochondrial protein import 6

1.1.5 Intrinsic (or 'mitochondrial') apoptosis pathway of cell death 7

1.2 EPEC and the type III secretion system 11

1.2.1 The T3SS and T3SS-secreted effectors 11

1.2.2 T3SS effectors regulate host cell death during infection 13

1.3 Proteases in human health and disease 15

1.3.1 Proteases are essential in the human immune system 15

1.3.2 Mitochondrial proteases as regulators of mitochondrial function 16

1.4 Terminomics as a tool to study mitochondria, apoptosis, and infection 17
1.4.1 Mitochondrial proteomics to understand mitochondrial function and regulation 17
1.4.2 Challenges to studying the mitochondrial proteome 20
1.4.3 Terminomics 22
1.4.4 Terminal amine isotopic labeling of substrates (TAILS) 23
1.4.5 Terminomics to study mitochondria 26
1.4.6 Terminomics to study apoptosis 28
1.4.7 Terminomics to study infection 29
1.5 Overall hypotheses 31
Chapter 2: A novel technique to study changes in the mitochondrial N-terminal proteome 33
2.1 Summary 33
2.2 Introduction 34
2.3 Methods 36
2.3.1 Cell culture and SILAC labeling 36
2.3.2 Induction of intrinsic apoptosis 37
2.3.3 Cell harvesting and mitochondrial enrichments 37
2.3.4 Inner mitochondrial membrane potential ($\Delta\Psi_m$) assays 38
2.3.5 SDS-PAGE and western blotting 38
2.3.6 Mitochondrial SILAC-TAILS N terminomics 38
2.3.7 LC-MS/MS analysis 39
2.3.8 N terminomics data analysis 40
2.3.9 Bioinformatics 41

2.4 Developing a mitochondrial terminomics workflow 43
2.5 Mitochondrial and cellular N-terminal peptide identification 48
2.6 The mitochondrial and whole cell N terminome profiles are unique 56
2.7 Identification of MTS neo N termini and novel mitochondrial proteolytic events..... 57
2.8 Discussion 58
Chapter 3: The induction of intrinsic apoptosis alters the mitochondrial and cellular N terminomes 62
3.1 Summary 62
3.2 Introduction 62
3.3 Methods 63
3.3.1 Cell culture, SILAC labeling, and mitochondrial enrichments 63
3.3.2 Induction of intrinsic apoptosis 65
3.3.3 Inner mitochondrial membrane potential ($\Delta\Psi_m$) assays 65
3.3.4 SDS-PAGE and western blotting 65
3.3.5 Mitochondrial SILAC (MS)-TAILS N terminomics and N terminome analysis 66
3.4 Proteomic analysis of BAM7- and STS-induced early intrinsic apoptosis 66
3.5 Global changes in the whole cell N terminome during early apoptosis 70
3.6 BAM7 and STS treatments affected a small core subset of the mitochondrial N terminome 74
3.7 Identification of novel neo N termini in mitochondrial import and fission proteins during early apoptosis 77
3.8 Novel early proteolytic events in mitochondrial pathways during apoptosis 80
3.9 Discussion 81

Chapter 4: EPEC type III secretion system-secreted effectors alter the mitochondrial and cellular N terminomes of infected human cells 85

4.1 Summary 85

4.2 Introduction 86

4.3 Methods 87

4.3.1 Cell culture and SILAC labeling 87

4.3.2 Infection of cultured cells 87

4.3.3 Lactate dehydrogenase (LDH) assay 88

4.3.4 Cell harvesting and mitochondrial enrichments 88

4.3.5 SDS-PAGE and western blotting 89

4.3.6 Mitochondrial SILAC (MS)-TAILS N terminomics and N terminome analysis 89

4.3.7 Transfection/knockdown 89

4.4 T3SS effectors localize to human mitochondria before the induction of cell death 90

4.5 The human mitochondrial N terminome is altered upon EPEC infection 93

4.6 EPEC T3SS effectors specifically alter the mitochondrial N terminome 100

4.7 EPEC infection and T3SS effectors mediate previously unknown proteolytic processing events in mitochondrial proteins 102

4.8 EPEC alters the whole cell N terminome during infection 103

4.9 EPEC infection and the T3SS affected a shared subset of mitochondrial protein neo N termini. 107

4.10 The majority of EPEC- and T3SS-mediated changes are unique from canonical intrinsic apoptosis 110

4.11 A unique infection-mediated mitochondrial event affects the first step in the induction of apoptosis 115
4.12 Discussion 120
Chapter 5: Conclusion 125
5.1 Overall significance of this work 125
5.2 Developing a suitable mitochondrial terminomics technique 127
5.3 Disturbing mitochondrial homeostasis to study mitochondrial regulation through proteolysis 133
5.4 Identifying mitochondrial consequences of bacterial infection 135
5.5 Value of studying microbial infection and the host-pathogen interface with terminomics 137
5.6 Future directions 140
References 143

List of Tables

Table 2.1 Summary of TAILS mass spectrometry data. 50

Table 2.2 Proteins identified by MS-TAILS that contained the most N termini. 53

Table 3.1 BAM7 and STS treatments affected the same subset of N termini in seven mitochondrial proteins. 77

Table 4.1 Summary of MS-TAILS mass spectrometry data. 95

Table 4.2 EPEC altered human mitochondrial N termini during infection. 98

Table 4.3 The presence of T3SS effectors altered human mitochondrial N termini during infection. 101

Table 4.4 EPEC altered human cellular N termini during infection. 103

Table 4.5 T3SS effectors altered cellular N termini during EPEC infection. 105

Table 4.6 EPEC infection- and T3SS-dependent N termini occurred in mitochondrial proteins with a known role in apoptosis. 113

List of Figures

Figure 1.1 Mitochondrial proteome import to the matrix. 7

Figure 1.2 Mitochondrial events in the induction of intrinsic apoptosis. 8

Figure 1.3 Structure of the type III secretion system (T3SS). 12

Figure 1.4 N-terminal amine isotopic labeling of substrates (TAILS) workflow..... 25

Figure 2.1 The Termini Annotation of Peptides (TAP) computer program. 42

Figure 2.2 The Center•Point computer program to normalize large ‘omics datasets. 43

Figure 2.3 Mitochondrial SILAC (MS)-TAILS workflow and set-up. 45

Figure 2.4 Enrichment of mitochondria from apoptotic and untreated cells. 47

Figure 2.5 MS-TAILS reproducibility and coverage at the protein, peptide, and N-terminal peptide levels..... 49

Figure 2.6 MS-TAILS identified multiple N-terminal peptides in individual proteins. 52

Figure 2.7 MS-TAILS successfully enriched mitochondrial N-terminal peptides. 55

Figure 3.1 Applying MS-TAILS to study BAM7- and STS-induced early apoptosis cleavage events. 67

Figure 3.2 MS-TAILS identified quantitative changes in high-confidence N-terminal peptides from mitochondria and whole cells. 69

Figure 3.3 Up-regulated neo N termini were not correlated with known events during late-stage apoptosis..... 70

Figure 3.4 BAM7- and STS-induced apoptosis resulted in global changes in the mitochondrial N terminome. 72

Figure 3.5 BAM7- and STS-induced apoptosis resulted in global changes in the cellular N terminome. 73

Figure 3.6 BAM7 and STS treatments altered a shared subset of mitochondrial and whole cell N termini, including a core subset of mitochondrial protein N termini. 76
Figure 3.7 Quantitative changes in mitochondrial N-termini during early apoptosis conditions. 79
Figure 4.1 EPEC significantly increases HeLa cell membrane permeability throughout infection. 91
Figure 4.2 EPEC infection results in characteristic T3SS-mediated processes. 92
Figure 4.3 EspZ and EspF are detected within enriched human mitochondria during EPEC infection. 93
Figure 4.4 EPEC MS-TAILS experimental layout. 94
Figure 4.5 EPEC infection resulted in quantitative changes in high-confidence N-terminal peptides from mitochondria and whole cells. 96
Figure 4.6 EPEC infection and T3SS effectors resulted in global changes in the mitochondrial N terminome. 99
Figure 4.7 EPEC infection significantly altered the abundance of mitochondrial N-terminal peptides in an infection-and effector-dependent manner. 107
Figure 4.8 MS-TAILS revealed a neo N terminus indicating a T3SS effector-mediated proteolytic processing event in VDAC1. 110
Figure 4.9 EPEC infection- and T3SS-dependent mitochondrial N termini are unique to infection and distinct from canonical apoptosis events. 112
Figure 4.10 ACAA2 was detected in infected cells and in mitochondria from infected cells.... 116
Figure 4.11 Levels of mitochondrial proteins were decreased with gene-targeted shRNA vectors transfection and knockdown by flow cytometry. 117

Figure 4.12 *ACAA2* knockdown altered mitochondrial membrane potential throughout EPEC infection. 119

List of Supplementary Materials

Supplemental File 1. The complete Mitochondrial SILAC (MS)-TAILS dataset comparing BAM7 *vs*. DMSO treated cells and mitochondria.

Supplemental File 2. The complete Mitochondrial SILAC (MS)-TAILS dataset comparing BAM7 *vs*. STS *vs*. DMSO treated cells and mitochondria.

Supplemental File 3. The complete Mitochondrial SILAC (MS)-TAILS datasets comparing uninfected *vs.* wild-type EPEC-infected cells and mitochondria as well as those from EPEC wild-type *vs.* Δ*escN* infection.

List of Abbreviations

2-DE, two-dimensional gel electrophoresis;

ACAA2, 3-ketoacyl-CoA thiolase, mitochondrial;

A/E, attaching and effacing;

BAM7, Bax activator molecule 7;

Bax, BCL-2-associated X protein;

BCL-2, B-cell lymphoma 2;

C, carboxyl;

COFRADIC, combined fractional diagonal chromatography;

DAVID, Database for Annotation, Visualization and Integrated Discovery;

DMSO, dimethyl sulfoxide;

Drp1, dynamin-related protein 1;

EHEC, enterohemorrhagic *Escherichia coli*;

EPEC, enteropathogenic *Escherichia coli*;

ETC, electron transport chain;

FAC, Functional Annotation Cluster;

FDR, false discovery rate;

GO, Gene Ontology;

HTRA2, high temperature-resistant protein A2;

I-MAP, infection-associated mitochondrial apoptosis pathway;

IAP, inhibitor of apoptosis protein;

IMM, inner mitochondrial membrane;

IMS, intermembrane space;

LC-MS/MS, liquid chromatography tandem mass spectrometry;

Met1, initiator methionine;

MFF, mitochondrial fission factor;

MOMP, mitochondrial outer membrane polarization;

MPP, mitochondrial processing peptidase;

mPTPC, mitochondrial permeability transition pore complex;

MS, mass spectrometry;

mtDNA, mitochondrial DNA;

MTS, mitochondrial targeting sequence;

N, amino;

OMM, outer mitochondrial membrane;

OXPHOS, oxidative phosphorylation;

ROS, reactive oxygen species;

SILAC, stable isotope labeling by amino acids in cell culture;

STS, staurosporine;

T3SS, type III secretion system;

TAILS, terminal amine isotopic labeling of substrates;

TAP, Termini Annotation of Peptides;

TIM, translocase of the inner mitochondrial membrane;

TopFINDer, TopFIND ExploRer;

MRPS30, mitochondrial ribosomal protein S30;

MS-TAILS, Mitochondrial SILAC-TAILS;

POLRMT, DNA-directed RNA polymerase, mitochondrial;

preTAILS, shotgun proteomics analysis of the sample before and parallel to MS-TAILS of the same sample;

VDAC1, voltage-dependent anion-selective channel protein 1.

Acknowledgements

No Ph.D. is easy. I will forever benefit from this degree because of all the people who helped me get there, and particularly those who helped me reach a balance between independence and collaboration for professional and personal growth. I thank Dr. Finlay for his guidance and encouragement, for the freedom to align my research with my interests, and for helping me keep them aligned. I thank Dr. Overall for his infectious excitement about science and for his patient guidance in a new field. I thank Drs. Sly and Fernandez for their patience and excellent advice through a constantly changing degree. This committee's questions and advice have undoubtedly made me a better scientist.

I thank the members of the Finlay, Overall, and Foster labs for their comradery and support of all kinds. I thank Dr. Wanyin Deng for being a scientific inspiration, a phenomenal colleague, and a general hoot – and for always looking out for me. I thank Dr. Theo Klein, who mentored me in my TAILS education and was endlessly patient with my questions. I thank Maichael Thejoe, Antonio Serapio-Palacios, and Niklas von Krosigk for their willing help with science when I could not. I thank Dr. James McCoy for rescuing me from a writing slump and equipping me to do better. I thank Drs. Nichollas Scott, Ulrich Eckhard, Nikolaus Fortelny, Jenny Moon, Nick Stoynov, and Jason Rogalski for patient technical support. I thank the Finlay lab for every single question and piece of advice on my project, despite studying something so different from many of you. And for all of the above, I thank Andrew Santos, who was a constant and unconditional source of encouragement and support.

I thank my family and friends for comradery and mental health support, particularly Willow, my sangha, and my cycling team, and my parents for their support and making it possible. You kept

me upright when times were tough. For the same reason, thanks to the team that kept me physically upright: Elliot, Peter, Tasha, Delphine, and Anie. There is no way I could have finished my Ph.D. or written my thesis so quickly without your care.

Thanks to the many resources available for UBC graduate students, particularly project and team management, and Dora, for structuring the ‘un-structurable.’ I also extend my gratitude to the UBC Graduate Student Society and the many opportunities there, for being a constant source of purpose, and for helping develop important skills while I didn’t even notice.

Thanks as well to the funding sources that supported my research and my travel to conferences. These broadened my horizons, got me out of my academic bubble, and allowed me to focus on the research at hand from new perspectives.

Chapter 1: Introduction

1.1 Mitochondria and apoptosis

Mitochondria are powerful and essential organelles that have earned their nickname, "the powerhouse of the cell." While mitochondria are primarily known for generating cellular energy, these small-but-mighty organelles have many important functions, including the cellular stress response, reactive oxygen species (ROS) generation, innate immunity, and the regulation of the intrinsic (or 'mitochondrial') pathway of apoptotic cell death[1–10].

Mitochondria typically measure 0.5 – 10 μm in diameter and contain several sub-compartments: the outer and inner mitochondrial membranes (OMM; IMM), the intermembrane space (IMS) between them, and the innermost matrix. The matrix contains the 17 kb mitochondrial genome (mtDNA). The IMM is impermeable, helping to maintain a proton gradient and membrane potential ($\Delta\Psi_m$) across the IMM that helps drive many mitochondrial processes. The IMM composition is unusually protein-dense, containing >70% protein, including proteins involved in metabolite transport, electron transport, and ATP synthesis[11]. IMM invaginations called cristae increase membrane surface area and dramatically increase mitochondrial efficiency[12].

Across the cytoplasm, mitochondria interact with each other in large networks, move directionally along microtubules, and interact directly with the endoplasmic reticulum (ER) in fission, calcium signaling, and apoptosis[1,13–15]. Mitochondria divide as their cells' energy requirements increase, and the total number of mitochondria per cell is highly variable, ranging from 1 – 10,000 based on the tissue type and the cell's metabolic requirements at the time, with ~200 per cell on average[1]. Mitochondrial shape also varies between tissues: they are typically

oval, but can be longer, spherical, toroidal, or branched tubular networks[16]. Even within a single cell, mitochondrial morphology and even function can differ: this is called 'heteroplasmy'[1].

1.1.1 Importance of mitochondria in cellular processes

A primary role of mitochondria is to produce cellular energy: ATP. Most energy comes from breaking down glucose and fatty acids in the cytoplasm (*e.g.* glycolysis), at which point pyruvate and fatty acids are transported to mitochondria and go through the Krebs cycle or oxidation, respectively, to form acetyl-CoA. Acetyl-CoA goes through the electron transport chain (ETC) at the IMM, producing ATP through oxidative phosphorylation (OXPHOS) with oxygen as a terminal electron acceptor. Several IMM protein complexes are involved in this process, pushing protons in the matrix out to the IMS and thereby creating potential energy in the form of a proton concentration gradient (*i.e.* $\Delta\Psi_m$) that is used to power ATP production by the ATP synthase complex[1,11]. This important role in cellular bioenergetics makes mitochondria essential for proper cellular function.

Mitochondria play many other roles, as well. Because mitochondria host the ETC, they are attuned to fluxes in electron flow and can thereby sense cell danger early as part of the highly conserved Cell Danger Response (unique from the general cell stress response)[2]. Mitochondria also protect cells from protein aggregation associated with heat shock[17,18].

OXPHOS and the Krebs cycle are the major producers of ROS as byproducts. Because ROS are damaging to many compounds (*e.g.* membranes; reviewed by Quinlan *et al.*[19]), mitochondria must also manage ROS accumulation[1]. Because ROS also function as cellular signaling molecules, mitochondria are also important for cellular ROS signaling[20].

Mitochondria are involved in several aspects of innate immunity, including pathogen recognition receptor pathways, ROS production, the 'MAVS' antiviral response, and the 'ECSIT' antibacterial response (reviewed by West *et al.*[3]). Mitochondria are central regulators of cell death, specifically (although not exclusively) the intrinsic pathway of apoptosis[21], which is introduced in Section 1.1.5.

1.1.2 Importance of mitochondria in human health

Mitochondrial dysfunction leads to a wide range of clinical pathologies, with the first reported case published in 1959[22]. One in every 5,000 people has a mitochondrial disorder[22] and an estimated 160 human diseases are linked with genetic defects in mitochondrial proteins, including several neuromuscular and metabolic diseases[23]. These mitochondrial disorders can be categorized as primary, secondary, or accessory. Primary mitochondrial disorders result from mtDNA mutations; all protein-coding mtDNA genes encode ETC components, therefore all mutations in mtDNA-encoded proteins are ETC disorders. Secondary disorders result from mutations in mitochondrial genes encoded in the nuclear genome. Accessory disorders result from a non-mitochondrial mutation that causes a mitochondrial defect[24].

Primary mitochondrial disorders can have isolated effects (*e.g.* deafness) or multisystem syndromes with (*e.g.*) neurological, gastrointestinal, and/or cardiac symptoms[24]. The most common disorders caused by OXPHOS defects are Leigh syndrome and encephalopathy[24]. Leigh syndrome is a neurological disease characterized by loss of movement and mental abilities, and ultimately respiratory failure. It typically results in patient death within only a few years of birth.

Defects in mitochondrial- or nuclear-encoded genes of the ETC present early in life and are typically fatal[24]. Other mutations in mtDNA or nuclear genes can result in decreased efficiency of ATP synthesis and increased production of ROS and other free radicals, which then decrease membrane potential across the IMM ($\Delta\Psi_m$) and shift the cell towards apoptotic cell death. Therefore it is important to remove damaged or defective mitochondria through a mitochondrial quality control process called mitophagy[24]. Mutations in mitophagy proteins are correlated with Parkinson's disease[24] (discussed further by Hang *et al.* and Ryan *et al.*[25,26]). Mutations in the *huntingtin* gene result in impaired mitochondrial trafficking and cause Huntington's disease[24]. Mitochondrial dysfunction characterizes several other diseases and disorders (*e.g.* Alzheimer's disease, amyotrophic lateral sclerosis) – although the mitochondrial abnormalities have not been shown to be causative and may merely be secondary[24] – and mitochondria are implicated in cardiovascular disease[27–29], auto-inflammatory diseases[30], aging[31,32], and altered cell metabolism in cancer, in which tumour cells shift metabolism towards glycolysis rather than OXPHOS and are therefore able to reliably produce energy regardless of oxygen supply for the increased metabolic demands of unregulated cell growth[1,33].

However, the presence of a mutation in a mitochondrial gene does not necessarily mean that a disease will manifest: there is a very high rate of asymptomatic carriers and the prevalence for specific mutations is very low[24]. Other factors help mask mtDNA mutations, including heteroplasmy, where multiple different mitochondrial genomes may be present in a single cell[24].

Mitochondria play vital roles in the heart, the lung, and in cancer. Dysfunctional mitochondrial respiration is characteristic of many heart conditions[34], including heart failure and ischemia/reperfusion[35]. Furthermore, mitochondria regulate apoptosis and autophagy, two

pathways involved in the development of cardiomyopathy and atherosclerosis[28]. Mitochondria are essential for lung function and protect lung cells from hypoxia during acute and chronic lung disease.[36] Finally, mitochondria are required for tumour initiation, growth, and metastasis[37] and mitochondrial dysfunction has been implicated in cancer progression[38]. Some clinically successful anti-cancer drugs affect mitochondrial function specifically in tumour cells[39–42].

1.1.3 The mitochondrial proteome

Because mitochondria are associated with so many pathologies, interest has increased in studying the mitochondrial proteome. The mitochondrial genome is a 17 kb circular, double-stranded DNA plasmid that is present in one to several copies within the mitochondrial matrix. Human mtDNA encodes 37 genes[1,11], encoding tRNA, rRNA, and 15 polypeptides[43,44], all of which are involved in OXPHOS. However, the mitochondrial genome does not encode all genes required for mitochondrial processes, such as mtDNA replication or transcription, the translation of mitochondrial mRNA, or most proteins required for OXPHOS or mitochondrial metabolism (*e.g.* enzymes of the TCA cycle)[11]. In fact, ~99% of mitochondrial proteins are encoded by nuclear genes, translated on cytosolic ribosomes, then imported into mitochondria through at least one of the mitochondrial membranes[11].

The mitochondrial proteome is estimated to include ~1,200 proteins[45] and is best represented by the MitoCarta protein compendium[46]. MitoCarta was built using multiple protein-targeted and proteomics approaches, including microscopy, mass spectrometry, and machine learning from experiments conducted in 14 mouse tissues[47]. MitoCarta was further updated in 2016 and now includes 1,158 mitochondrial genes from mice and the human homologs; it is thought to include >85% of the mitochondrial proteome[48].

1.1.4 Mitochondrial protein import

With >99% of the mitochondrial proteome encoded by nuclear genes, each mitochondrion must import the vast majority of its proteome in order to function. Defects in proteome import lead to metabolic disorders and other human diseases (reviewed by MacKenzie and Payne[49]). Import of nuclear-encoded mitochondrial protein precursors is controlled by cross-talk within the cell, including cellular metabolic demands[50], where the OMM import translocase acts as a communication hub to control mitochondrial function and cellular distribution based on signaling from OMM-bound and cytosolic protein kinases[50]. Based on the wide variety of mitochondrial functions and constant anterograde and retrograde signaling between mitochondria and other cellular compartments, the mitochondrial proteome and import are very dynamic[46,51]. For example, during stress, levels of mitochondrial protein import decrease[51].

In yeast, five distinct translocase systems are involved in mitochondrial protein transport through the translocases of the outer/inner mitochondrial membranes (TOM; TIM). For proteins destined for the mitochondrial matrix, a cleavable N-terminal mitochondrial targeting signal (MTS) directs chaperoned, unfolded polypeptides[51] from the cytoplasm through TOM and TIM and into the matrix, as shown in Figure 1.1. Once imported, the ATP-dependent chaperone mitochondrial heat shock protein 60 is essential for the correct folding of imported proteins. An MTS is typically 20 – 100 amino acids long[52,53] with multiple positively charged amino acids and no negative charges[54] and may form amphipathic α-helices with both positive and hydrophobic faces[55,56]. Different but interconnected protein import pathways occur for proteins destined for the IMM, IMS, and OMM (reviewed by Rehling *et al.*[57]).

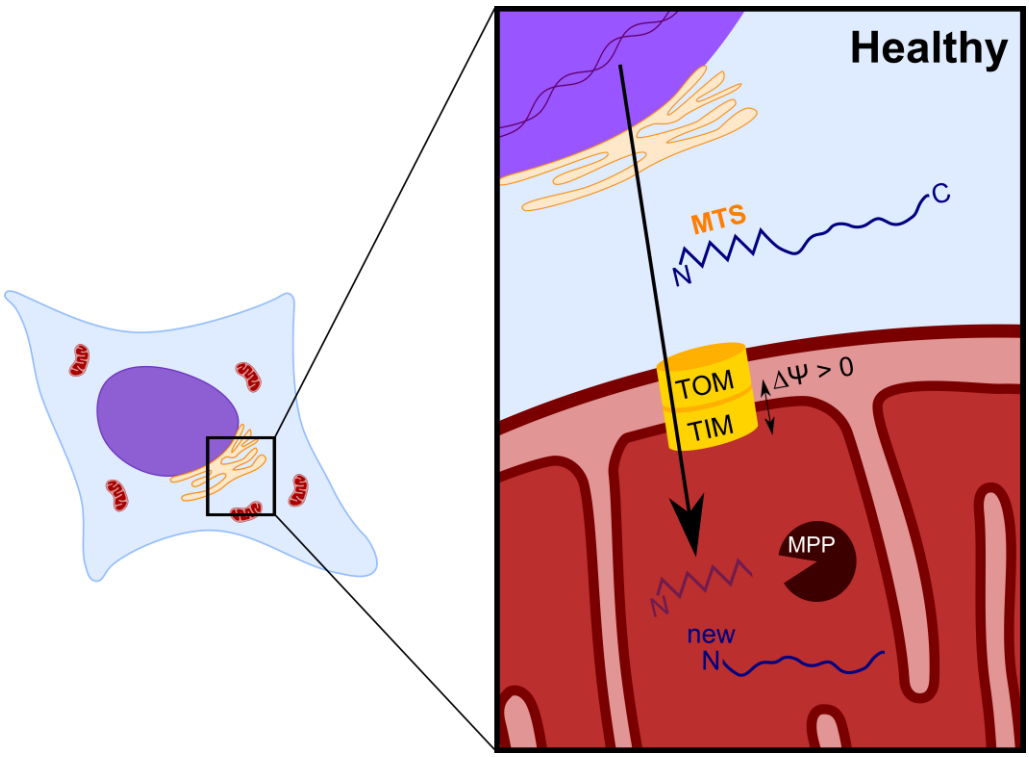

Figure 1.1 Mitochondrial proteome import to the matrix. Many proteins that are encoded in the nuclear genome but destined for the mitochondrial matrix possess an N-terminal mitochondrial targeting signal (MTS). Proteins with an MTS are imported across the outer and inner mitochondrial membranes (OMM; IMM) via the translocases of the OMM/IMM (TOM; TIM). Within the matrix, the mitochondrial processing peptidase (MPP) and Icp55 cleave the MTS, which is degraded, creating a 'neo' N terminus on the imported mitochondrial matrix protein.

1.1.5 Intrinsic (or 'mitochondrial') apoptosis pathway of cell death

Mitochondria are the site of the first steps of intrinsic apoptosis: a highly regulated and broadly conserved process that plays an essential role in cell life and death, human development, tissue homeostasis[58], and the removal of potentially dangerous cells[59]. Apoptosis often occurs as an active process in healthy tissues; for example, apoptosis plays an integral part in the turnover of human intestinal epithelium, which is wholly regenerated and replaced by new cells every 4-5 days[60].

The international Nomenclature Committee on Cell Death defines intrinsic apoptosis as:

> A cell death process that is mediated by [mitochondrial outer membrane permeabilization] MOMP and hence is always associated with (*i*) generalized and irreversible $\Delta\Psi_m$ dissipation, (*ii*) release of IMS proteins into the cytosol (and their possible relocalization to other subcellular compartments) and (*iii*) respiratory chain inhibition[61].

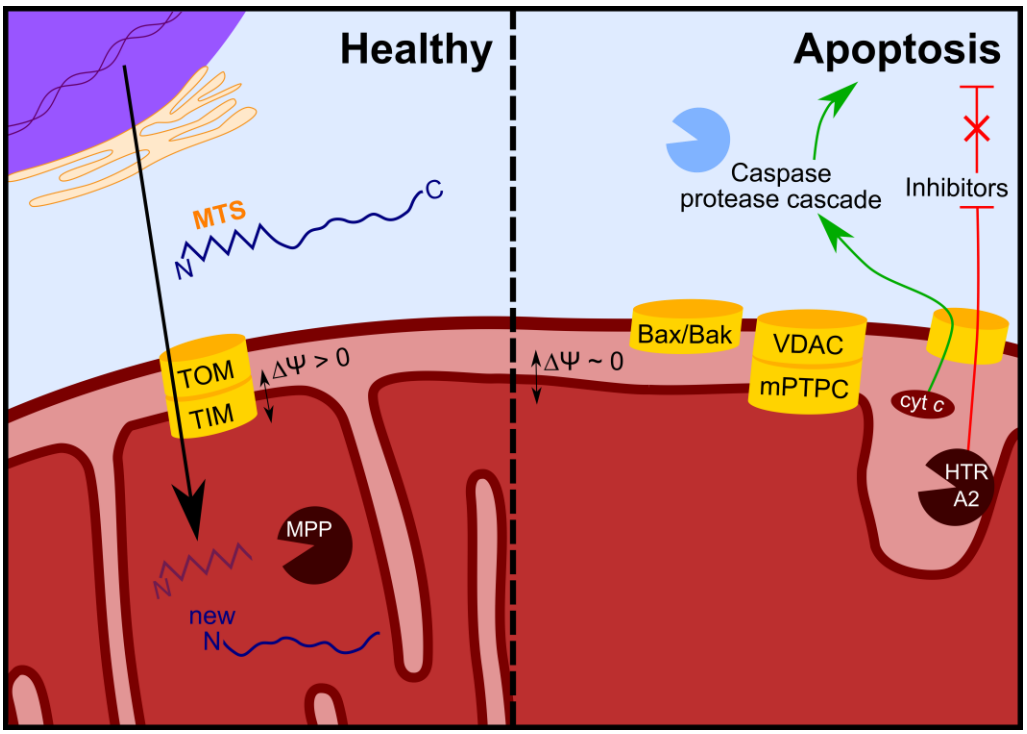

Figure 1.2 Mitochondrial events in the induction of intrinsic apoptosis. In healthy mitochondria (*Left*), inner and outer mitochondrial membranes and membrane potential ($\Delta\Psi_m$) are intact, sequestering toxic, pro-apoptotic molecules in the intermembrane space (IMS), such as cytochrome *c*, HtrA2, and SMAC/DIABLO. During intrinsic apoptosis (*Right*), $\Delta\Psi_m$ dissipates and toxic IMS molecules are released through pores in the OMM. Some of these IMS molecules (*e.g.* HtrA2) inhibit cytoplasmic proteins in the Inhibitor of Apoptosis Proteins family, thereby promoting apoptotic signaling through caspase-independent mechanisms. Other IMS molecules help assemble a cytoplasmic apoptosome with procaspase-9, resulting in caspase-9 cleavage and activation, which subsequently activates caspase-3 and thereby initiates rampant, indiscriminate, and cell-wide proteolysis during the late-stage apoptosis, at which point the cell dies.

The intrinsic apoptosis pathway is responsive to intracellular danger signals such as DNA damage and ROS[59]. When these pro-apoptotic damage signals abound, MOMP occurs. MOMP can occur from the IMM, resulting in a massive, open permeability transition pore complex (mPTPC) from the matrix through the OMM[1,61]. Alternatively, MOMP can occur from the OMM

due to the pore-forming abilities of two oligomerizing B-cell lymphoma 2 (BCL-2) proteins: BCL-2-associated X protein (Bax) and BCL-2 homologous antagonist/killer (Bak). Bax/Bak pore formation in the OMM increases membrane permeability, which irreversibly dissipates $\Delta\Psi_m$ and allows for the cytoplasmic release of toxic IMS components including cytochrome *c*, SMAC/DIABLO, high-temperature resistant protein A2 (HTRA2), apoptosis-inducing factor (AIF), and endonuclease G (Figure 1.2). These previously sequestered mitochondrial proteins then disrupt several essential cellular functions in a series of distinct but co-occurring caspase-independent and –dependent processes. Dissipation of cytochrome *c* further inhibits the ETC, leads to further ROS production, and amplifies the signal for apoptosis[61]. In the nucleus, endonuclease G and AIF mediate DNA fragmentation. In the cytoplasm, HTRA2 and SMAC/DIABLO inhibit Inhibitor of Apoptosis (IAP) family proteins – enabling caspase activation – and cytochrome *c*, apoptotic protease-activating factor 1 (APAF1), and dATP activate the cytosolic zymogen procaspase-9, forming the apoptosome protein complex with active caspase-9. The activated apoptosome then activates effector caspases, including caspase-3, which cleaves caspases-6 and -7, resulting in destructive and indiscriminate proteolysis of cellular proteins in the caspase-dependent stages of intrinsic apoptosis[1]. Ultimately, the cell dies.

Mitochondria therefore are the site of the early events of intrinsic apoptosis, regulating cell death through processes regulated by mitochondrial proteins and mitochondrial bioenergetic failure[61]. However, while the late, 'executioner' stages of intrinsic apoptosis (following MOMP and caspase-3 activation) are well-characterized and often studied, the specific, molecular events early in intrinsic apoptosis have remained unclear – particularly those in mitochondria.

The roles of mitochondria in apoptosis are further reviewed by Jeong and Seol[62], Galluzzi *et al.*[63], and Tait and Green[8].

Cells can also die through other cell death processes, including the extrinsic pathway of apoptosis, which is triggered by sensing extracellular stress signals using transmembrane receptors in the cell plasma membrane. Extrinsic apoptosis is defined as:

> Extrinsic apoptosis is a caspase-dependent cell death subroutine, and hence can be suppressed (at least theoretically) by pancaspase chemical inhibitors… or by the overexpression of viral inhibitors of caspases like cytokine response modifier A (CrmA). Extrinsic apoptosis would feature one among three major lethal signaling cascades: (i) death receptor signaling and activation of the caspase-8 (or -10)-caspase-3 cascade; (ii) death receptor signaling and activation of the caspase-8-tBID-MOMP-caspase-9-caspase-3 pathway; or (iii) ligand deprivation-induced dependence receptor signaling followed by (direct or MOMP-dependent) activation of the caspase-9-caspase-3 cascade[61].

During extrinsic apoptosis, an extracellular danger signal binds to death receptors, inducing the association of a cytoplasmic Death-Inducing Signaling Complex (DISC). The DISC contains the cytoplasmic domains of the death receptors and recruits and oligomerizes the FAS-associated death domain (FADD) and procaspase-8 or procaspase-10, both initiator caspases. When the DISC forms, pro-caspase-8 (or-10) dimerizes and self-cleaves into active caspase-8. Caspase-8 can cleave the BH3-interacting domain death agonist (BID), forming truncated BID (tBID), which permeabilizes mitochondria (*i.e.* MOMP)[61]. However, MOMP is dispensable to extrinsic apoptosis, whereas it is a defining feature in intrinsic apoptosis. Alternatively, caspase-8 can directly cleave procaspase-3 to activate it, propelling the cell directly into the 'executioner phase' of apoptosis in a caspase-dependent but mitochondrion-independent process[61]. Caspase-3 activation is one example of overlap between the intrinsic and extrinsic apoptosis pathways through different signaling pathways.

1.2 EPEC and the type III secretion system

Several human pathogens target mitochondria to control apoptosis and the host response to infection[21]. This work aims to examine how enteropathogenic *Escherichia coli* affects mitochondria during infection of human cells.

Pathogenic *Escherichia coli* are a leading cause of childhood death, worldwide[64]. The attaching and effacing (A/E) pathogens enteropathogenic and enterohemorrhagic *E. coli* (EPEC; EHEC) cause significant morbidity and mortality worldwide[65,66]. EPEC infects the human intestine and causes severe infantile diarrhea and enteric colitis; outbreaks have occurred in Canadian childcare centres[67,68]. Enterohemorrhagic *E. coli* (EHEC) causes outbreaks of severe diarrhea, hemorrhagic colitis, and fatal hemolytic uremic syndrome[67]. In Canada, EHEC causes an estimated 50,000 infections/year, numerous deaths, and a substantial financial burden, costing the Canadian healthcare system ~$400 million/year[65,66].

1.2.1 The T3SS and T3SS-secreted effectors

During infection, EPEC and EHEC attach to intestinal epithelial cells and locally efface microvilli, resulting in characteristic attaching/effacing (A/E) lesions[69]. Their virulence requires a type III secretion system (T3SS; Figure 1.3), a highly conserved molecular syringe that injects bacterial effector proteins directly into the cytoplasm of intestinal cells[69]. The EPEC/EHEC T3SS is encoded by the locus of enterocyte effacement (LEE) pathogenicity island, which contains the genes required for T3SS assembly as well as several effectors[70]. Bioinformatic and proteomic analysis of the EPEC O127:H6 strain genome predicts at least 23 effector proteins[71,72],

many of which are not fully characterized. Effector proteins manipulate cellular processes and are responsible for the characteristic features of EPEC and EHEC disease, including intimate bacterial-host cell attachment[73], actin pedestal formation[74], mitochondrial dysfunction[75,76], tight junction disruption[77], and intestinal cell death[78].

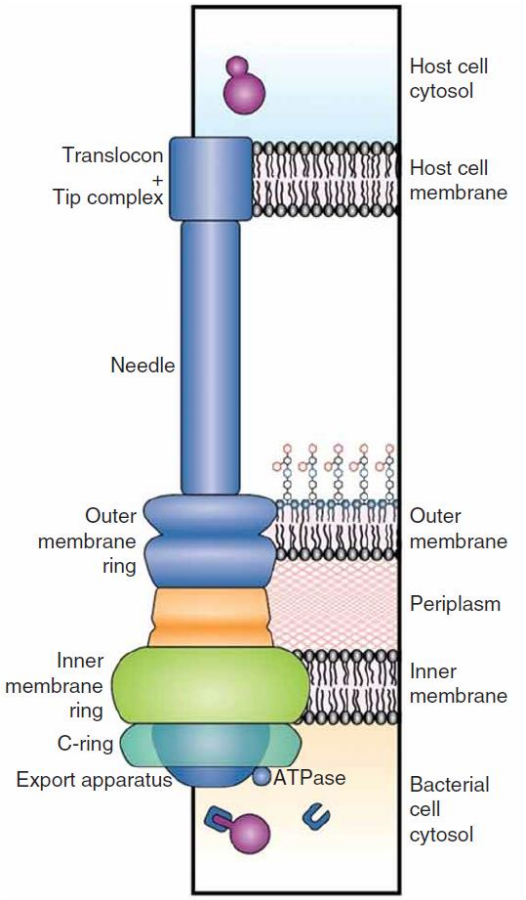

Figure 1.3 Structure of the type III secretion system (T3SS). T3SS effectors (purple) are bound in the bacterial cytosol to their chaperones (blue). Once recognized at the export apparatus, they travel through a hollow channel in the T3SS body that circumvents the two Gram-negative bacterial membranes and directly connects through the host cell membrane. In EPEC, type III secretion is powered by the dedicated EscN ATPase until effector translocation and release directly into the host cell cytosol. Reproduced from [79] with permission.

These two pathogens cause disease in a very similar manner, and both require their T3SS to cause disease. Because the histopathology and virulence mechanisms of EPEC and EHEC are

remarkably similar, EPEC has become the classical model with which to study EHEC, T3SS-mediated processes, and the host response to these *E. coli* pathotypes and their T3SS. EPEC infection is modeled in mice using a natural A/E pathogen of mice: *Citrobacter rodentium*[80].

Research on these pathogens has focused on identifying the function and mechanism of single effectors[78,81], but with dozens of effectors – some with several functions[78] – this approach is slow and inefficient. Identifying the mechanisms of >20 T3SS effector proteins is a substantial challenge. For example, several effectors target mitochondria, however, the mechanisms by which they induce apoptosis and promote colonization and transmission are unknown.

1.2.2 T3SS effectors regulate host cell death during infection

Early signs of apoptosis are evident during EPEC infection (*e.g.* cellular DNA damage, expression of phosphatidylserine on the host cell surface early in infection), while late signs of apoptosis are not (*e.g.* membrane blebbing, nuclear fragmentation)[82,83]. In contrast, *Salmonella, Shigella,* and *Yersinia* cause apoptosis earlier during infection and to a greater degree[82]. Due to the natural rapid shedding of host epithelial cells in the human gut, and because EPEC adheres to the mucosa and does not invade these cells, EPEC may benefit from slowing host cell apoptosis[82].

In fact, many bacterial and viral pathogens manipulate intrinsic apoptosis during infection (reviewed by Rudel *et al.*[21]), and because mitochondria regulate intrinsic apoptosis, they are valuable and frequent targets for pathogens to subvert during infection[21,84–88].

EPEC encodes several T3SS effectors that regulate apoptosis both inside and outside of mitochondria, including NleF, NleC, and NleD. NleF directly binds to cytosolic caspases-4, -8,

and -9, and inserts its C-terminus into the active cleft of caspase-9 to inhibit apoptosis[89]. The effectors NleD and NleC are zinc metalloproteases that specifically cleave and inactivate the c-Jun N-terminal kinase and the p65 subunit of NF-κB, respectively[90]. c-Jun N-terminal kinase promotes apoptosis from the cytoplasm and NF-κB can either promote or inhibit apoptosis from within the nucleus, depending on the stimulus[91,92]. Accordingly, NleD and NleC inhibit the pro-apoptotic activities of these two proteins in the cytoplasm and nucleus, respectively[90].

Within mitochondria, EspF contributes to the activation of intrinsic apoptosis, specifically: (*i*) dissipating mitochondrial membrane potential (Ψ_m), (*ii*) releasing sequestered cytochrome *c*[93], and (*iii*) activating caspases-3 and -9[94]. Ectopic expression of *espF* alone in uninfected HeLa or COS cells caused cell death with hallmark signs of apoptosis[83]. EspF possesses an N-terminal MTS that allows it to exploit host mitochondrial machinery and be imported into host mitochondria by canonical import pathways. Its mitochondrial localization has profound effects on the course of disease: mice infected with a mutant strain of *C. rodentium* where EspF is unable to target mitochondria demonstrate improved survival rates, decreased *C. rodentium* colonization, decreased intestinal inflammation, and decreased host cell death[95].

EspZ also localizes to mitochondria during infection. In contrast to EspF, EspZ delays apoptosis by stabilizing $\Delta\Psi_m$, preventing the rapid death of infected cells[96] and even protecting against intrinsic apoptosis in the presence of a chemical apoptosis inducer: staurosporine[97]. As expected, infection with an EPEC strain lacking EspZ caused increased cytotoxicity of infected cells[98]. Recent work shows that EspZ interacts with Tim17b[96], a component of the TIM complex that is essential for the voltage-gating and requires an intact $\Delta\Psi_m$ to sustain mitochondrial protein import, which is itself required for mitochondrial function and cellular health[99,100].

Despite the importance of mitochondria in cell death, no study to date has yet examined T3SS effector mechanisms within host mitochondria. Understanding how T3SS effectors alter the mitochondrial proteome would provide valuable insight into how EPEC causes cell death.

1.3 Proteases in human health and disease

This work aims to examine dynamics of the mitochondrial proteome (*e.g.* import); however, the mitochondrial proteome is fundamentally 'sculpted' by proteases, which also play important roles across the entire cellular proteome. Therefore, to understand how the mitochondrial proteome is affected by a treatment of interest, proteases must also be examined.

1.3.1 Proteases are essential in the human immune system

Proteases play important roles in countless human cellular processes (reviewed by Marshall *et al.*[101]). At 566 members, proteases are one of the largest enzyme families, representing 1.7% of human genes, therefore larger than the kinase family (456 members) and second only to ubiquitin ligases[102]. Proteases are essential immune regulators, performing precise proteolytic processing to regulate signaling and rapidly deploy innate immune defenses including: complement; antigen and MHC peptide processing; cytokine and chemokine activation/inactivation; and immune cell activation through NF-κB[103–105]. During infection, these many human pathways must interface to protect against virulence processes, resolve the infection, and achieve homeostasis once more.

The inflammatory response to infection and associated tissue damage involves a complex interplay of pathways and mediators including Toll-like receptors, NF-κB-transcribed cytokine

induction, innate and adaptive immune cell activation and recruitment, matrix metalloproteinases, and the coagulation and complement proteolytic systems[105–107]. These protease-regulated processes can be further regulated by crosstalk from other proteases[108,109]. These protease webs can modulate essential functions (*e.g.* alter cytokine activity) while remaining functionally invisible to transcriptomic and proteomic analyses. These hidden events obstruct our understanding of biological processes that are important to develop new diagnostic tests and therapeutics. It is therefore important to identify both intact and cleaved proteins, particularly for those involved in host immune processes.

1.3.2 Mitochondrial proteases as regulators of mitochondrial function

Mitochondrial and cytoplasmic proteases alike play a central role in apoptosis, most notably the caspase protease cascade[110,111], including initiator and executioner caspases, *e.g.* caspases-9 and -3, respectively.

Within mitochondria, proteases play a crucial role in the import of the mitochondrial proteome[49,112,113] and are therefore important to consider when studying the mitochondrial proteome and dynamics. Mitochondrial proteases sculpt the mitochondrial proteome, regulating and executing mitochondrial functions by altering substrate activity and turnover, and affecting processes such as: mitochondrial fusion and fission; apoptosis; and the synthesis, import, and quality control of mitochondrial proteins (reviewed by Quirós *et al.*[114]). Mitochondrial protease mutation or down-regulation can be catastrophic for cellular function and survival[115] and several human diseases arise from genetic defects in mitochondrial proteases, such as cerebral, ocular, dental, auricular, skeletal syndrome[116]. Due to the associations between the mitochondrial generation of reactive oxygen species and cancer cell metabolism[117], mitochondrial proteases

have been recently identified as possible therapeutic targets in cancer. Thus, mitochondrial proteases are also essential for human health and involved in human disease.

For example, upon import to the matrix, the matrix processing peptidase (MPP) cleaves the N-terminal MTS[118,119], which is typically rapidly degraded, leaving the mature, imported protein with a new N terminus[57]. Following MTS removal, several other mitochondrial proteases may further cleave the imported protein: the Intermediate Cleaving Peptidase (Icp55) removes one terminal amino acid[53]; the intermediate peptidase Oct1 removes eight[120,121]; the inner membrane protease (IMP) removes a hydrophobic sorting signal at the new N terminus[119,120]; the rhomboid protease Pcp1 and the mitochondrial m-AAA protease further process imported proteins[122,123].

Identifying the substrates of mitochondrial proteases would help elucidate their functions and exact mechanisms of action; however, little is known about the substrates of mitochondrial proteases[117].

1.4 Terminomics as a tool to study mitochondria, apoptosis, and infection

1.4.1 Mitochondrial proteomics to understand mitochondrial function and regulation

Research on the mitochondrial proteome has greatly advanced since the first study of the mitochondrial proteome in 1998[124], in stride with concurrent advances in proteomics and bioinformatics. Mitochondrial proteomes have now been characterized in human[125,126], rat[127,128], mouse[129], and yeast[130,131] cells, as well as in several tissues. The earliest study of the mitochondrial proteome used two-dimensional gel electrophoresis (2-DE) and peptide mass fingerprinting and identified 46 proteins, though most were cytoplasmic contaminants[124]. Studies

continued[128], with various attempts to increase mitochondrial proteome coverage and decrease contaminants[132]. A particularly significant advance was the utilization of liquid chromatography-tandem mass spectrometry (LC-MS/MS)[133], which circumvented the bias of 2-DE against hydrophobic proteins, including the IMM protein complexes in the ETC. More recent mitochondrial proteomics studies using LC-MS/MS have identified upwards of 600 mitochondrial proteins[126,134] and dramatically improved mitochondrial proteome coverage by combining several different technical approaches[134].

Mitochondrial proteomics has considerably advanced since the first study 20 years ago[124]. While the early studies focused on characterizing the members of the mitochondrial proteome[47], more recent studies have aimed to characterize tissue-specific mitochondrial proteomes, characterize mitochondrial sub-proteomes, improve the quality of mitochondrial enrichments to minimize proteome contamination, and understand mitochondrial proteome dynamics, including post-translational modifications.

To identify tissue-specific mitochondrial functions, we can study mitochondria from different tissues, This is important because mitochondria have different structures, functions, gene expression, and overall morphologies in different tissues. In the first study of mitochondrial tissue-specific proteome, Mootha *et al.* purified mitochondria from mouse liver, heart, kidney, and brain and identified 163 proteins that had not been associated with mitochondria before[135]. Only ~50% of these proteins were detected in all four tissues, suggesting substantial variety between tissue-specific mitochondrial proteomes, which has been corroborated by several other tissue studies on the mouse and rat mitochondrial proteomes[47,127,136]. In 2010, Pagliarini *et al.* studied the mitochondrial proteomes from 14 different mouse tissues and combined their data

with other mitochondrial 'omics dataset and protein localization studies to produce a "mitochondrial protein compendium" called MitoCarta, which is regarded as the most comprehensive database of the mitochondrial proteome available[47].

Just as the mitochondrial proteome varies between tissues, it varies between the four mitochondrial compartments: the OMM, IMS, IMM, and matrix. The mitochondrial matrix contains the bulk (~2/3) of mitochondrial protein, the IMM ~29%, and the OMM ~4% of mitochondrial protein[137]. Because of the high abundance of soluble proteins in the mitochondrial matrix, it is a challenge in mitochondrial proteomics to detect low abundance and hydrophobic membrane proteins. To detect these low abundance proteins, and particularly membrane proteins, many studies have characterized mitochondrial sub-proteomes[133]. In addition to these four compartments, several studies have focused on mitochondrial ribosomes[138–142]. Mitochondrial ribosomes consist of a small (28S) and large (39S) subunit, where the small subunit has a 12S rRNA and ~30 protein components; the large subunit has a 16S rRNA and ~50 protein components[140]. For example, Suzuki *et al*. identified 31 proteins in the large subunit and 21 in the small subunit using proteomics[141,142].

An Achilles' heel of mitochondrial proteome and sub-proteome characterization is sample purity. Therefore, recent mitochondrial proteomics research has focused on improving mitochondrial yield and purity. A multi-lab research consortium from the Mitochondrial Human Proteome Project conducted a series of studies to optimize and standardize mitochondrial enrichments for proteomic studies[143]. Using ten model cell lines, this study compared three mitochondrial enrichment methods: differential centrifugation, sucrose gradient separation, and a commercial surfactant-based kit. They found that no single mitochondrial enrichment performed best for all

cell lines, and therefore suggested that researchers should choose mitochondrial enrichment techniques based on the standardized results provided for each model cell line. For this reason, modular 'omics techniques are valuable to ensure optimal mitochondrial purity and technical consistency between cell lines.

Recent research has focused on understanding mitochondrial proteome dynamics, including protein turnover[144], metabolism[138], and responses to stress induced by ethanol[145,146] and chemical ETC blockers[147]. Research has also pursued important mitochondrial post-translational modifications, including acetylation[148], phosphorylation[149], nitrosylation[150], carbonylation[150], and methylation[138].

Overall, 'omics tools have contributed significantly to the characterization of the mitochondrial proteome and our understanding of how it changes with different stimuli and in different tissues.

1.4.2 Challenges to studying the mitochondrial proteome

Studying the mitochondrial proteome has several inherent challenges.

First, the mitochondrial proteome is incompletely characterized. While the human mitochondrial proteome is estimated to consist of ~1,200 proteins[48,151], the mitochondrial genome encodes only ~1% of the whole human mitochondrial proteome; the remaining 99% of mitochondrial proteins are encoded across the nuclear genome. Therefore, due to the evolutionary dissection and adaptation of the mitochondrial genome with the eukaryotic nuclear genome, the constituents of the mitochondrial proteome cannot be inferred directly from gene annotations and cannot be unambiguously identified through conserved signals.

Second, the mitochondrial proteome is not static. In fact, it is highly dynamic and responsive to varying cell requirements (reviewed by Lau *et al.*[152]). Mitochondria regulate and are also regulated by signal transduction with the cytoplasm, including anterograde signaling from the cytoplasm to mitochondria and retrograde signaling from mitochondria to the cytosol (reviewed by Jazwinski[153] and Weinberg *et al.*[154]). For example, nearly the entire mitochondrial proteome is imported into mitochondria, involving complex, coordinated pathways of protein targeting and import systems (reviewed by Neupert and Herrmann[119] and Schulz *et al*.[155]). Mitochondrial protein import is also regulated by metabolic needs and cell stress (recently reviewed by Harbauer *et al.*[51]), and is important in cellular homeostasis and implicated in human disease[49]. When unfolded proteins accumulate within mitochondria but without the mitochondrial chaperone mtHsp60, they are digested by the mitochondrial protease ClpP; the resulting peptides are exported to the cytoplasm and may act as a cue to stop further protein import[156]. Many dynamic processes occur for fundamental mitochondrial processes. The levels of Krebs cycle intermediates can alter cellular transcription[154]. When cytoplasmic calcium levels spike, calcium is rapidly sequestered into mitochondria[157]. Mitochondrial 'omics tools must consider these dynamics and be robust to them.

Furthermore, the mitochondrial proteome is sculpted by mitochondrial proteases. While some mitochondrial proteases are nonspecific and degradative, others are tightly regulated for proteolytic post-translational modification that can alter the function, localization, or turnover of mitochondrial proteases substrates. Mitochondrial proteases are essential for human health and are implicated in human diseases[114], affecting processes such as apoptosis[88], antimicrobial defense[85], mitochondrial protein synthesis, import, and quality control, mitophagy, mitochondrial

biogenesis, fusion, and fission[114]. When mitochondrial protease regulation goes awry, consequences can include metabolic syndromes, cancer, and neurodegenerative diseases[114]. Therefore, with the increasing recognition of the importance of mitochondrial proteases in mitochondrial processes, a complete understanding of mitochondrial proteome dynamics must identify not only proteins but also proteolytic events.

Therefore, when studying the mitochondrial proteome, it is important to use techniques that also capture proteolytic events, due to the importance of mitochondrial proteases (Section 1.3.2). Mitochondrial proteomics tools that captured proteolytic events could greatly contribute to our understanding of mitochondrial processes, including but not limited to mitochondrial protein import, mitochondrial proteolysis, and the early mitochondrial events in intrinsic apoptosis.

1.4.3 Terminomics

In classical proteomics, naturally-occurring proteolytic events are buried and obscured by 100,000s of tryptic peptides, particularly those from high abundance proteins. Therefore, conventional approaches are unable to reliably detect naturally-occurring proteolytic events and miss this fertile field of functional information of identified proteins and global protease networks.

Recently, terminal proteomics (‘terminomics’) techniques have been invented that can identify protease substrates across an entire proteome by identifying terminal proteomes (‘terminomes’), including original termini of mature unprocessed proteins and precise sites of ‘neo’ termini created by proteolytic events. Terminomic techniques can therefore simultaneously profile global changes in protein abundance and proteolysis.

Two of the leading terminomics techniques are terminal amine isotopic labeling of substrates (TAILS)[158,159] and combined fractional diagonal chromatography (COFRADIC)[160]. Both involve the selective negative enrichment of terminal peptides from a digested proteome and the use of MS and bioinformatics to identify: the terminal peptide sequence, the protein that the terminal peptide originated from, and the position of the terminal peptide within the mature protein, accordingly. Other degradomics techniques include the 1D gel-based approaches PROtein TOpography and Migration Analysis Platform (PROTOMAP) and Global Analyzer of SILAC-derived Substrates of Proteolysis (GASSP), as well as subtiligase-catalyzed biotinylation of protein N termini for subsequent capture and enrichment[161–163].

Terminomics has been successfully applied to many studies, as it enables: characterization of protease specificity[164]; identification of signal peptide cleavage sites[53] and N-terminal protein acetylation[165]; identification of novel protease substrates[166–169]; and characterization of downstream effects of particular proteolytic events[168,170]. Accordingly, terminomics has been applied to study topics as diverse as apoptotic cell death[161,162,171,172]; protease-protease crosstalk[173]; biomarker identification[174]; and validation or correction of genome annotations[175] (reviewed by Eckhard *et al.*[176]).

1.4.4 Terminal amine isotopic labeling of substrates (TAILS)

TAILS is a commonly used terminomics approach: N-TAILS for neo N termini[158] and C-TAILS for neo C termini[177]. N-TAILS is depicted in Figure 1.4. The key to this technique is labeling α-amines at the protein level, thereby labeling and chemically blocking mature protein N termini and neo-N termini resulting from proteolysis. Labeled N-terminal α-amines are strong evidence for their presence *in vivo* and their proteolytic generation in the biological sample and are

therefore considered true positives. However, careful handling and the use of protease inhibitors during sample collection are essential to prevent post-harvest cleavage by proteases still active in the sample. Nonetheless, background proteolysis in the sample or inadvertently through sample handling is identifiable from labeled peptides having isotopic ratios centered on 1:1, whereas the protease-exposed sample will have high isotope ratios (*i.e.* +protease sample / -protease sample) for true positive cleaved peptides. Later in sample preparation, internal tryptic peptides display newly exposed free α-amines arising from trypsin cleavage that were not blocked earlier in the procedure[159]. These unblocked tryptic peptides are depleted from the sample using a polyaldehyde polymer that binds to free α-amines under reductive conditions, leaving the original sample N terminome unbound and easily recoverable. TAILS is amenable to many different protein labeling techniques, including dimethylation, SILAC, iTRAQ, and most recently isobaric Tandem Mass Tags (TMT)[105,159]. These labeling techniques allow up to 10 samples to be analyzed simultaneously, reducing experimental error due to technical variability. In quantitative proteomics, metabolic labeling approaches such as SILAC are the gold standard, though they are practically impossible in humans *in vivo*[101].

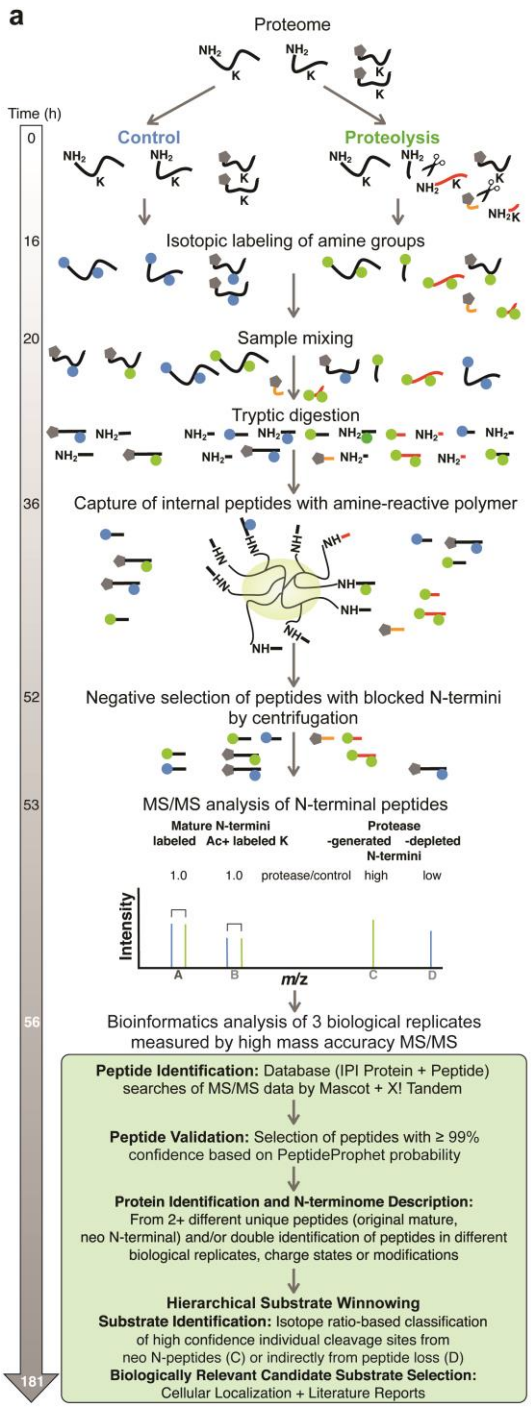

Figure 1.4 N-terminal amine isotopic labeling of substrates (TAILS) workflow. Cellular proteomes are prepared to compare a proteolysis condition (*e.g*. the addition of an exogenous active protease) *vs*. a control condition. In each proteome, each protein contains a primary α amine group (NH2) at its mature amino (N) terminus as well as additional primary α amine groups at 'neo' N termini arising from proteolysis. Formaldehyde is typically used to label and block all primary amines at the protein level, including mature and neo protein N termini and lysine (K) side chains, which contain an ε amine group. Following labeling, samples can be pooled 1:1 and digested with trypsin, which creates new, unblocked N termini. Peptides containing unblocked primary amines from trypsin digestion are bound by an aldehyde-rich polymer and

mature and neo N termini are negatively enriched, as well as any naturally blocked N termini, e.g. those with N-terminal acetylation or cyclization. N-terminal peptides are analyzed by tandem mass spectrometry and are identified and quantified using bioinformatics. Modified from [159] with permission.

1.4.5 Terminomics to study mitochondria

Terminomics is exceptionally well-suited to study changes in the mitochondrial proteome, including import and proteolysis. Because N-terminal peptide enrichment techniques allow for the identification of low abundance proteins that may not be detected by shotgun proteomics, these complementary methods may enable the further characterization of the mitochondrial proteome, including the identification of new members of the mitochondrial proteome. Due to the important role of proteolysis in both mitochondria and apoptosis, proteomics techniques that can identify proteolytic events are valuable in the study of mitochondrial events and dynamics, including those associated with other important mitochondrial functions and processes. Furthermore, because 99% of the mitochondrial proteome is imported, often involving proteolysis, a terminomics approach would be sensitive to the import state of a given protein and able to identify the exact site of import-associated cleavage.

The exact site of mitochondrial MTS cleavage has been an area of recent interest[178], with great strides made in yeast mitochondria using terminomics[53]. Several import-associated proteases can further modify mitochondrial proteins following import. Proteins destined for the mitochondrial matrix are typically cleaved by MPP, but then may also be cleaved by several other import-associated proteases, including Icp55[53], MIP[120], and IMP[119,120]. Several groups have applied terminomics to characterize proteolysis during mitochondrial protein import, specifically the site of MTS removal[53,179]. The first mitochondrial terminomics study was published in 2009; it

demonstrated that an MTS can be as long as 100 amino acids – rather than 20-65 amino acids, as was accepted then[52] – and also distinguished between the cleavage sites of two MTS-cleaving proteases (MPP and Icp55) with a single amino acid resolution to refine two distinct cleavage motifs in yeast[53]. Similarly, mitochondrial terminomics has been valuable in identifying low-abundance members of mitochondrial sub-compartments, namely the IMS proteome[180].

TAILS specifically has been successfully applied to study complex plastids, organelles that also contains cleavable import signals[181]. Other terminomics approaches have contributed to the characterization of the yeast mitochondrial proteome[53] and IMS proteome[180], and more recently human[179] and mouse mitochondria[182]. By identifying biological protein N termini, terminomics techniques are able to infer biological consequences, *e.g.* import.

Furthermore, N-terminomics techniques can identify further chemical modifications in protein N termini, including co-translational acetylation – which affects protein turnover – and the presence or removal of formylated initiator methionine (fMet) residues: a chemical modification of the Met1 residue of proteins translated within mitochondria. fMet modifications are associated with the mitochondrial N-end rule and protein half-life, similar to Met1 removal and acetylation in proteins translated in the cytoplasm, and are the topic of recent interest[183,184].

Finally, studying the mitochondrial proteome under different biological conditions, such as altered metabolism or stress, may allow for the identification of mitochondrial proteins not expressed in healthy conditions, and of proteolytic events that may not occur in healthy conditions.

Because terminomics approaches can quantitatively compare proteomes and also identify and quantify terminal peptides from proteolysis, we hypothesized that a mitochondrial terminomics approach would be valuable and well-suited to study both mitochondrial dynamics as well as cell-wide events in the early stages of intrinsic apoptosis and infection. Furthermore, this approach could identify the pathways affected during early apoptosis as well as specific proteolytic events pointing to mechanisms necessary for the later stages of intrinsic apoptosis or infection, respectively.

1.4.6 Terminomics to study apoptosis

Terminomics is well suited to study the complex interplay between signaling pathways and cellular responses in apoptosis and infection *in vivo*. Proteomics studies have been successfully applied to study apoptosis[185,186], as have several terminomics studies[187], though none have examined early apoptosis or mitochondrial events.

During apoptosis, late stages are mediated by a well-established caspase protease cascade and early events are mediated by mitochondrial proteases; the consequences of each would be detectable in protein N termini. N terminomics has been successfully applied to study cells undergoing the late stages of apoptosis. The Wells lab developed a subtiligase-based technique to positively enrich for protein N termini and applied it to study chemically-induced apoptosis in Jurkat cells[162]. Terminomics enabled them to study the relative frequencies of cleavage motifs across the cellular proteome and they found that the canonical caspase cleavage motif (DEVD) represented <1% of their observed caspase-like cleavage sites. Proteomics[185,186] and terminomics[161,162,171,172,188] have been applied to study late-stage apoptosis. However, there

appear to be no terminomics or mitochondrial proteomics studies of early apoptosis, providing an interesting avenue for further research.

1.4.7 Terminomics to study infection

Terminomics techniques are also well-suited to study infection, which occurs at the interface of protease-regulated immune pathways and inflammatory events. Proteomics applications have contributed significantly to the study of pathogens and host-pathogen interactions (reviewed by Bhavsar *et al.*[189], Malmström *et al.*[190], Walduck *et al.*[191], and Fels *et al.*[192]). For example: stable isotope labeling by amino acids in cell culture (SILAC) and quantitative proteomics have enabled the identification of virulence factors and the cataloguing of the virulence-associated secreted protein repertoires, known as secretomes, of many pathogens[71,193–197]. Furthermore, enrichment techniques and MS have enabled the identification of virulence factor substrates and host binding partners[198–200], and shotgun proteomics has allowed the characterization of the host cellular response to infection at a global level[201–203]. Finally, proteomics techniques specific for various PTMs, including phosphorylation, have further characterized bacterial regulation[204] and the host cellular response, as well as identifying mechanisms of virulence factors[205,206].

Despite the breadth of prior terminomics applications, relatively few have studied pathogens and host-pathogen interactions in infection, and none have examined an active infection, despite the importance of proteases in host immunity and microbial virulence strategies (reviewed by Marshall *et al.*[101]). Terminomics can identify substrates of pathogen-encoded proteases, both intracellular and secreted. Furthermore, for pathogens that do not encode known proteases, terminomics of infected host cells would be valuable to glean mechanistic information on how the host cell proteome and global proteolysis change during infection, including how infection

impacts host processes. This approach could identify mechanistic causes of disease symptoms and map the pathways behind it.

Furthermore, many pathogens manipulate proteases as a virulence strategy, ultimately causing injury to host tissues or evasion from the host immune system. Indeed, many bacterial proteases play a direct and substantial role in disease; terminomics approaches would be capable of identifying proteolytic events and the global consequences of a microbial protease. For example, *Clostridia* species secrete potent collagenases that aid infection by disrupting tissue barriers while providing amino acids as a carbon source[207].

Some bacterial pathogens encode proteases that assist with escape from the host immune system: their most imminent and significant threat during infection. For example, many pathogens that infect mucosal surfaces encode proteases that cleave immunoglobulin A1 (IgA1), including *Neisseria meningitidis* and *Neisseria gonorrhoeae*, which cause human meningitis and sexually-transmitted infections[208]. IgA1 proteases separate the pathogen-recognition (Fab) and host signaling (Fc) components of the antibody, thereby severing communication with host defense cells. This also leaves pathogens coated with cleaved Fab fragments and camouflaged from the immune system. IgA1 proteases disable this immune defense molecule allowing for direct escape of the invading pathogen from host immunity.

Bacterial pathogens can also cause disease without encoding their own proteases for virulence; many target and disrupt host proteases, instead. For example, some pathogens make use of host proteases, such as *Salmonella enterica* serovar Typhimurium, which infects the human gut, causing neutrophil recruitment to the gut lumen and secretion of neutrophil elastase. In a mouse model, elastase causes shifts in the composition of the gut microbiome and ultimately creates a

more favourable environment for *Salmonella* colonization and the initiation of disease[209]. Rather than activating host proteases, some bacterial pathogens directly inhibit host proteases. EPEC delivers its virulence factors, including NleF, into intestinal epithelial cells. Within the host cell cytoplasm, NleF directly binds to and blocks the activity of host caspases-4, -8, and -9[89].

These examples demonstrate the broad and vital roles of bacterial proteases and bacterial manipulation of host proteases in infectious diseases. These paradigms of bacterial pathogenesis have all been established in the field using microbiology, biochemistry, and molecular biology techniques, and notably without 'omics techniques. In recent decades, 'omics techniques have made a substantial impact in understanding virulence mechanisms and host-pathogen interactions. Unlike other 'omics techniques, terminomics is sensitive to alterations made by proteases. Its success in other applications shows that terminomics techniques can identify substrates of a protease of interest, the specific sites of proteolysis, and motifs to identify protease specificity. The importance of proteases in host-pathogen interactions highlights both the need for such knowledge as well as its potential impact.

1.5 Overall hypotheses

Although proteomic studies have great potential to illustrate how complex mitochondrial processes are coordinated, we lack useful proteomic tools to capture the crucial roles of protease networks and proteolysis across the mitochondrial proteome as well as the whole cell consequences of mitochondrial changes.

Recently, advances in proteomics and bioinformatics have better equipped us to characterize organelle proteomes[133]. Because proteases play important roles in mitochondrial functions[101], terminomics is particularly well-suited to study the mitochondrial proteome and proteolysis. In particular, regulation of intrinsic apoptosis is a key mitochondrial function, and although the later stages of caspase protease-driven apoptosis are well established, the early events in mitochondria are unclear. Ergo I hypothesize that examining how the mitochondrial N terminome changes during the induction of intrinsic apoptosis will reveal novel mechanistic insights into the regulation and execution of apoptosis.

Furthermore, because of the important role that mitochondria play in regulating intrinsic apoptosis and innate immunity, they are also valuable and frequent targets for pathogens to subvert during infection[21,84–88]. For example, EPEC targets mitochondria[68,79] with T3SS effectors EspF and EspZ, which traffic to mitochondria[21] and regulate mitochondrial functions including host cell apoptosis[61].

Although we know the mitochondrial phenotypes of these effectors, we currently lack a mechanistic understanding of what these effectors do within mitochondria to produce these contrasting pro- *vs.* anti-apoptotic effects, and how other effectors might affect mitochondria. Understanding how mitochondria change in the presence *vs*. absence of these effectors would help us understand how EPEC controls apoptosis. Ergo, I hypothesize that identifying unique changes in the human mitochondrial N terminome during EPEC infection will uncover mechanisms by which mitochondria-targeted T3SS effectors contribute to disease.

Chapter 2: A novel technique to study changes in the mitochondrial N-terminal proteome

2.1 Summary

Mitochondria are essential for many vital processes in eukaryotic cells. In turn, mitochondrial proteases are essential for mitochondrial function, including the import of 99% of the mitochondrial proteome from the cytoplasm, which often requires the proteolytic removal of a mitochondrial targeting sequence (MTS). However, little is known about how the mitochondrial proteome is sculpted by the >20 mitochondrial proteases, nor how proteolysis changes during key mitochondrial processes. We developed a new terminal proteomics workflow to study the global proteolytic landscape in mitochondria and whole parent cells simultaneously. By applying this workflow to enriched human mitochondria, we identified amino (N) termini from 26% of all known mitochondrial proteins: the highest coverage of the human mitochondrial terminome to date. Mitochondrial N termini indicated 97 novel sites of proteolysis, 99 known MTS sites, and 135 novel MTS sites that displayed a characteristic cleavage motif for the Mitochondrial Processing Peptidase. Together, these demonstrate the utility of this approach to study mitochondrial proteolysis, proteases, and import. Overall, this work provides a novel approach to study global dynamics in mitochondrial proteolysis between conditions and, therefore, can be used to characterize mitochondrial dynamics, processes, pathologies, and proteases, including and beyond apoptosis.

2.2 Introduction

Mitochondria are vital to many cellular activities due to their key role in bioenergetics[2]. Mitochondria have additional roles in innate immunity[3] and the regulation of the intrinsic or 'mitochondrial' pathway of apoptotic cell death[7,8], with genetic defects in mitochondrial proteins linked to an estimated 160 human diseases, including several neuromuscular and metabolic diseases[23]. However, there are inherent challenges to studying mitochondrial function; only 15 mitochondrial proteins are encoded on the mitochondrial chromosome[44], with the remaining ~1,200 proteins[48,151] imported from the cytosol, often involving the proteolytic removal of an N-terminal mitochondrial targeting sequence (MTS). Adding further complexity, mitochondrial proteases regulate and execute mitochondrial functions by sculpting the mitochondrial proteome, altering substrate activity and turnover, and affecting processes such as mitochondrial fusion and fission, apoptosis, and the synthesis, import, and quality control of mitochondrial proteins (reviewed by Quirós *et al.*[114]). Mitochondrial protease mutation or down-regulation can be catastrophic for cellular function and survival[115], and several human diseases arise from genetic defects in mitochondrial proteases, including cerebral, ocular, dental, auricular, skeletal syndrome[116]. More recently, mitochondrial proteases have been identified as possible therapeutic targets in cancer, due to the associations between the mitochondrial generation of reactive oxygen species and cancer cell metabolism[117]. Thus, mitochondrial proteases are important for both human health and disease.

Proteomic studies have the potential to illustrate how these complex processes are coordinated for mitochondrial function and perturbed in disease. However, appropriate mitochondrial proteomic tools are lacking that can capture the dynamic state of the mitochondrial proteome as

regulated by mitochondrial proteases, including mitochondrial protein import and maturation, proteolytic events within mitochondria that drive mitochondrial processes and regulation, and the consequence of these mitochondrial proteolytic events across the whole cell proteome. Conventional shotgun proteomics obscures naturally occurring proteolytic events among tryptic peptides and is therefore unable to detect proteolytic events reliably. In contrast, terminal proteomics, or 'terminomics,' identifies protein termini, including original termini of mature unprocessed proteins and precise sites of 'neo' termini created by proteolytic events. Terminomic techniques can therefore simultaneously profile global changes in protein abundance and proteolysis.

Three of the leading terminomics techniques are terminal amine isotopic labeling of substrates (TAILS), combined fractional diagonal chromatography (COFRADIC), and subtiligase-based positive enrichment of protein termini[158,160,162]. All three techniques selectively enrich terminal peptides from a sample proteome, using either a polymer to retain internal peptides (TAILS), direct chemical modification to alter internal peptide HPLC elution profiles (COFRADIC), or terminal peptide biotinylation and capture (subtiligase). Mass spectrometry of the collected terminal peptides then reveals terminal peptide sequences, the proteins that terminal peptides originated from, and accordingly the position of each terminal peptide within the mature proteins. Terminomics has already helped characterize the mitochondrial proteome of yeast, mouse, and human cells, as well as the exact sites of MTS removal in imported proteins[53,179,180,182]. Furthermore, quantitative comparisons of protein abundance and proteolysis between conditions are possible by using isotopic labels to differentiate the terminomes of different cell populations before mass spectrometry. Therefore terminomics is a powerful tool to

compare global proteolysis between different states and an excellent tool with which to study mitochondrial processes and regulation.

This chapter describes a quantitative TAILS-based approach to simultaneously study the dynamics of the whole cell and mitochondrial terminomes for a comprehensive view of mitochondrial processes.

2.3 Methods

2.3.1 Cell culture and SILAC labeling

HeLa cells (CCL-2, American Type Culture Collection, Manassas, Virginia, USA) were cultured in Dulbecco's Modified Eagles Medium (DMEM; HyClone) with 10% (v/v) heat-inactivated fetal bovine serum (Gibco), 1% (v/v) non-essential amino acids (HyClone), and 1% (v/v) GlutaMax (HyClone) and found to be *Mycoplasma* negative. All experiments were performed between passages 5 – 20. For stable isotope labeling by amino acids in cell culture (SILAC) experiments, HeLa cells were grown in DMEM lacking arginine and lysine (Caisson Labs) and supplemented with 10% (v/v) heat-inactivated, dialyzed fetal bovine serum (Gibco), 1% GlutaMax (HyClone), 'light' L-lysine (1.0 M; Sigma-Aldrich), and 0.12 M of either 'light' L-arginine, 'medium' L-[13C6]arginine, or 'heavy' L-[13C6,15N4]arginine (Cambridge Isotope Laboratories). Following six cell doublings in SILAC medium, arginine incorporation was verified as described[210]. For experiments, 2.0 x 10^6 cells were seeded per 150 mm tissue culture dish per condition and repeated for each biological replicate. Experiments were performed at 75% cell confluence.

2.3.2 Induction of intrinsic apoptosis

Before inducing apoptosis, HeLa cells were rinsed with phosphate-buffered saline containing calcium and magnesium (HyClone) and synchronized with serum-free DMEM for 24 h. Bax agonist molecule 7 (BAM7, Calbiochem) was dissolved in DMSO. HeLa cells were treated with 30 μM BAM7 or the DMSO control for 24 h, both to a final DMSO concentration of 0.6% (v/v).

2.3.3 Cell harvesting and mitochondrial enrichments

Following treatments, the SILAC-labeled cells and spent medium were collected from each culture, rinsed and resuspended in cellular isolation buffer containing 10 mM Tris-MOPS, 10 mM EGTA/Tris, and 0.2 M sucrose[211] supplemented with 5 mM EDTA plus EDTA-free HALT Protease Inhibitor Cocktail (Thermo Fisher). Whole labeled cells were pooled 1:1:1 from the light-, medium-, and heavy-labeled populations according to protein concentration, which was determined using the bicinchoninic acid assay. Pooled cells were pelleted at 600 x g for 10 min at 4 °C and resuspended in 2 mL of ice-cold isolation buffer, then gently homogenized on ice with a pre-chilled glass-Teflon Potter-Elvehjem homogenizer until > 90% cell lysis was achieved as monitored by Trypan blue staining. A 1 mg aliquot of cell homogenate protein was snap-frozen in liquid nitrogen for storage before terminomics analysis. For the remaining cell homogenate, intact cells, nuclei, and heavier cell components were pelleted at 600 x *g* for 10 min at 4 °C in microfuge tubes and mitochondria were enriched from the supernatant by five serial centrifugations at 7,000 x *g* for 10 min in 1 mL volumes after each spin. Microfuge tubes and 1 mL volumes were used to avoid sample dilution from the use of 50 mL tubes as initially described by Frezza *et al.*[211]. The final pellet was rinsed three times in ice-cold isolation buffer

and resuspended in a minimal volume of the remaining supernatant, snap frozen in liquid nitrogen, and stored at -80 °C until samples were prepared for terminomics analysis.

2.3.4 Inner mitochondrial membrane potential ($\Delta\Psi_m$) assays

The inner mitochondrial membrane potential was measured according to manufacturer's instructions (Cayman Chemical) on a Tecan M200 plate reader. Cells were treated with BAM7, STS, DMSO, or DMEM only, as indicated. J-aggregates/J-monomers ratios (representing the ratios of healthy:unhealthy mitochondria) were normalized to the average DMSO control for each time point. A Kruskal-Wallis (unpaired, non-parametric) test was used to compare each experimental treatment and its respective control.

2.3.5 SDS-PAGE and western blotting

Cells and enriched mitochondria were lysed and proteins resolved by 15% SDS-PAGE and immunoblotted using anti-caspase-9 (1:1,000, Cell Signaling Technology #9508), anti-caspase-3 (1:500, Cell Signaling Technology #9662), and anti-β-tubulin (1:5,000, Sigma-Aldrich #T4026) antibodies overnight at 4 °C.

2.3.6 Mitochondrial SILAC-TAILS N terminomics

Mitochondrial samples (0.5 mg) were heated at 90 °C in 6 M GuHCl to 500 µL for 1 h, as described[212], and diluted two-fold in HEPES buffer (100 mM HEPES, 1 x HALT Protease Inhibitor Cocktail, 10 mM EDTA, pH 7.4). Whole cell samples (0.5 mg) were thawed on ice and diluted in HEPES buffer to a final volume of 1 mL. All samples were then centrifuged at 10,000 x g for 10 min to pellet cell debris and insoluble proteins and protein was extracted using methanol-chloroform precipitation before drying on a SpeedVac[159]. The dry protein pellet was solubilized in 500 µL of 6 M GuHCl and diluted two-fold in HEPES buffer. Sample pH was

adjusted to 7.5 and dimethylation terminal Amine Isotopic Labeling of Substrates (TAILS) was performed on all samples as previously described[159], but modified to perform mitochondrial and whole cell analyses in parallel, which we termed Mitochondrial SILAC-TAILS (MS-TAILS). In brief, whole protein was selectively blocked at N-terminal and neo-N terminal α-amines and lysine ε-amines by reductive dimethylation with light formaldehyde. Following trypsin digestion, 20 μg of peptides were collected for a parallel shotgun proteomics analysis ('preTAILS') to compare overall changes in protein abundance, as described before[159]. Blocked N-terminal peptides were negatively enriched from the tryptic digest by covalent linkage of the tryptic and C-terminal peptides to polyaldehyde-HPG-ALD polymer (http://flintbox.com/public/project/1948/), which selectively binds peptides containing free primary amines, thereby separating tryptic peptides from the N-terminally dimethylated and naturally blocked N-terminal peptides (*e.g.* acetylated or cyclized).

2.3.7 LC-MS/MS analysis

Lyophilized peptide samples (MS-TAILS and preTAILS) were redissolved with 1% (v/v) formic acid before loading ~1 μg total peptide on a 45-cm capillary HPLC column (75-μm i.d.) packed in-house with ReproSil-Pur 120 C18-AQ 1.9 μm reversed phase particles (Dr. Maisch, Ammerbuch, Germany). Peptides were resolved by a linear gradient of acetonitrile with 0.1 % (v/v) formic acid in H2O with 0.1 % (v/v) formic acid (250 nL/min; 2 – 35% v/v over 90 min) delivered by an Easy-nLC system (Thermo Fisher Scientific). The column was maintained at 50 °C during the separation. MS/MS analysis was performed using an Impact-II Q-TOF mass spectrometer (Bruker) fitted with a captive spray ESI source using acetonitrile as dopant. Spectra were acquired from 200 – 2000 Th with the oTOF control focus mode enabled in a fixed cycle

time of 3 s. Ions were automatically targeted for MS/MS analysis using data-dependent selection of the maximum top 20 precursor ions, with a 30 s active exclusion window. Base collision energy for CID was set to 23 eV, with stepping to 70 eV scaling on deconvoluted ion mass enabled.

2.3.8 N terminomics data analysis

Raw data was analyzed using MaxQuant version 1.5.2.8[213] using the built-in Andromeda search engine. Data for duplex and triplex SILAC experiments were analyzed separately, as well as preTAILS and MS-TAILS data sets. Spectra were matched against the UniProt/SwissProt human protein database (version 2013_10, 84,843 entries) with common contaminants added to the database using the feature in MaxQuant. The false discovery rate (FDR) set to 0.01 at both protein and PSM level using the MaxQuant "revert" option for decoy database generation. The "match-between-runs" option was enabled using a 2-min search window. Carbamidomethylation (Cys) and dimethylation (Lys) were set as fixed modifications, and acetylation (peptide N terminus), pyroglutamation (Gln and Glu) and dimethylation (peptide N terminus) were set as variable modifications with the minimum score for modified peptides set to 25. Enzyme specificity was set to semi-ArgC (free N terminus) due to the inability of trypsin to cleave dimethylated lysine. Two miscleavages were allowed. Peptide mass tolerance was set to 0.07 Da for the first search and 6 mDa for the main search, and 40 ppm for MS/MS peak matching. Quantification was performed using the MaxQuant SILAC option, with 13C(6) (Arg) and/or 13C(6)15N(4) (Arg) used as quantitative labels, depending on the experiment. Peptide output lists were filtered to remove decoy hits prior to further analysis.

The mass spectrometry proteomics data have been deposited to the ProteomeXchange Consortium (http://proteomecentral.proteomexchange.org) via the PRIDE partner repository[214] with the dataset identifier PXD009054.

2.3.9 Bioinformatics

Identified peptides were annotated by an in-house developed Java program we called Termini Annotation of Peptides (TAP; Figure 2.1). TAP annotates TAILS data matching protein isoforms, P6 – P6' of the identified cleavage site, N terminus classification (*e.g.* original, neo-from proteolysis), protein function, subcellular location, and Gene Ontology (GO) annotations for Biological Processes, Molecular Functions, and Cellular Components. N-terminal peptides were identified as original, initiator methionine (Met1) removals, pro-peptide or signal peptide removals, MTS removals, or endoproteolytic processing by the TopFIND ExploRer (TopFINDer) web program (clipserve.clip.ubc.ca/topfind/topfinder), which incorporates data from the MEROPS database and community uploaded TAILS and COFRADIC studies[215]. When known, TopFINDer also annotated proteases known to cleave at the TAILS–identified sites. Mitochondrial proteins were identified as known members of the human mitochondrial proteome through the MitoCarta2.0 database[47,48]. To identify potential cleavage site consistency in proteolytic processing events, the amino acid sequence surrounding each N-terminal event was analyzed using WebLogos (http://weblogo.berkeley.edu/)[216]. Enrichment of Functional Annotation Clusters (FACs) was conducted using the Database for Annotation, Visualization and Integrated Discovery (DAVID) v. 6.8 (https://david.ncifcrf.gov)[217,218], comparing the query dataset with all proteins identified using MS-TAILS, or all mitochondrial proteins, as

appropriate. Quantitative data was normalized and centered using a $\log_2$ transformation using Center•Point, an in-house developed Java program (Figure 2.2).

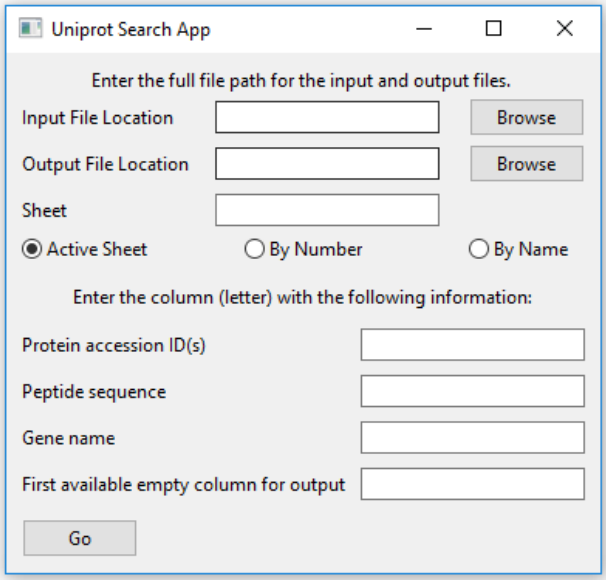

Figure 2.1 The Termini Annotation of Peptides (TAP) computer program. TAP, a Java software program that within Microsoft Excel annotates matching protein isoforms, P6 – P6' amino acids of the identified cleavage site, type of N terminus (e.g. original, neo N-terminal), protein function, subcellular location, and Gene Ontology annotations for Biological Processes, Molecular Functions, and Cellular Components.

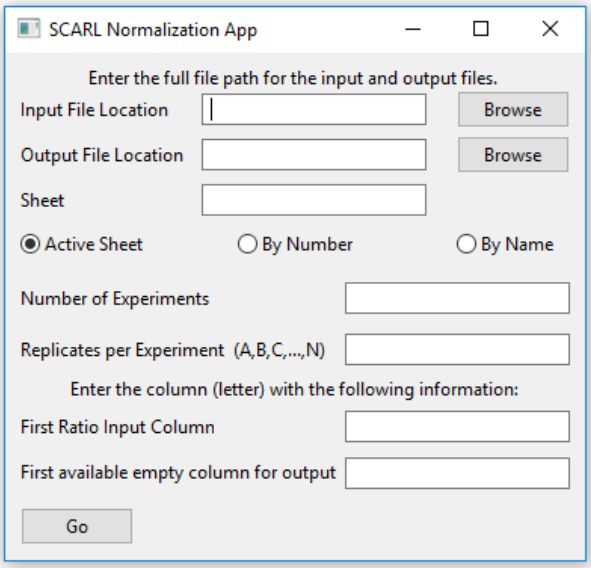

Figure 2.2 The Center•Point computer program to normalize large 'omics datasets. Center•Point is a Java software program that individually $\log_2$ transforms up to thousands of peptide ratios from separate biological replicates, normalizes these to center around a fold change of 1:1 ($\log_2(1) = 0$), and outputs the average, normalized fold-change across all replicates and all computations throughout the process within Microsoft Excel.

2.4 Developing a mitochondrial terminomics workflow

To analyze and compare the N terminomes of enriched mitochondria and the parent cell lysate, we metabolically labeled cellular proteins by stable isotope labeling by amino acids in cell culture (SILAC), and performed TAILS on both cell fractions, a procedure we modified and so termed Mitochondrial SILAC-TAILS (MS-TAILS; Figure 2.3A). By combining SILAC and TAILS techniques, N terminome changes could be easily quantified by comparing the relative abundance of SILAC-labeled peptides originating from different treatment conditions, either heavy, medium, or light labeled. Accordingly, the label on each N-terminal peptide and the cell fraction of origin together provide information on treatment-specific changes and how these change in the cell overall or within mitochondria. A change in a SILAC ratio for a proteolytic

neo N terminal peptide therefore indicates sites of altered proteolysis (provided that preTAILS or mature N termini can control for changes in the overall abundance of that protein). While MS-TAILS does not provide information on the overall proportion of the substrate protein that is cleaved, MS-TAILS identifies substrates and specific proteolytic sites as well as quantitative changes in proteolysis between conditions of interest, which is exceedingly valuable in the search for cleaved proteins. Such sites of altered proteolysis may cause a gain or loss of protein function, which could be confirmed by subsequent experiments based on MS-TAILS data.

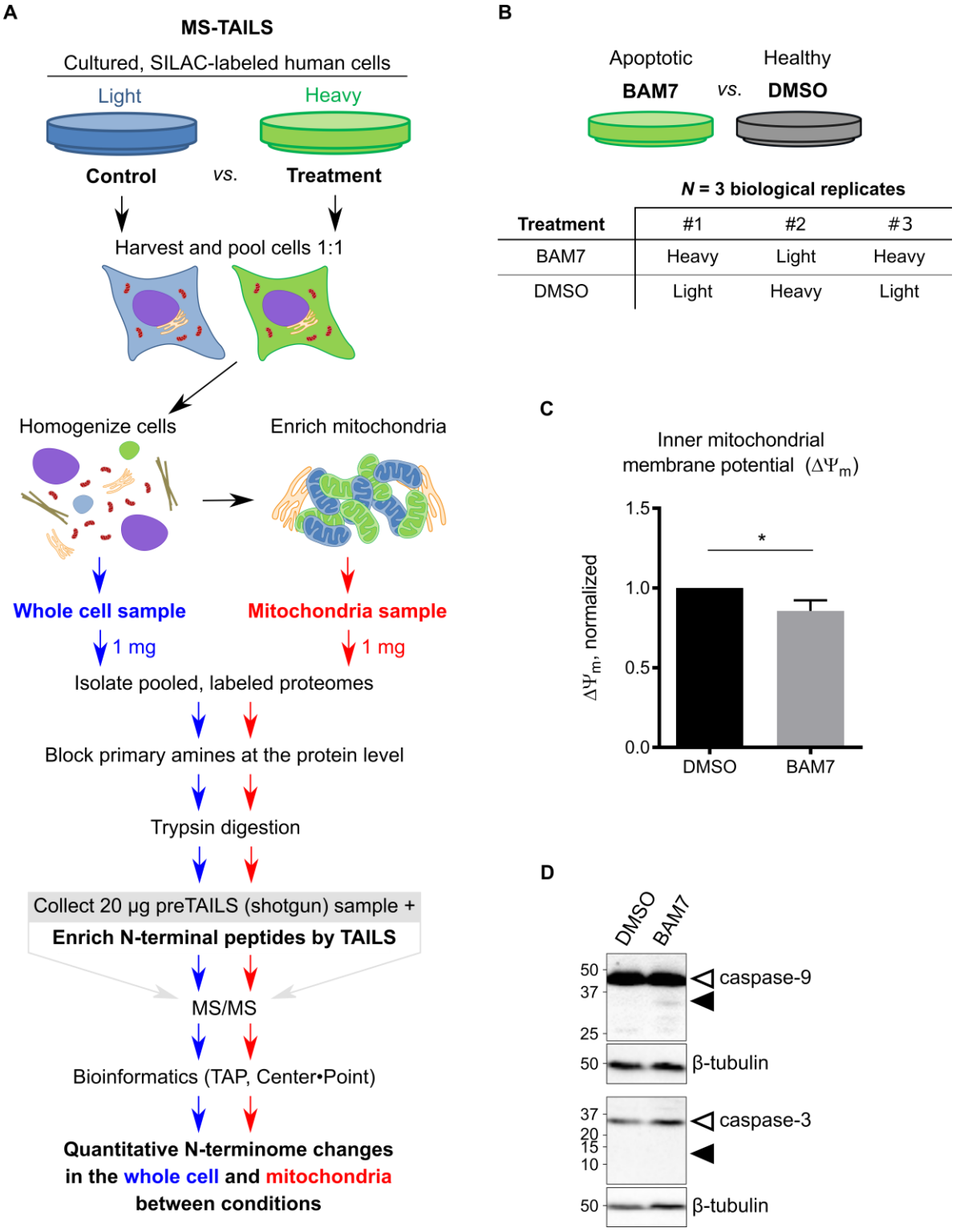

Figure 2.3 Mitochondrial SILAC (MS)-TAILS workflow and set-up. *A,* Isotope-labeled HeLa cell populations were prepared using SILAC. Cells were treated, pooled 1:1, and then homogenized. Whole cell protein (1 mg) was retained for a parallel, complementary analysis of the whole cell N terminome, whereas mitochondria were isolated from the remaining cell homogenate. Cellular and mitochondrial proteomes

were isolated, and 20 μg were collected for a shotgun proteomics analysis. In parallel, N terminomes were prepared by TAILS[159] and analyzed by tandem mass spectrometry. Peptides were identified and quantified using MaxQuant, and further analyzed with TAP, Center•Point, and TopFINDer. *B,* Experimental setup of TAILS experiments to compare apoptotic and untreated cells and their mitochondria. HeLa cells were treated with 30 μM BAM7 or an equal volume of a DMSO vehicle control for 24 h. $N = 3$ biological replicates were prepared for all experiments, wherein isotope-coded arginine label swaps were performed as shown. *C,* Inner mitochondrial membrane potential ($\Delta\Psi_m$) of treated HeLa cells was measured and normalized to the vehicle control. Mean and standard deviation are shown. *D,* Cells were harvested and lysates were analyzed by western blotting with α-caspase-9 and α-caspase-3 antibodies, and α-β-tubulin as a protein loading control. Expected masses of the full-length zymogen (white arrow) and the cleaved, active forms of each caspase (black arrow) are shown. SILAC, stable isotope labeling by amino acids in cell culture. TAILS, terminal amine isotopic labeling of substrates. TAP, Termini Annotation of Peptides. BAM7, Bax activator molecule 7.

To assess the performance of the MS-TAILS technique, we first compared the N terminomes of untreated cells and mitochondria with those executing an active mitochondrial function by treating human epithelial cells with Bax activator molecule 7 (BAM7, a specific activator of intrinsic apoptosis[219]) or a DMSO vehicle control (Figure 2.3B). As expected of early stage apoptosis, BAM7-treated cells displayed significantly decreased inner mitochondrial membrane potential ($\Delta\Psi_m$; $p = 0.0203$; Figure 2.3C) and increased activating cleavage of procaspase-9 compared to the vehicle control, with no detectable procaspase-3 cleavage, consistent with the early stages of intrinsic apoptosis prior to caspase-3 activation (Figure 2.3D).

In MS-TAILS, cells were grown in either ‘light’ or ‘heavy’ SILAC labeling medium for two weeks. SILAC labeled cells were treated with BAM7 or DMSO and then pooled and homogenized. An aliquot was retained for separate whole-cell lysate analysis and then mitochondria were enriched from the remaining sample. Enriched mitochondria highly increased the abundance of the mitochondrial marker cytochrome *c* oxidase subunit IV and undetectable levels of β-tubulin, a cytoplasmic marker, indicating successful mitochondrial enrichment (Figure 2.4). In Chapter 3, I used this technique to further study apoptosis using similar techniques and including a second inducer of intrinsic apoptosis: staurosporine (STS). These

conditions were optimized simultaneously, although in this Chapter I focus on establishing the technique and in Chapter 3 I use MS-TAILS to examine the biological impacts of apoptosis, specifically. Mitochondria from STS-treated cells contained more carryover from the cytoplasm, which may indicate differing mitochondrial ultrastructure or differing interactions between cell compartments. Aliquots from both mitochondria-enriched and whole cell fractions were retained for shotgun proteomics ('preTAILS') analysis to assess changes in individual protein levels prior to N terminome enrichment by dimethylation TAILS[158], where dimethylation was used to block protein primary amines for the negative enrichment of blocked N termini. Following TAILS, cellular and mitochondrial N terminomes were analyzed in parallel by tandem mass spectrometry.

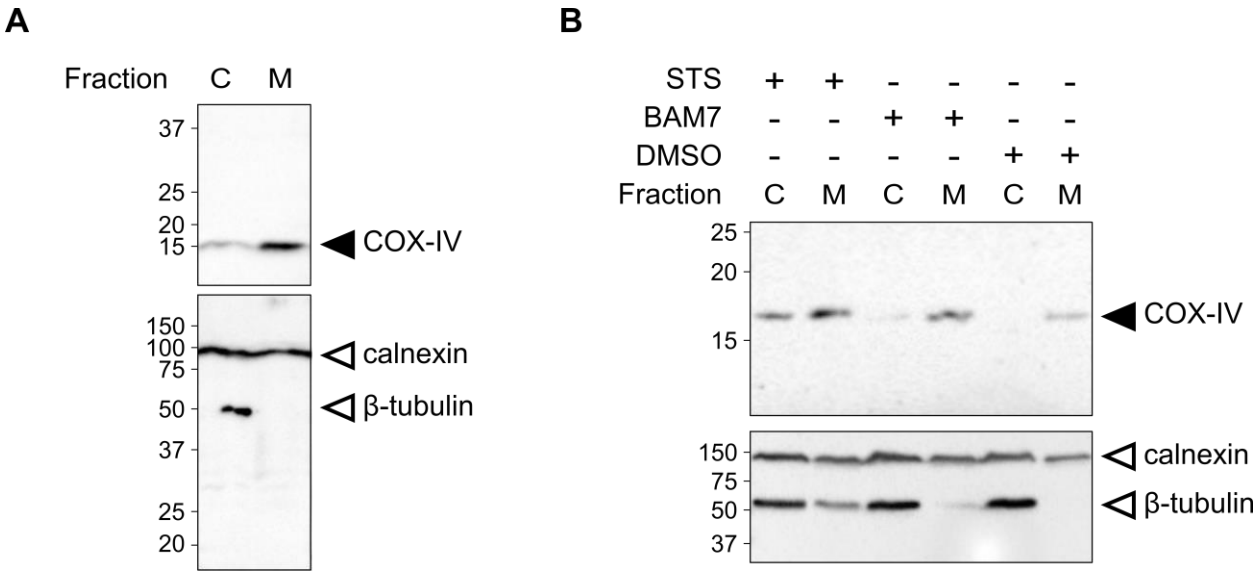

Figure 2.4 Enrichment of mitochondria from apoptotic and untreated cells. *A,* Mitochondria were enriched from HeLa cells. Mitochondria-enriched (M) cell fractions were compared to whole cell lysates (C) and analyzed by western blotting using antibodies specific to the proteins as indicated. Mitochondria-enriched samples demonstrated increased abundance of the mitochondrial marker (cytochrome *c* oxidase subunit IV, COX-IV) and decreased abundance of the cytoplasmic marker (β-tubulin). The endoplasmic reticulum marker (calnexin) was detectable in both fractions. *B,* HeLa cells were treated with 0.2 μM STS, 30 μM BAM7, or an equal volume of DMSO vehicle control. Mitochondria were enriched from each cell population and analyzed by western blot to the proteins indicated following 15% SDS-PAGE.

2.5 Mitochondrial and cellular N-terminal peptide identification

MS-TAILS of mitochondria and whole cells identified in total 2,237 N-terminal peptides from 1,789 proteins at a peptide-level FDR of 1.13% (Figure 2.5A; Supplemental File 1). These N-terminal peptides represented 94% of all N-terminal peptides identified by MS-TAILS and preTAILS combined (n = 2,377; Table 2.1), confirming high N terminome enrichment by MS-TAILS and hence unique peptide identification and proteome coverage missed by conventional shotgun (preTAILS) analyses alone (Figure 2.5A). Three biological replicates were used to increase proteome coverage and to increase confident identifications of N termini (Figure 2.5B). In mitochondria, 72% of proteins and 63% of N-terminal peptides were identified in all three biological replicates; in whole cell samples, 66% of proteins and 57% of N-terminal peptides were identified in all three biological replicates. Thus, while also showing reproducible identification of peptides and proteins, increasing the number of biological replicates further increased peptide and proteome coverage as expected.

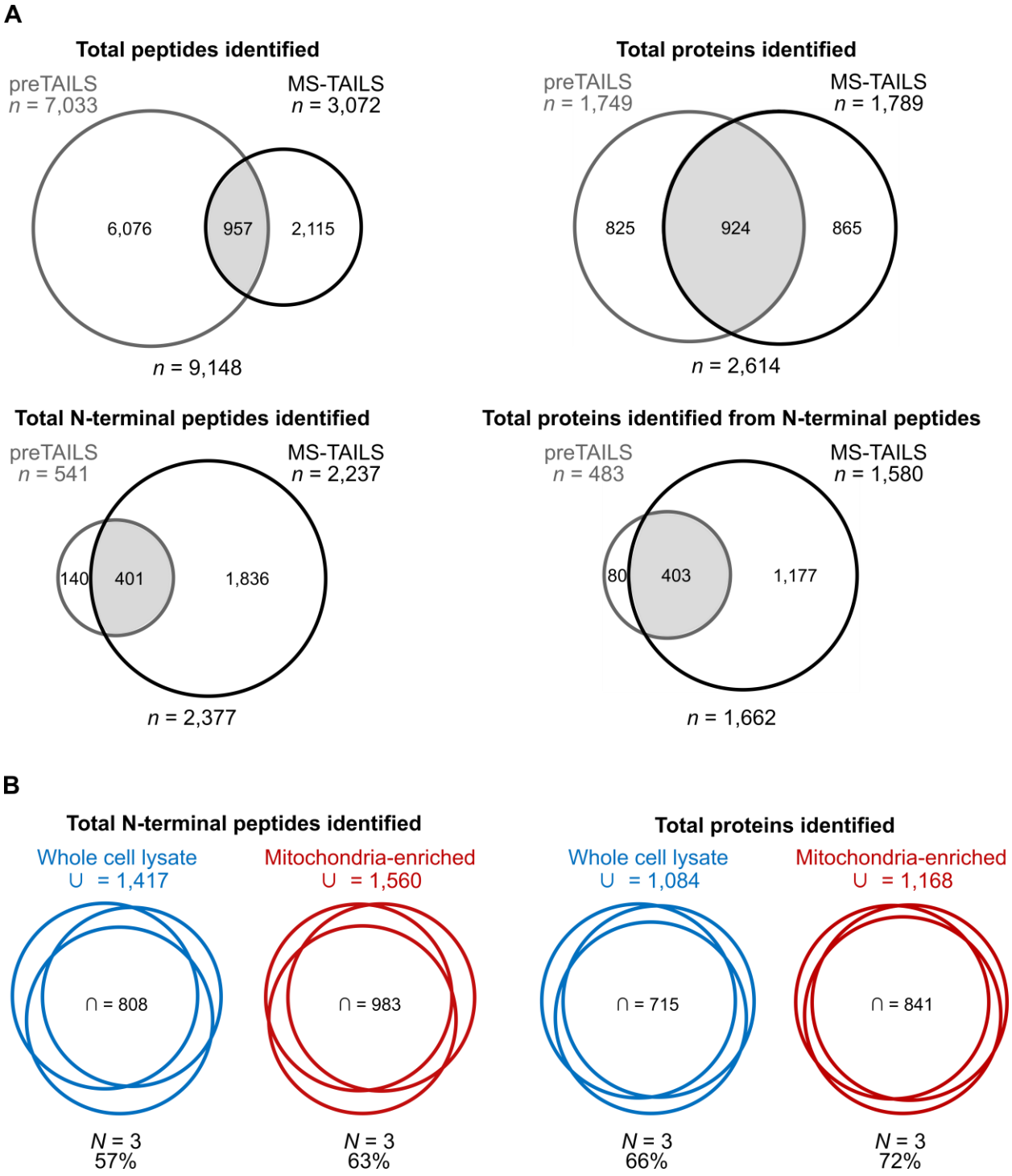

Figure 2.5 MS-TAILS reproducibility and coverage at the protein, peptide, and N-terminal peptide levels. *A*, Unique peptides (top right), unique proteins (top left), unique N-terminal peptides (bottom left), and proteins identified from all N-terminal peptides (bottom right) identified by preTAILS *vs*. MS-TAILS in either cell fraction. *B*, Reproducibility of N-terminal peptides (left) and proteins (right) identified with MS-TAILS between $N = 3$ biological replicates. The union (∪) of all peptides and proteins identified in any of the three pooled replicates is shown as well as the intersect (∩) of all peptides and proteins identified in all

three replicates. The percent of all peptides and proteins observed in all three biological replicates (*i.e.* ∩/∪) is displayed beneath each Venn diagram.

Table 2.1 Summary of TAILS mass spectrometry data. The number of unique proteins, peptides, and N-terminal peptides identified from $N = 3$ biological replicates of MS-TAILS and preTAILS experiments of mitochondria and whole cells.

	Total	Mitochondria	Whole cell
Unique proteins	2,614	1,935	1,750
Unique peptides	9,148	5,667	5,972
Unique N-terminal peptides	2,377	1,638	1,524
Proteins identified by N-terminal peptides	1,662	1,219	1,133
Unique mitochondrial proteins	516	492	154
Coverage of the mitochondrial proteome	44.6 %	42.5 %	13.3 %
Unique peptides from mitochondrial proteins	2,102	1,830	601
Unique N-terminal peptides from mitochondrial proteins	502	446	155

We next addressed whether the types of N termini identified in the mitochondrial N terminome globally differed from those in the whole cell. These comprised both mature protein N termini — including the original N-terminal Met at position 1 as well as a mature N terminus at position 2 following removal of the initiator methionine (Met1) — and neo N termini arising from proteolytic processing of a signal peptide (from ER carryover), pro-peptide, MTS, or deeper within the protein chain. To distinguish between these types of protein N termini, we developed Termini Annotation of Peptides (TAP; Figure 2.1), an in-house software program to mine the UniProt database and thereby annotate TAILS data, including P6 – P6' of the identified cleavage site and the type of N terminus. Altogether, we found that 17.7% of proteins displayed multiple N-terminal peptides ($n = 276$) with an average of 1.4 N-terminal peptides identified per protein (Figure 2.6A; Table 2.1). Of all proteins identified, 26.0% displayed an original genetic encoded N terminus ($n = 405$), 49.6% displayed Met1 removal ($n = 773$), 2.0% displayed an N terminus from a known alternative translational start site ($n = 31$), and 11.1% displayed neo N termini

from a known, annotated site of signal peptide or pro-peptide removal (n = 173). Furthermore, ≥1 neo N terminus from other proteolytic processing events were detected in 26.1% of all proteins identified (n = 407; Figure 2.6).

As only 1.9% of all proteins contained ≥3 neo N termini, this showed that the vast majority of cellular lysate proteins were not extensively processed, yet one-third of proteins containing ≥5 proteolytic N termini were mitochondrial (n = 10; Table 2.2). The highest numbers of detected N termini were found in some of the most abundant proteins in the cell, *e.g.* actin and tubulin (Table 2.2). This suggests that the N termini detected are likely underestimates of the true number of N termini per protein, where other proteins may have additional yet undetected N termini due to their lower abundance in cellular and mitochondrial samples.

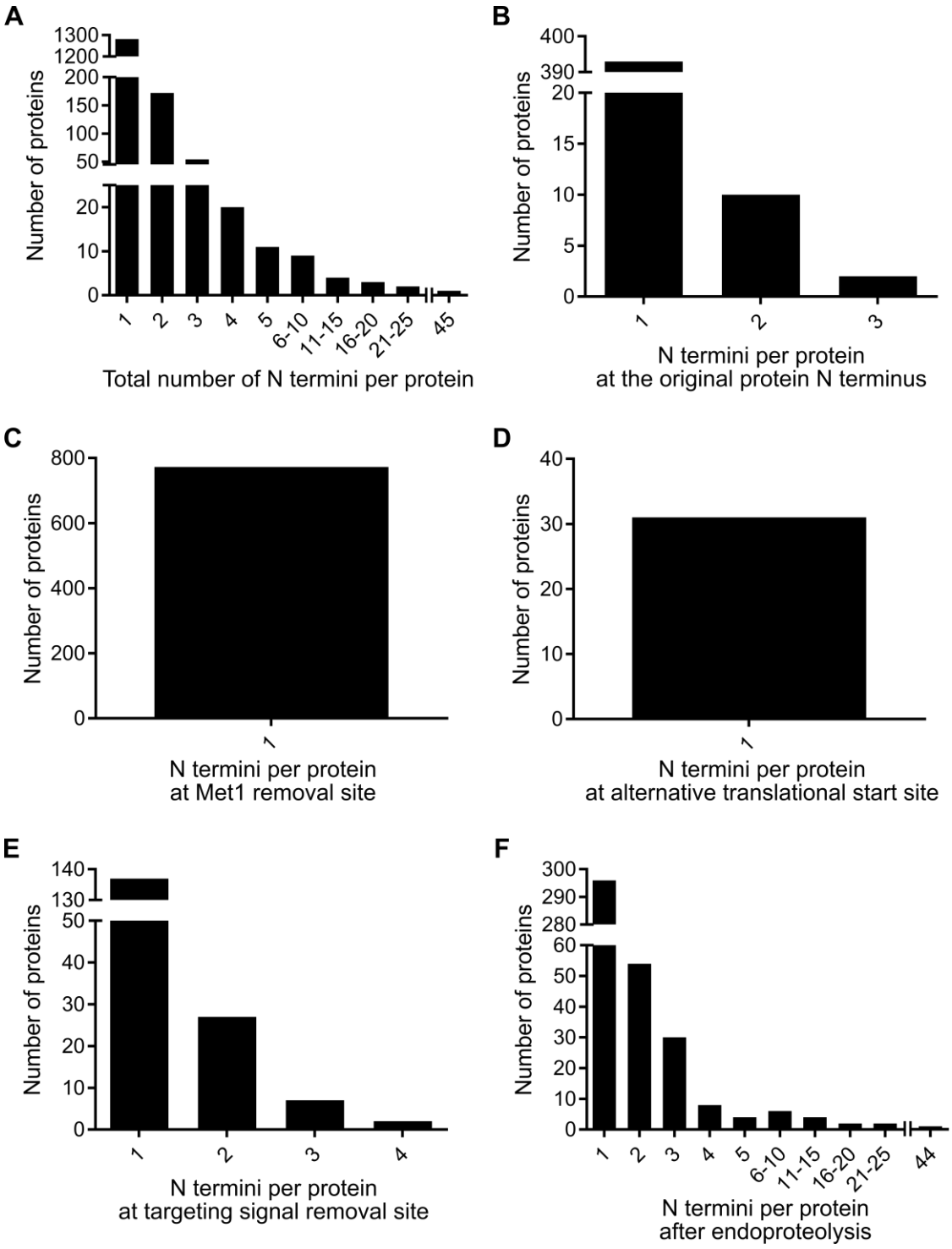

Figure 2.6 MS-TAILS identified multiple N-terminal peptides in individual proteins. *A*, Number of N-terminal peptides classified as shown that were identified for each protein by MS-TAILS. *B – E*, Number of proteins having a N terminus indicative of: *B*, original (genetic encoded) N terminus; *C*, initiator methionine (Met1) removal; *D*, known alternative translational start site; *E*, known signal peptide or pro-peptide removal; or *F*, neo N termini remaining after other (unidentified) proteolytic processing events.

Table 2.2 Proteins identified by MS-TAILS that contained the most N termini. The proteins with five or more unique N-terminal peptides identified by MS-TAILS in mitochondrial or whole cell fractions. Proteins in the MitoCarta 2.0 database of known mitochondrial proteins are indicated in red.

Gene	Protein	Mitochondrial	Total	Mature	Original	Met1 removal	Targeting/pro-peptide	Endoproteolysis
ACTB	Actin, cytoplasmic 1	No	45	1	0	1	0	44
PKM	Pyruvate kinase PKM	No	25	3	2	1	0	22
TUBA1A	Tubulin alpha-1A chain	No	22	0	0	0	0	22
HSPD1	60 kDa heat shock protein, mitochondrial	Yes	19	0	0	0	2	17
HSPA8	Heat shock cognate 71 kDa protein	No	17	1	0	1	0	16
ALDOA	Fructose-bisphosphate aldolase A	No	16	1	0	1	0	15
TUBB	Tubulin beta chain	No	15	1	1	0	0	14
EEF1A1P5	Putative elongation factor 1-alpha-like 3	No	14	0	0	0	0	14
GAPDH	Glyceraldehyde-3-phosphate dehydrogenase	Yes	12	1	0	1	0	11
VCP	Transitional endoplasmic reticulum ATPase	No	12	2	0	2	0	10
ATP5B	ATP synthase subunit beta, mitochondrial	Yes	10	0	0	0	4	6
ANXA2	Annexin A2	No	9	1	0	1	0	8
HSP90AB1	Heat shock protein HSP 90-beta	No	9	0	0	0	0	9
PPIA	Peptidyl-prolyl cis-trans isomerase A	No	9	2	1	1	0	7
EEF2	Elongation factor 2	No	8	2	1	1	0	6
ATP5A1	ATP synthase subunit alpha, mitochondrial	Yes	7	0	0	0	3	4
SLC25A5	ADP/ATP translocase 2	Yes	6	2	1	1	0	4
HSPA9	Stress-70 protein, mitochondrial	Yes	6	0	0	0	1	5
ENO1	Alpha-enolase	No	6	2	1	1	0	4
FTH1	Ferritin heavy chain	Yes	5	1	0	1	0	4
SDHA	Succinate dehydrogenase [ubiquinone] flavoprotein subunit, mitochondrial	Yes	5	0	0	0	2	3
TUFM	Elongation factor Tu, mitochondrial	Yes	5	0	0	0	2	3
ACLY	ATP-citrate synthase	Yes	5	1	0	1	0	4
HNRNPA1	Heterogeneous nuclear ribonucleoprotein A1	No	5	3	2	1	0	2
FLNA	Filamin-A	No	5	0	0	0	0	5
CALR	Calreticulin	No	5	0	0	0	2	3
HNRNPH1	Heterogeneous nuclear ribonucleoprotein H	No	5	2	1	1	0	3
HNRNPK	Heterogeneous nuclear ribonucleoprotein K	No	5	2	2	0	0	3
YBX1	Nuclease-sensitive element-binding protein 1	No	5	0	0	0	0	5
HNRNPU	Heterogeneous nuclear ribonucleoprotein U	No	5	0	0	0	0	5

To validate our modified mitochondrial enrichment procedure, we assessed how mitochondrial enrichment contributed to the identification of mitochondrial proteins. With TAILS and preTAILS combined, we identified 516 mitochondrial proteins, comprising ~45% of the known human mitochondrial proteome in the MitoCarta2.0 database of human mitochondrial proteins; MS-TAILS alone identified 310 mitochondrial proteins (26%) and MS-TAILS identified mitochondrial proteins not found by shotgun preTAILS analyses (Table 2.1; Figure 2.7A). Neither MS-TAILS nor preTAILS identified any of the 15 endogenous mitochondrial proteins encoded by the mitochondrial genome, despite searches including an N-terminal formyl-methionine variable modification (data not shown). Furthermore, MS-TAILS identified 475 unique N-terminal peptides from proteins in the MitoCarta2.0 database of known mitochondrial proteins, including 386 mitochondrial neo N termini (Table 2.1). Mitochondria-enriched samples contained 1,829 unique peptides from mitochondrial proteins, corresponding to 95% of all mitochondrial proteins identified by MS-TAILS and preTAILS combined; whole cell lysates identified a further 24 mitochondrial proteins with an additional 56 mitochondrial protein N termini identified (Figure 2.7A). In total, mitochondrial N-terminal peptides were identified a total of 3,631 times; 94% of these identifications originated from the mitochondria-enriched sample, with whole cell lysates contributing ~30% (Figure 2.7B). Thus, our modified mitochondrial enrichment procedure with MS-TAILS markedly increased the identification of mitochondrial proteins and N-terminal peptides.

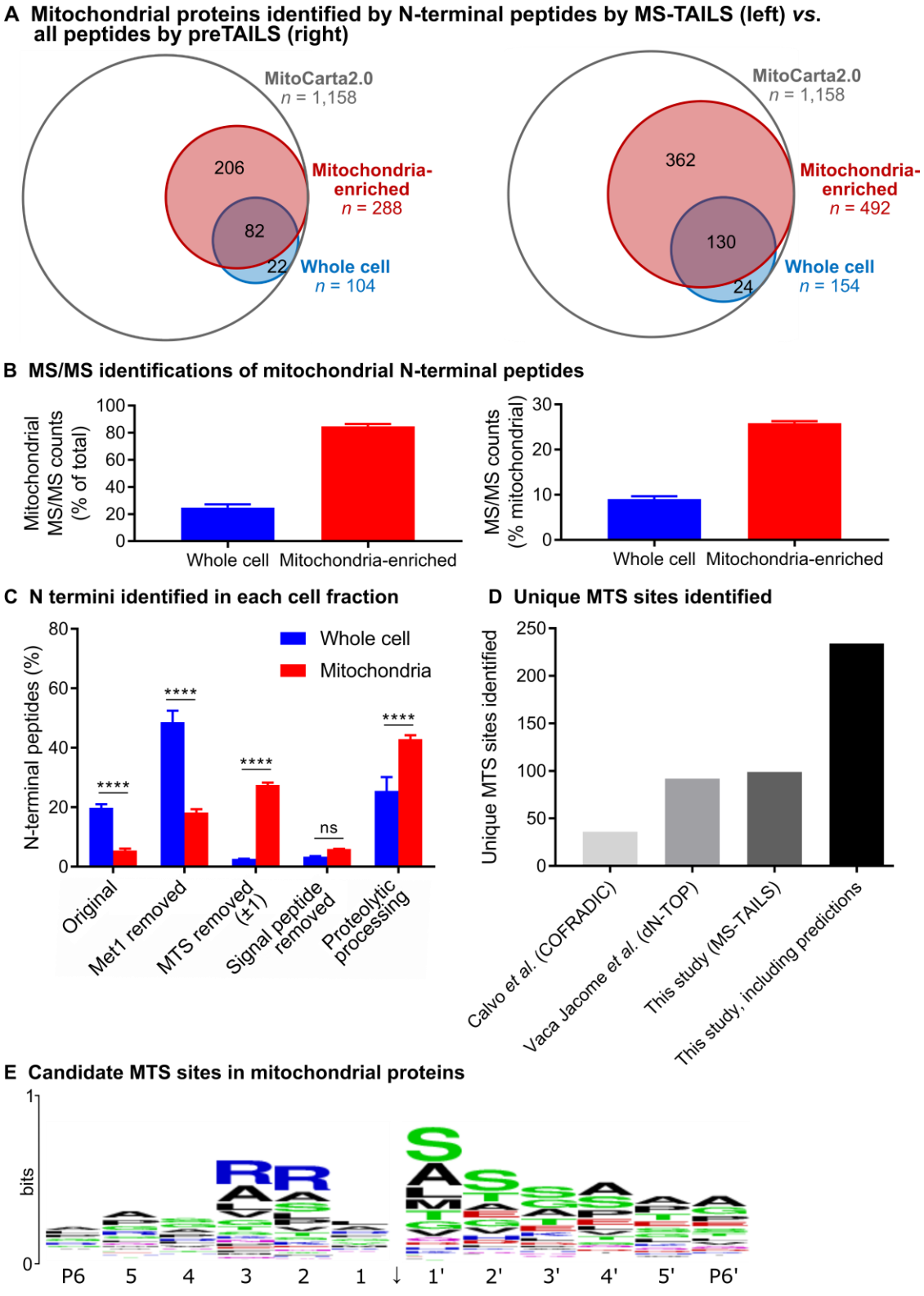

Figure 2.7 MS-TAILS successfully enriched mitochondrial N-terminal peptides. *A*, Coverage of the mitochondrial proteome by N-terminal peptides (left) and all peptides (right) identified by TAILS and

preTAILS. *B,* Proportion of N-terminal peptide MS/MS identifications belonging to mitochondrial proteins from (left) all mitochondrial protein MS/MS counts and (right) all MS/MS counts from each cell fraction. *C,* Types of N-terminal peptides identified in each TAILS cell fraction, including only known mitochondrial proteins from the MitoCarta2.0 database in the 'mitochondria' sample. *D,* Number of unique N-terminal peptides corresponding to MTS sites identified by Calvo *et al.*[182] in mouse tissues and Vaca Jacome *et al.*[179] in human monocytes compared to this study. *E,* Sequence logo of the amino acid sequence surrounding each neo N-terminus in the first 100 amino acids of mitochondrial proteins lacking an annotated mitochondrial targeting sequence[53]. '↓', predicted cleavage site.

2.6 The mitochondrial and whole cell N terminome profiles are unique

We then asked whether the types of N termini identified in the mitochondrial N terminome globally differed from those in the whole cell. An average of 1.4 N-terminal peptides were identified for each protein (Figure 2.5A; Table 2.1) ranging from 1.5 N termini/protein in the mitochondrial N terminome to 1.3 N termini/protein in the whole cell lysates (Table 2.1). These included both mature protein N termini, including the original N-terminal Met at amino acid 1 and termini following removal of the initiator methionine (Met1) creating a mature N terminus at position 2. Neo N termini also arose from proteolytic processing of the pro-peptide, signal peptide, MTS, or deeper within the protein chain.

To precisely annotate each type of N terminus, MS-TAILS N-terminal peptide sequences were compared with protein sequences in UniProt using TopFINDer[215]. As expected, the mitochondrial N terminome contained significantly fewer mature N termini ($p < 0.0001$) with a corresponding significantly higher proportion of N termini corresponding to signal and transit peptide removals ($p < 0.0001$) and other cleavage events ($p < 0.0001$) compared to the whole cell N terminome (Figure 2.7C). As expected from protein import requirements, where an estimated 30-35% of mitochondrial proteins contain an N-terminal MTS that is proteolytically removed during import[220], the mitochondrial N terminome also contained a significantly higher

proportion of N termini from MTS removal than the cellular terminome: a total of 28% of mitochondrial terminal peptides corresponded to MTS removal events.

2.7 Identification of MTS neo N termini and novel mitochondrial proteolytic events

We then sought to use mitochondrial N termini to annotate the sites of MTS removal using MitoCarta2.0 and TopFINDer annotations of the MS-TAILS data. We identified 74 neo N termini at precisely the P1' site of a known MTS removal site in UniProt, 27 within one amino acid of that site, and 24 within five amino acids of the annotated site (Supplemental File 1). Protein termini like this are frequently generated by "ragging" by amino-exopeptidase activity. Of these 125 total N-terminal peptides in 93 proteins, 99.2% (n = 124) were identified in the mitochondria-enriched sample, and 29.6% (n = 37) in the whole cell sample.

To evaluate MS-TAILS performance in annotating MTS sites, we conducted the same analysis on published data from other mitochondrial N terminomics studies. From mouse tissues, N termini were identified at 36 sites within one amino acid of an MTS[182] and at 92 sites from cultured human monocytes[179]. In comparison, MS-TAILS identified more MTS sites (n = 99) and an additional 81 MTS sites that were not previously detected by published N terminomics studies (Figure 2.7D); because mouse and human genes and proteins from different species have different names and different sequences, specific termini and proteins identified in this study could not be directly compared with that from mouse tissues[182]. Furthermore, such low numbers of mouse MTS sites (n = 36) precluded orthologue mapping.

To determine whether MS-TAILS annotated protein targeting signals in mitochondrial proteins

without a yet known MTS, mitochondrial proteins were searched for proteolytic neo N termini within the first 100 amino acids, because these sequences are up to 100 amino acid residues long[53]. By this strategy, we identified an additional 135 unique proteolytic events in 108 mitochondrial proteins within the first 100 amino acids that did not contain an annotated MTS site. Using WebLogos, we identified an enrichment of arginine at P2 and P3 as well as serine at P1' and P2' surrounding each N-terminal event (Figure 2.7E), *i.e.* Arg-Arg-Xxx↓Ser-Ser motif, a characteristic of the mitochondrial processing peptidase[53], thus potentially being novel MTS sites in mitochondrial proteins.

To further examine the neo N termini, we identified 217 cleavage sites in 133 mitochondrial proteins (Supplemental File 1), including 97 corresponding to novel proteolytic events in 67 mitochondrial proteins, 102 observed in published N terminomics studies[215], and 27 cleaved at sites of known proteolysis with a known protease. Hence, MS-TAILS correctly annotated MTS sites and known proteolytic events in mitochondrial proteins and also identified N termini suggestive of novel proteolytic events in mitochondrial proteins. Thus, within the first 100 amino acids, MS-TAILS identified 116 unique proteins from 170 neo N termini.

2.8 Discussion

Mitochondrial proteases play essential roles in mitochondrial processes – including mitochondrial import, fission, and apoptosis[114] – therefore it is important to understand how proteases regulate mitochondrial and cellular processes. However, this is challenging due to the limited tools to quantitatively characterize mitochondrial proteolysis on a proteome-wide scale. Therefore, we developed MS-TAILS and applied it to study mitochondria during early intrinsic

apoptosis. MS-TAILS provides increased sensitivity, enabling excellent coverage across the mitochondrial proteome, which here allowed us to identify novel sites of proteolysis in mitochondrial proteins and more MTS removal sites than any other previous terminomics studies. MS-TAILS enables the simultaneous study of the whole cell and mitochondrial N terminomes and is therefore capable of quantitatively comparing biological conditions, which will allow for greater insights into the mitochondrial and whole cell events during any mitochondrial process.

MS-TAILS increased sensitivity by enriching N-terminal peptides within mitochondria, which enabled excellent coverage across the mitochondrial proteome. When combined with a parallel shotgun proteomics sample, this study identified 45% of the known human mitochondrial proteome. Independently, MS-TAILS N terminomics identified 26% of the known human mitochondrial proteome: 65% more coverage than the only other published human mitochondrial terminomics study[179]. MS-TAILS also identified mitochondrial proteins that were not detected in the whole cell sample and that were not detected by shotgun proteomics of the same mitochondria-enriched samples, highlighting the value of using terminomics approaches when profiling mitochondria in initiatives like the Human Mitochondrial Proteome Project. Notably, MS-TAILS of one epithelial cell line here identified 95% as many mitochondrial proteins as were identified from studies of mitochondria from 14 different tissues[48,182]. The MS-TAILS workflow is less laborious, requires less instrument time, and is modular, where the crude mitochondrial enrichment could be easily replaced by mitochondrial isolation or enrichment of a different cellular compartment. This modularity is an important function when working with different cell types, which require custom protocols for equivalent mitochondrial enrichment, as

Alberio *et al.* recently demonstrated by comparing three mitochondrial enrichment protocols across 10 cell lines[143].

Within the mitochondrial N terminome, MS-TAILS identified 175% more MTS sites than a recent subtiligase-based terminomics study of mitochondria from two mouse tissues[182], 81 sites not previously identified by N terminomics of human mitochondria, and 8% more sites than a study of four parallel experiments on mitochondria from human monocytes[179]. MS-TAILS also identified putative novel MTS sites in mitochondrial proteins with no yet-annotated MTS, with an Arg-Arg-Xxx↓Ser-Ser cleavage motif matching that of the Mitochondrial Processing Peptidase: the mitochondrial protease known to cleave the MTS from mitochondrial proteins upon import[53]. As expected from protein import requirements, where 30-35% of mitochondrial proteins are thought to encode a cleavable N-terminal import signal and the remaining ~70% contain mature protein N termini[220], MTS removal events accounted for 28% of mitochondrial N-terminal peptides and altogether the mitochondrial N terminome contained a significantly higher proportion of N termini from MTS removal ($p < 0.0001$) and significantly fewer mature N termini ($p < 0.0001$) compared to the whole cell N terminome (Fig. 5*A*). In addition, MS-TAILS identified 97 putative novel sites of proteolysis in 67 mitochondrial proteins, demonstrating its suitability to study mitochondrial proteases and identify new functions of cleaved mitochondrial proteins.

By analyzing both the mitochondrial and parent whole cell N terminomes in parallel, MS-TAILS revealed distinct N terminome profiles in each cellular compartment, wherein mitochondria contained more N termini per protein on average and a significantly higher proportion of neo N termini corresponding to MTS removals and other proteolytic events. Monitoring the cellular

terminome depicts how mitochondrial processes impact the entire cell. Simultaneously, the mitochondrial enrichment decreases sample complexity, increasing sensitivity for mitochondrial proteins and peptides.

In conclusion, MS-TAILS is a powerful approach to profile the mitochondrial N terminome and to study both the mitochondrial and cellular N terminomes in parallel to comprehensively study mitochondrial events, processes, and their cell-wide consequences.

Chapter 3: The induction of intrinsic apoptosis alters the mitochondrial and cellular N terminomes

3.1 Summary

Mitochondrial proteases are essential for many vital processes in eukaryotic cells and within mitochondria, including the regulation and execution of intrinsic apoptosis. However, little is known about how the >20 mitochondrial proteases sculpt the mitochondrial proteome to regulate key mitochondrial processes such as intrinsic apoptosis. Here, I examined quantitative changes in proteolysis during the induction of intrinsic apoptosis by enriching mitochondria from untreated and early apoptotic cells then applying our technique to mitochondria and whole parent cells in parallel. Two different inducers of apoptosis (staurosporine and Bax activator molecule 7) altered the mitochondrial N terminome in unique ways. Global analysis of >400 apoptosis-dependent N-terminal peptides implicated specific cellular and mitochondrial pathways affected by each treatment, including mitochondrial protein import, fission, and iron regulation. Seven mitochondrial and 85 cellular amino termini were significantly altered during both apoptotic treatments and may indicate a core set of conserved early apoptotic events, including crucial early steps committing cells to death.

3.2 Introduction

The induction of intrinsic apoptosis is a core mitochondrial role. Intrinsic apoptosis is a dynamic, highly regulated, and broadly conserved process that is essential in cell life and death, human development, and tissue homeostasis[58]. Intrinsic apoptosis is initiated when intracellular danger signals are sensed, cueing outer mitochondrial membrane (OMM) permeabilization, dissipation

of inner mitochondrial membrane potential ($\Delta\Psi_m$), and release of toxic intermembrane space components into the cytoplasm[1]. Whereas the late 'executioner' stages of intrinsic apoptosis following caspase-3 activation are well studied[161,162,188], the early stages of intrinsic apoptosis within mitochondria remain poorly described, particularly the specific, molecular events within mitochondria that regulate the induction of intrinsic apoptosis. Because apoptosis consists of both mitochondria-localized events and cell-wide events, a thorough understanding of this process requires capturing the interaction of both mitochondrial and cellular terminomes. Both mitochondrial and cytoplasmic proteases play a central role in apoptosis, including the caspase protease cascade[110,111]. Therefore, the approach developed in the previous Chapter (MS-TAILS), which can study both mitochondrial and whole cell changes in the N terminome, has the potential to identify how specific proteolytic events in mitochondrial and cellular pathways during early apoptosis trigger the signaling events that lead to the later events of intrinsic apoptosis.

3.3 Methods

3.3.1 Cell culture, SILAC labeling, and mitochondrial enrichments

HeLa cells (CCL-2, American Type Culture Collection, Manassas, Virginia, USA) were cultured in Dulbecco's Modified Eagles Medium (DMEM; HyClone) with 10% (v/v) heat-inactivated fetal bovine serum (Gibco), 1% (v/v) non-essential amino acids (HyClone), and 1% (v/v) GlutaMax (HyClone) and found to be Mycoplasma negative. All experiments were performed between passages 5 – 20. For stable isotope labeling by amino acids in cell culture (SILAC) experiments, HeLa cells were grown in DMEM lacking arginine and lysine (Caisson Labs) and

supplemented with 10% (v/v) heat-inactivated, dialyzed fetal bovine serum (Gibco), 1% GlutaMax (HyClone), 'light' L-lysine (1.0 M ; Sigma-Aldrich), and 0.12 M of either 'light' L-arginine, 'medium' L-[13C6]arginine, or 'heavy' L-[13C6,15N4]arginine (Cambridge Isotope Laboratories). Following six cell doublings in SILAC medium, arginine incorporation was verified as described[210]. For experiments, 2.0 x 10^6 cells were seeded per 150 mm tissue culture dish per condition and repeated for each biological replicate. Experiments were performed at 75% cell confluence.

Following treatments, the SILAC-labeled cells and spent medium were collected from each culture, rinsed and resuspended in cellular isolation buffer containing 10 mM Tris-MOPS, 10 mM EGTA/Tris, and 0.2 M sucrose[211] supplemented with 5 mM EDTA plus EDTA-free HALT Protease Inhibitor Cocktail (Thermo Fisher). Labeled cells were pooled 1:1:1 from the light-, medium-, and heavy-labeled populations according to protein concentration, which was determined using the bicinchoninic acid assay. Pooled cells were pelleted at 600 x g for 10 min at 4 °C and resuspended in 2 mL of ice-cold isolation buffer, then gently homogenized on ice with a pre-chilled glass-Teflon Potter-Elvehjem homogenizer until > 90% cell lysis was achieved. A 1 mg aliquot of cell homogenate protein was snap-frozen in liquid nitrogen for storage before terminomics analysis. For the remaining cell homogenate, intact cells, nuclei, and heavier cell components were pelleted at 600 x *g* for 10 min at 4 °C in microfuge tubes and mitochondria were enriched from the supernatant by five serial centrifugations at 7,000 x *g* for 10 min in 1 mL volumes. Microfuge tubes and 1 mL volumes were used to avoid sample dilution from the use of 50 mL tubes as initially described by Frezza *et al.*[211]. The final pellet was rinsed three times in ice-cold isolation buffer and resuspended in the minimal remaining volume of the

supernatant, snap frozen in liquid nitrogen, and stored at -80 °C until samples were prepared for terminomics analysis.

3.3.2 Induction of intrinsic apoptosis

Prior to inducing apoptosis, HeLa cells were rinsed with phosphate-buffered saline containing calcium and magnesium (HyClone) and synchronized with serum-free DMEM for 24 h. Staurosporine (STS, Sigma-Aldrich) and Bax agonist molecule 7 (BAM7, Calbiochem) were dissolved in DMSO. HeLa cells were treated with 0.2 μM STS for 6 h, 30 μM BAM7 for 24 h, or the DMSO control for 6 or 24 h, all to a final DMSO concentration of 0.6% (v/v).

3.3.3 Inner mitochondrial membrane potential ($\Delta\Psi_m$) assays

The inner mitochondrial membrane potential was measured according to manufacturer's instructions (Cayman Chemical) on a Tecan M200 plate reader. Cells were treated with BAM7, STS, DMSO, or DMEM only, as indicated. J-aggregates/J-monomers ratios were normalized to the average DMSO control for each time point. A Kruskal-Wallis (unpaired, non-parametric) test was used to compare each experimental treatment and its respective control.

3.3.4 SDS-PAGE and western blotting

Cells and enriched mitochondria were lysed and proteins resolved by 15% SDS-PAGE and immunoblotted using anti-caspase-9 (1:1,000, Cell Signaling Technology #9508), anti-caspase-3 (1:500, Cell Signaling Technology #9662), and anti-β-tubulin (1:5,000, Sigma-Aldrich #T4026) antibodies overnight at 4 °C.

3.3.5 Mitochondrial SILAC (MS)-TAILS N terminomics and N terminome analysis

Performed as described in Chapter 2. All apoptosis treatments were tested alongside a vehicle control with the same final concentration and duration. For triplex MS-TAILS experiments, STS and BAM7 treatments were compared with the 6 h DMSO control condition; there were no significant differences in caspase activity or $\Delta\Psi_m$ between 6 h and 24 h of DMSO treatment. MS-TAILS experiments were conducted using $N = 3$ biological replicates to confirm reproducibility of the technique. Alternating SILAC label swaps were performed across the three biological replicates to employ randomization. To compare BAM7 and STS, three treatment conditions were used (24 h BAM7 treatment *vs.* 6 h STS treatment *vs.* 6 h DMSO treatment) and compared in mitochondrial and whole cell fractions across $N = 3$ biological replicates using MS-TAILS. To compare differences across all conditions mitochondrial protein enrichment and the distribution of the various N-terminal peptides *e.g.* original, ± Met1, ± pro-peptide, ± signal peptide, ± MTS, or proteolytic processing were assessed using a two-way ANOVA without matching and with a Šídák correction to account for multiple comparisons.

3.4 Proteomic analysis of BAM7- and STS-induced early intrinsic apoptosis

To identify core mitochondrial apoptotic regulators and events, MS-TAILS was used to study quantitative changes in the mitochondrial N terminome during the early events of intrinsic apoptosis before caspase-3 activation. Cells treated with the intrinsic apoptosis inducers BAM7 or STS displayed significantly decreased $\Delta\Psi_m$ ($p = 0.0203$ and 0.0092, respectively), and cleaved caspase-9 with intact caspase-3 compared with DMSO vehicle control, indicative of early apoptosis (Figure 3.1A-C).

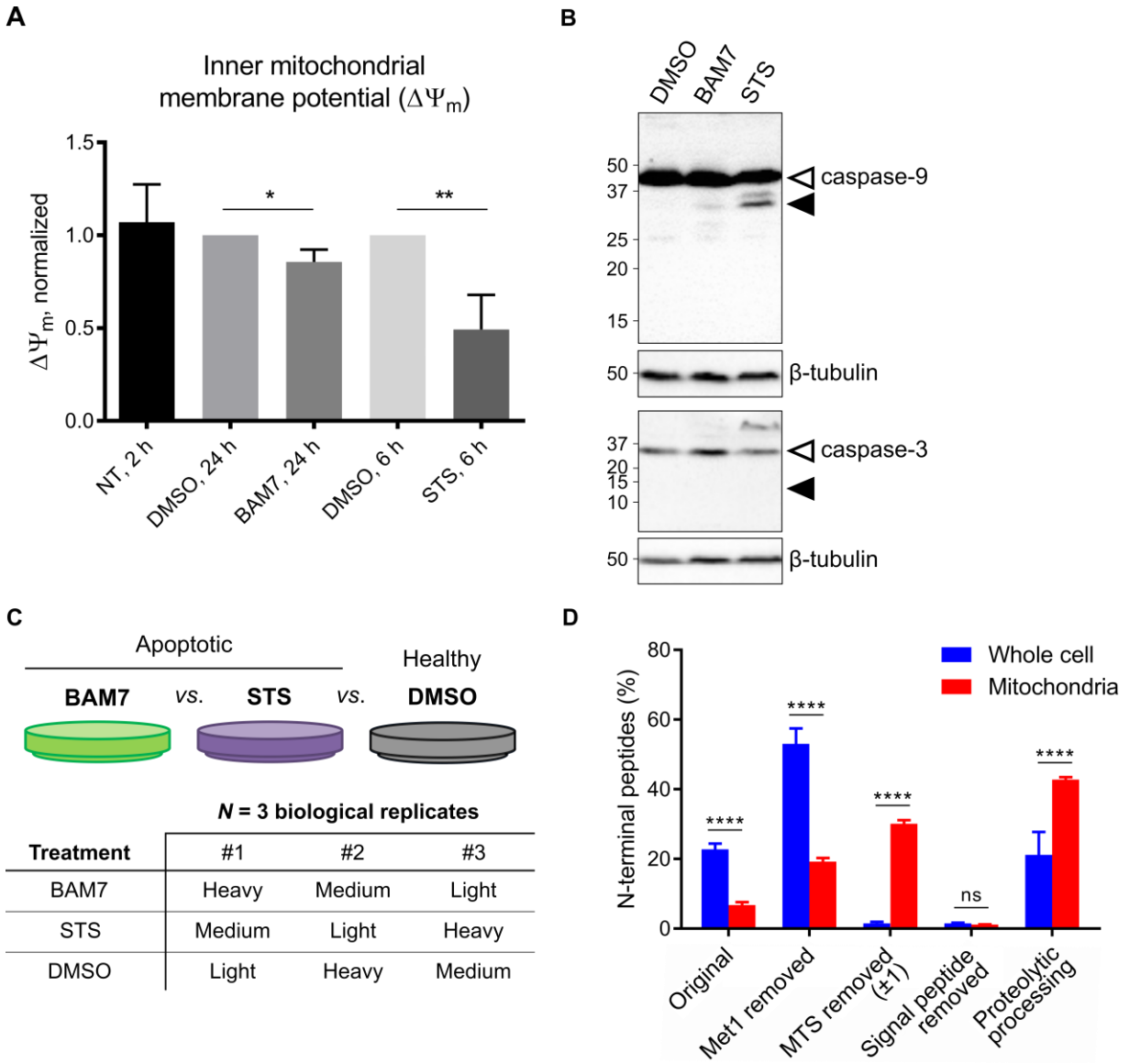

Figure 3.1 Applying MS-TAILS to study BAM7- and STS-induced early apoptosis cleavage events. *A,* Inner mitochondrial membrane potential ($\Delta\Psi_m$) of BAM7- and STS-treated HeLa cells was measured and normalized to the respective vehicle controls, with a non-treated (NT) cell baseline for comparison. The full experimental data from Figure 2.3C is shown here. *B,* Cells were harvested and analyzed by western blot with antibodies against caspases-9 and -3, with β-tubulin as a protein loading control. Expected masses of the full-length zymogen (white arrow) and the cleaved, active forms of each caspase (black arrow) are shown. The full western image from Figure 2.3D is shown here. *C,* Experimental setup of Mitochondrial SILAC (MS)-TAILS experiments to compare apoptotic and untreated cells and mitochondria. HeLa cells were treated with 30 μM BAM7 for 24 h, 0.2 μM STS for 6 h, or an equal volume of the DMSO vehicle control for 24 h. *N* = 3 biological replicates were prepared for all MS-TAILS experiments, wherein isotope-coded arginine label swaps were performed as shown. *D,* Classification of N-termini identified in each MS-TAILS cell fraction.

High-confidence, apoptosis-dependent changes in protein original and neo N termini were

identified by filtering MS-TAILS data for N-terminal peptides having an absolute fold change > 1.5 between either apoptotic treatment *vs.* the vehicle control with a *p*-value of identification < 0.05 (Figure 3.2; Supplemental File 2). N terminome changes were quantified by comparing the relative abundance of SILAC-labeled peptides originating from different treatment conditions, either heavy, medium, or light labeled (Figure 2.3A). Accordingly, the label on each N-terminal peptide and the cell fraction of origin together provide information on treatment-specific changes and how these change in the cell overall or within mitochondria. N-terminal peptides were annotated by the type of N terminus and location within each protein. Like the untreated cells above, neo N termini resulting from MTS removal represented 30% of all N termini identified: a significantly higher proportion than seen in the whole cell N terminome ($p < 0.0001$; Figure 3.1D).

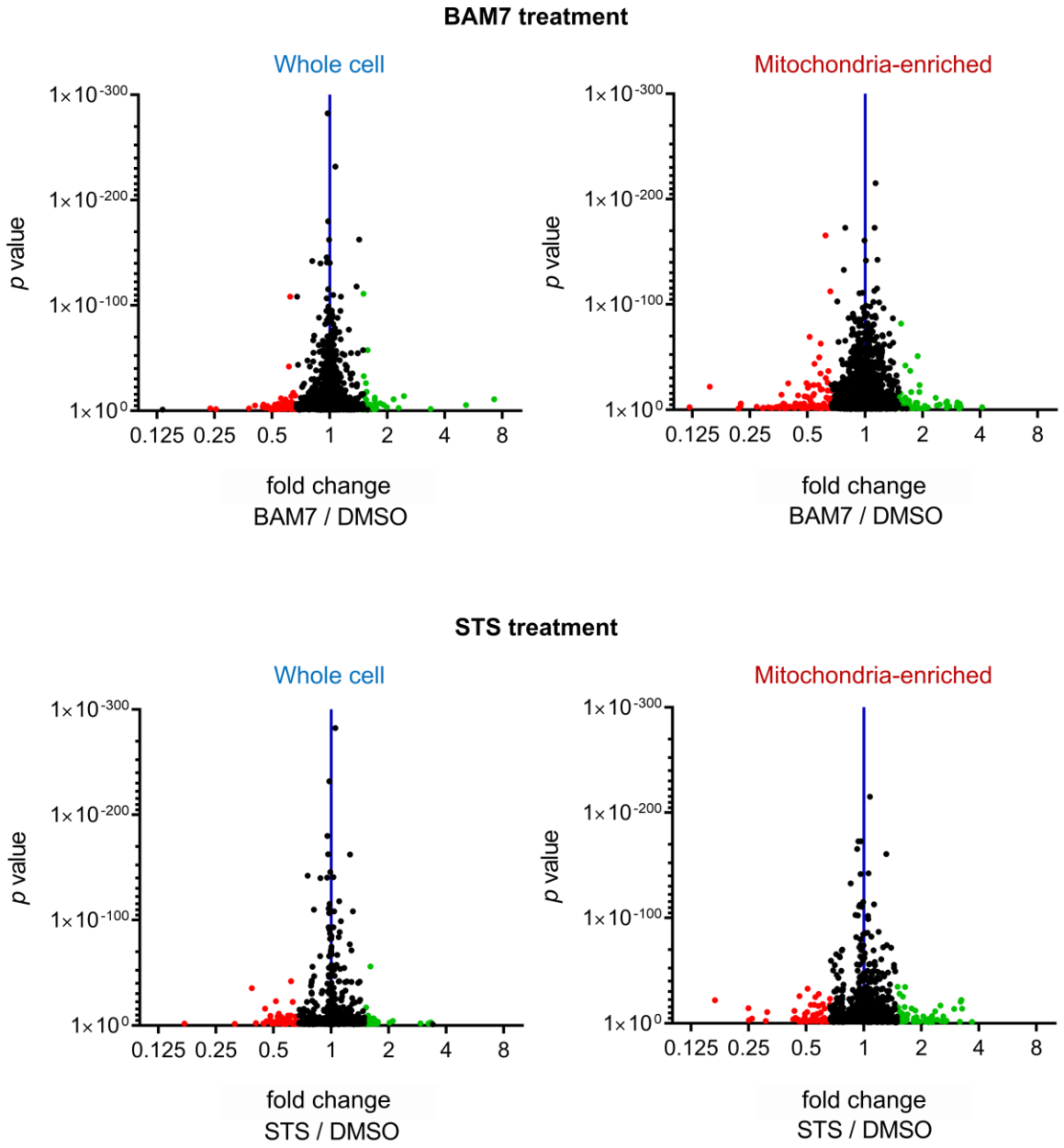

Figure 3.2 MS-TAILS identified quantitative changes in high-confidence N-terminal peptides from mitochondria and whole cells. N-terminal peptides identified by MS-TAILS in BAM7- or STS-treated HeLa cells and mitochondria were assessed as volcano plots depicting the relative abundance of each N-terminal peptide between apoptosis *vs.* control conditions against the posterior error probability (PEP), or *p* value of identification.

To ensure that BAM7 and STS conditions did not yet induce the late stages of apoptosis, I investigated whether late-stage apoptotic markers were evident in BAM7- and STS-treated cells,

such as known proteolytic events from the DegraBase N termini database of apoptotic cells that are largely generated from apoptosis studies that directly initiate apoptosis at late stages (*e.g.* etoposide)[188]. Significantly increased neo N termini from the BAM7 or STS treatments covered 0.3% of the human N termini from the DegraBase (14 in BAM7; 11 in STS), including no mitochondrial N termini, and 18.0% of all significantly increased neo N termini from BAM7 or STS treatments were detected in the DegraBase (n = 23; Figure 3.3). Therefore, neither apoptotic treatment greatly affected known proteolytic events associated with late-stage apoptosis, but probably set the stage for these later cleavage events. Thus, our BAM7 and STS treatment conditions were validated to focus on early apoptotic events.

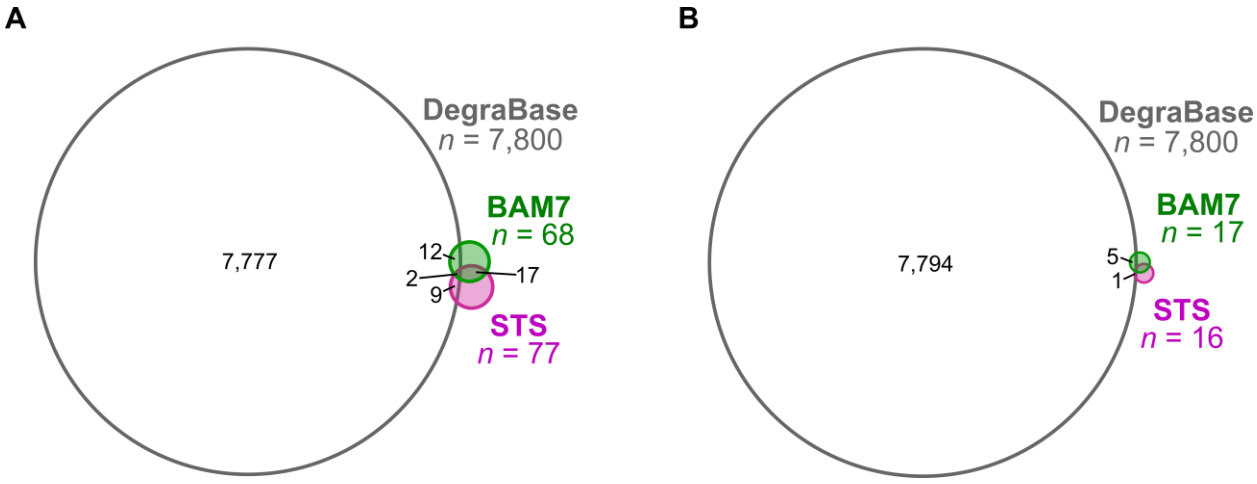

Figure 3.3 Up-regulated neo N termini were not correlated with known events during late-stage apoptosis. Up-regulated neo N termini from BAM7 and STS treatments that were identified in the DegraBase database of apoptosis-associated N-termini from: *A*, the whole cell and *B*, mitochondrial proteins.

3.5 Global changes in the whole cell N terminome during early apoptosis

In mitochondria-enriched samples, MS-TAILS identified 66 apoptosis-dependent N termini from 56 mitochondrial proteins. These proteins were analyzed for enriched mitochondrial processes using DAVID to identify mitochondrial processes altered during early apoptosis, prior to

caspase-3 activation. Both apoptotic conditions were enriched in proteins related to carboxylic acid metabolism and the outer mitochondrial membrane, potential core mitochondrial functions affected during apoptosis induction (Figure 3.4A). Within whole cell fractions, MS-TAILS revealed apoptosis-dependent changes in 471 N termini from 377 proteins. To identify cellular processes altered during early apoptosis by BAM7 and/or STS, proteins with apoptosis-dependent neo N termini were analyzed using DAVID as before. I found that both BAM7-and STS-dependent changes occurred that were enriched for processes affected during apoptosis, cell-cell adhesion and glycolysis (Figure 3.5).

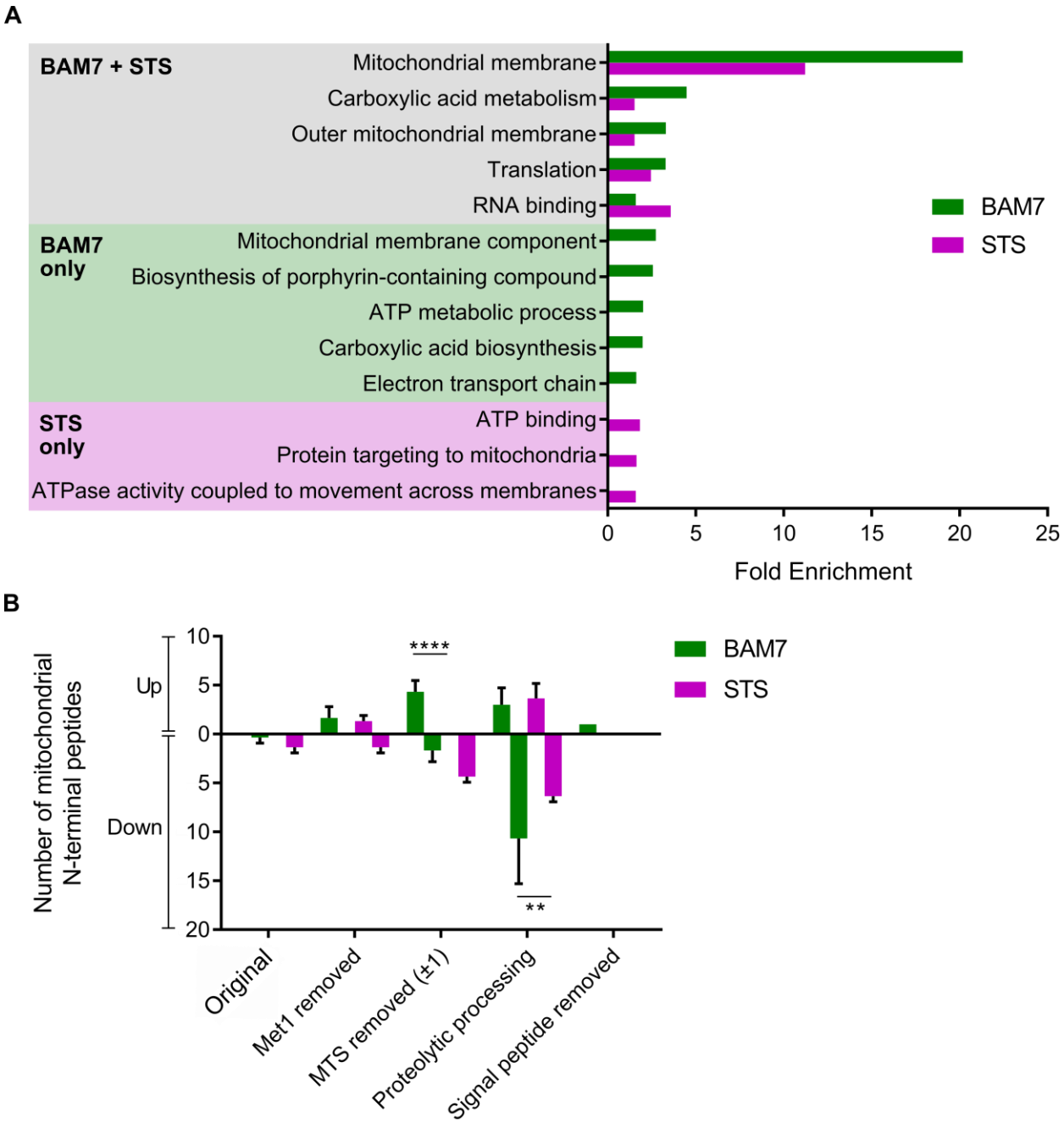

Figure 3.4 BAM7- and STS-induced apoptosis resulted in global changes in the mitochondrial N terminome. *A*, Mitochondrial proteins containing apoptosis-dependent N termini were analyzed using DAVID to identify Functional Annotation Clusters enriched in the mitochondrial N terminome of cells treated with BAM7 (green) or STS (pink). *B*, Mitochondrial N-terminal peptides that were up-regulated (top) during BAM7 and STS treatments were compared with those that were down-regulated (bottom) relative to the shared vehicle control, and displayed according to the type of N terminus. *, $p < 0.05$; ****, $p < 0.0001$.

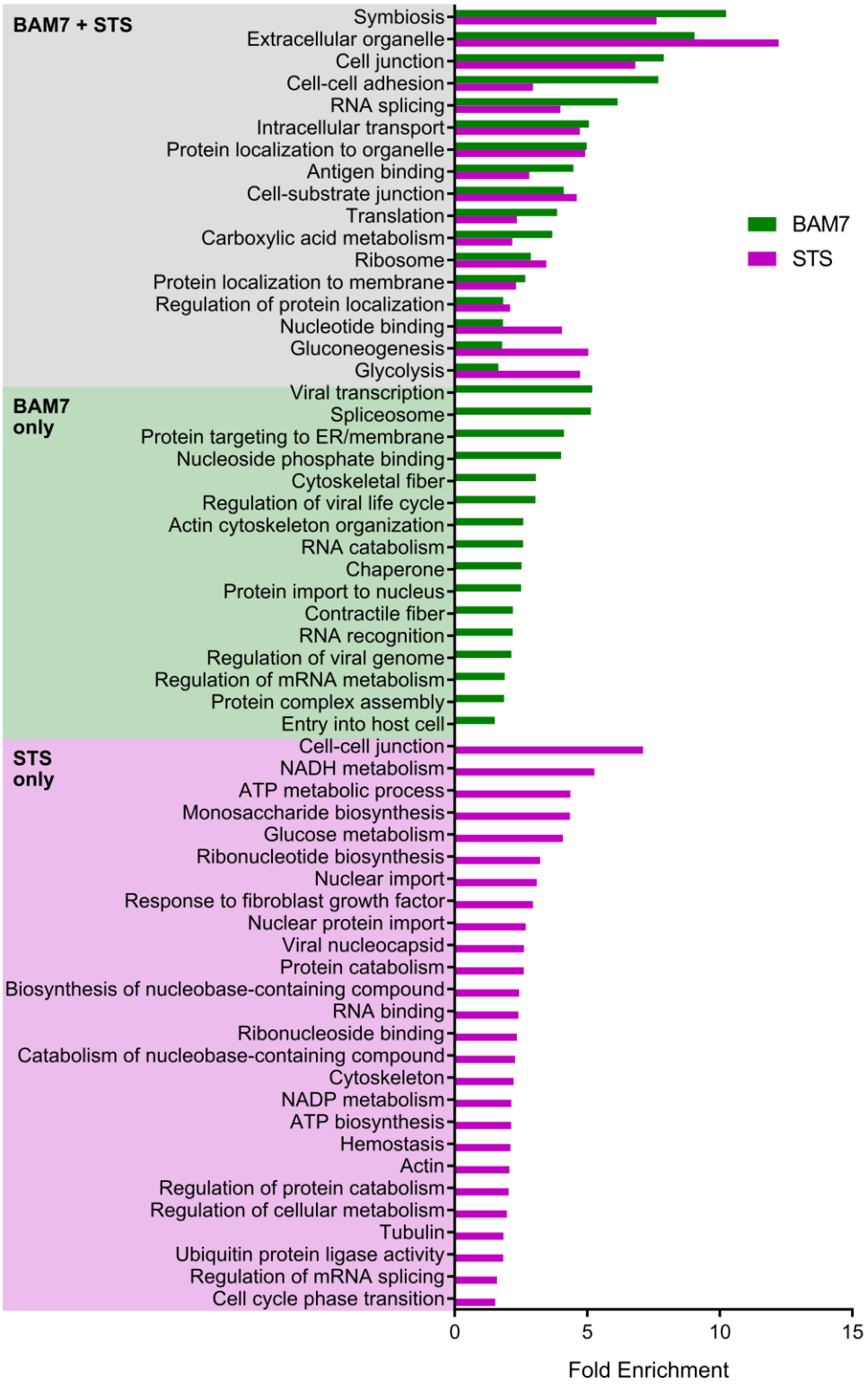

Figure 3.5 BAM7- and STS-induced apoptosis resulted in global changes in the cellular N terminome. Proteins containing apoptosis-dependent N termini in the whole cell sample were analyzed using DAVID to identify Functional Annotation Clusters enriched in the cellular N terminome when treated with BAM7 or STS.

BAM7 and STS treatments also altered unique mitochondrial processes specific to each treatment condition: only BAM7-dependent protein N termini were enriched in porphyrin biosynthesis and the electron transport chain (2.6- and 1.6-fold, respectively), and only STS-dependent protein N termini were enriched for protein targeting to mitochondria (1.6-fold; Figure 3.4A). Similarly, when the number of mitochondrial N termini that were up- or down-regulated by each chemical was calculated, global trends in mitochondrial protein targeting and proteolysis were observed: BAM7-dependent mitochondrial N termini were significantly enriched in MTS removal N termini compared to STS ($p < 0.0001$; Figure 3.4B), suggesting increased mitochondrial import of targeted mitochondrial proteins. Significantly more proteolytic N termini were also observed at decreased abundance during BAM7 treatment compared to DMSO ($p < 0.005$), indicating decreased proteolysis of specific mitochondrial proteins. Thus, MS-TAILS tracked global N-terminomic changes in apoptotic cell populations and identified chemical-specific differences during apoptosis induction.

3.6 BAM7 and STS treatments affected a small core subset of the mitochondrial N terminome

Of the 66 apoptosis-dependent changes within the mitochondrial N terminome, seven were common to both BAM7 and STS treatments (10.6%; Figure 3.6A). Within the entire cell, 85 of 471 apoptosis-dependent changes were significantly altered by both BAM7 and STS (18.0%; Figure 3.6B). Because both BAM7 and STS induce intrinsic apoptosis, this small overlap in mitochondrial and cellular N termini indicates substantial differences in how these chemicals

induce this pathway, thought the extent of this was previously unknown. This small subset of shared BAM7- and STS-dependent N termini is also more likely to contain central events in the induction of apoptosis rather than chemical-specific effects, and therefore may represent core mitochondrial events that regulate or execute early apoptosis. Therefore, I further examined the seven common mitochondrial N termini affected by both BAM7 and STS. Of these, four were up-regulated during both apoptotic treatments, one was down-regulated, and two were differently regulated (Figure 3.6C); none contained caspase cleavage motifs. Notably, these core mitochondrial N termini included increased abundance of a protein involved in mitochondrial protein import, increased proteolysis of two iron homeostasis proteins, differential proteolysis of a mitochondrial fission protein, differential MTS removal of the DNA-directed RNA polymerase (POLRMT), and N termini that predict novel sites of proteolytic processing in mitochondrial proteins (Figure 3.6D; Table 3.1). Because none of these proteins were identified in the preTAILS samples – which identify changes in protein levels – these N termini may either reflect changes in protein abundance or proteolysis. One exception existed, where the abundance of ferritin heavy chain increased 1.37-fold (BAM7/DMSO) in the mitochondrial preTAILS sample, corroborated by a 1.26-fold increase (BAM7/DMSO) in the Met1 removal N-terminal peptide in MS-TAILS. Similarly, multiple neo N termini from endoproteolysis were identified along the mitochondrial fission factor (MFF) protein chain, each with different abundances, suggesting altered relative abundance of these proteolytic events (Table 3.1).

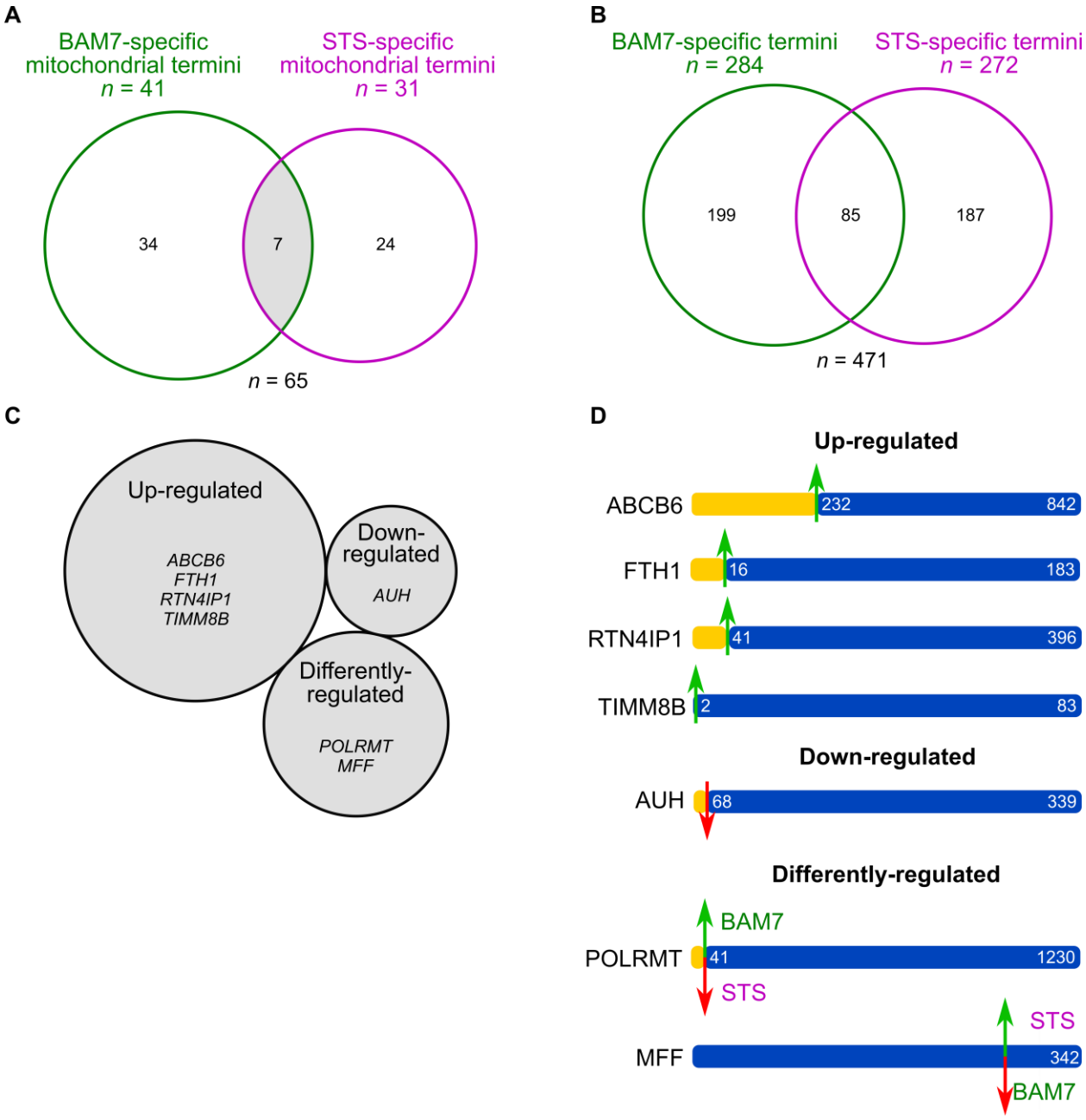

Figure 3.6 BAM7 and STS treatments altered a shared subset of mitochondrial and whole cell N termini, including a core subset of mitochondrial protein N termini. *A,* Mitochondrial N-termini that were significantly altered in enriched mitochondria during BAM7 or STS treatments relative to the vehicle control. *B,* Cellular protein N-termini that were significantly altered during BAM7 or STS treatments relative to the vehicle control. *C,* Mitochondrial proteins containing core N-terminal peptides that were significantly altered during both BAM7 and STS treatments. *D,* Sites of up- and down-regulated N-terminal peptides in mitochondrial proteins during apoptosis, with yellow regions indicating a known MTS. ABCB6, ATP-binding cassette sub-family B member 6, mitochondrial. FTH1, ferritin heavy chain. RTN4IP1, reticulon-4-interacting protein 1, mitochondrial. TIMM8B, mitochondrial import inner membrane translocase subunit Tim8 B. AUH, methylglutaconyl-CoA hydratase, mitochondrial. POLRMT, DNA-directed RNA polymerase, mitochondrial. MFF, mitochondrial fission factor.

Table 3.1 BAM7 and STS treatments affected the same subset of N termini in seven mitochondrial proteins. Mitochondrial proteins containing N-terminal peptides that were significantly altered within the mitochondrial samples from both BAM7- and STS-treated cells. Significantly up- and down-regulated N-terminal peptides are shown at ratios in green and red, respectively, compared with the shared vehicle control. '*' indicates a novel N terminus site.

Gene	Protein name	Type of N terminus	Cleavage site	Fold change	
				BAM7:DMSO	STS:DMSO
ABCB6	ATP-binding cassette sub-family B member 6, mitochondrial	Proteolytic processing	ERSQVR↓S232*	**1.66**	**2.54**
FTH1	Ferritin heavy chain	Met1 removed	M↓T2	1.26	1.45
		Proteolytic processing	RQNYHQ↓D16*	**2.46**	**1.54**
RTN4IP1	Reticulon-4-interacting protein 1, mitochondrial	MTS	TTSPRS↓T41	**1.51**	**1.54**
TIMM8B	Mitochondrial import inner membrane translocase subunit Tim8 B	Met1 removed	M↓A2	**1.84**	**1.66**
AUH	Methylglutaconyl-CoA hydratase, mitochondrial	MTS	APKRGY↓S68	**0.22**	**0.45**
POLRMT	DNA-directed RNA polymerase, mitochondrial	MTS	VCGPRR↓S41	**1.79**	**0.58**
MFF	Mitochondrial fission factor	Proteolytic processing	SRIQYE↓M37*	1.01	1.12
		Proteolytic processing	PLDFLD↓L132	0.78	**3.18**
		Proteolytic processing	HDNVRY↓G273*	**0.43**	**1.68**

3.7 Identification of novel neo N termini in mitochondrial import and fission proteins during early apoptosis

Because both chemicals globally affected MTS removal N termini and STS enriched for protein targeting to mitochondria (Figure 3.4), I examined apoptosis-mediated changes in mitochondrial protein import. Furthermore, a core mitochondrial N terminus was identified in the mitochondrial import inner membrane translocase subunit Tim8 B (Table 3.1), a protein directly involved in the mitochondrial protein import process and whose mature N terminus was detected more with both

apoptosis treatments, suggesting increased import of this protein (Tim8 B does not encode an MTS itself) and a possible effect on import.

To examine how early intrinsic apoptosis affected mitochondrial protein targeting, I queried MS-TAILS data for the specific MTS neo N termini that were altered during BAM7 and STS treatments. I identified 10 BAM7-dependent and six STS-dependent MTS removal N termini within one amino acid from the annotated site (Figure 3.7A). MS-TAILS was also able to identify N termini from both the 'immature' (pre-) and post-MTS removal forms of mitochondrial proteins (Figure 3.7A, inset). Of the MTS neo N termini affected during STS treatment, 83% (n = 5/6) were less abundant in STS compared to the control. For example, the ↓Val36 MTS removal of the mitochondrial intermediate peptidase was observed 2.3-fold less in the STS treatment compared to the control; this peptidase is also involved in mitochondrial protein import. Of BAM7-dependent MTS removal N termini, 70% (n = 7/10) were increased relative to the control, corroborating the global trends in apoptosis-dependent mitochondrial N termini observed previously (Figure 3.4B). For example, during BAM7 treatment, MTS removal at ↓Ser41 in the mitochondrial DNA-directed RNA polymerase was detected 1.7-fold less in mitochondria from BAM7-treated *vs*. untreated cells, whereas the same N-terminal peptide in this protein was detected 1.8-fold more in mitochondria from STS-treated *vs.* untreated cells (Figure 3.7A; Table 3.1). Collectively, MS-TAILS identified quantitative changes in N termini corresponding to MTS removal during early intrinsic apoptosis and generated data to analyze mitochondrial protein import.

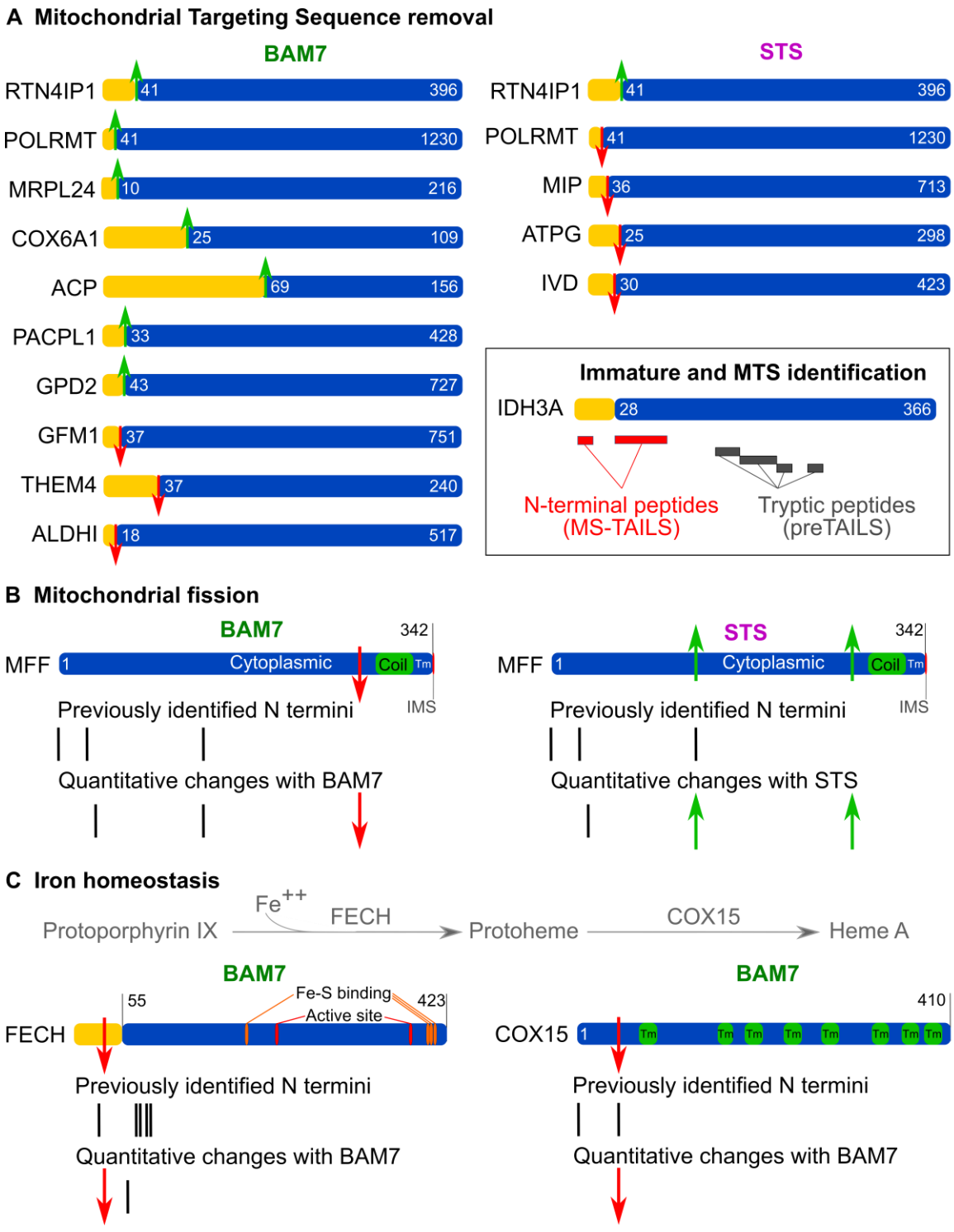

Figure 3.7 Quantitative changes in mitochondrial N-termini during early apoptosis conditions. *A*, Sites of up- and down-regulated mitochondrial targeting sequence (MTS) removals corresponding to N-termini significantly increased or decreased during BAM7 or STS treatments relative to the vehicle control, with yellow regions indicating a known MTS. The inset box displays the mitochondrial isocitrate dehydrogenase [NAD] subunit alpha (IDH3A) and all corresponding peptides identified in this study, namely N-terminal

peptides identified by MS-TAILS (red) and tryptic peptides identified by preTAILS (grey). MS-TAILS N-terminal peptides detect the Met1 removal N terminus and the MTS removal neo N terminus in IDH3A, which are not detected by preTAILS (shotgun) analysis. *B,* Sites of neo N termini identified in the mitochondrial fission factor (MFF) protein during BAM7 and STS treatment. *C,* Sites of neo N-termini identified in proteins identified in mitochondrial iron homeostasis during BAM7 treatment: mitochondrial ferrochelatase (FECH) and the cytochrome *c* oxidase assembly protein COX15. Coil, coiled-coil domain. Tm, transmembrane domain. IMS, mitochondrial intermembrane space. Fe-S, iron-sulfur cluster.

A second core N terminus belonged to the mitochondrial fission factor (MFF), which plays important roles in mitochondrial membrane dynamics and might coordinate the enriched outer membrane processes observed with both chemicals (Figure 3.4A; Table 3.1). MS-TAILS identified several neo N termini in MFF, including three N termini in its cytoplasmic tail at ↓Met37, ↓Leu132, and ↓Gly273 (Figure 3.7B). Two of these neo N termini (↓Met37 and ↓Gly273) have not previously been identified. The N-terminal peptide commencing at ↓Gly273 was observed 2.3-fold less during BAM7 treatment compared to DMSO-treated cells. However, the ↓Gly273 and ↓Leu132 N termini were observed 1.7- and 3.2-fold more during the STS treatment compared to untreated cells. Therefore, MS-TAILS identified different proteolytic profiles in a mitochondrial protein during apoptosis, including potential novel proteolytic events.

3.8 Novel early proteolytic events in mitochondrial pathways during apoptosis

To identify how specific protein termini were involved in other enriched mitochondrial processes, I analyzed MS-TAILS data for N termini related to biosynthesis of porphyrin-containing compounds: a mitochondrial process enriched 2.6-fold in BAM7-dependent N termini (Figure 3.4A). Two core mitochondrial N-terminal peptides play important roles in iron homeostasis (Table 3.1), including porphyrin metabolism, and corroborate the importance of this enriched pathway.

I applied the TAP program (Figure 2.1) – which mines the UniProt database to identify protein function, subcellular location, and GO annotations – to identify proteins with GO annotations related to iron, heme, and porphyrins due to their importance in iron metabolism[221] and the potential involvement of iron in apoptosis[222]. MS-TAILS identified BAM7-dependent neo N termini involved in the biosynthesis of heme A from iron and protoporphyrin IX: mitochondrial ferrochelatase and cytochrome *c* oxidase assembly protein COX15 (Figure 3.7C). Neo N termini in these proteins were decreased 1.8- and 1.6-fold at ↓Ser44 and ↓Lys37, respectively, suggesting decreased proteolysis of these proteins during BAM7 treatment (or increased protein abundance as no mature N termini were identified to quantify changes in overall protein abundance). Both neo N termini are novel in this study and have not previously been identified in the TopFIND or MEROPS databases.

In conclusion, MS-TAILS identified novel protein N termini in mitochondrial proteins, highlighting a potentially uncharacterized early apoptotic signaling pathway.

3.9 Discussion

Mitochondrial proteases play essential roles in mitochondrial processes, including mitochondrial import, fission, and apoptosis[114]. Because mitochondria regulate apoptosis, it is important to understand how proteases regulate mitochondrial and cellular processes during the earliest steps of apoptosis. Because MS-TAILS is the first approach that can simultaneously and quantitatively study the whole cell and mitochondrial N terminomes, this work is the first to quantitatively compare the mitochondrial and cellular terminomes between biological conditions. Here, this allowed for greater insights into the mitochondrial and whole cell events during apoptosis before

caspase-3 activation, importantly identifying seven core mitochondrial events that occur during early apoptosis with two different chemical inducers. Recently, Scott *et al.* identified caspase-independent shifts in mitochondrial membrane interactomes[171], demonstrating the importance of looking beyond caspases to identify important changes within mitochondria during apoptosis. Here, MS-TAILS successfully identified novel mitochondrial neo N termini from proteolytic events that may be important to understand the full complexity of the earliest events in intrinsic apoptosis, prior to caspase-3 activation and rampant cell-wide proteolysis.

MS-TAILS terminome coverage provided biologically meaningful data by comparing the global changes in cells and mitochondria from multiple conditions. Unlike previous terminomics applications to study mitochondria, MS-TAILS provides quantitative and therefore comparative data between up to three conditions of interest. MS-TAILS identified 66 mitochondrial N termini that were significantly altered during apoptosis, 11% of which were significantly changed during both BAM7 and STS treatments compared to an untreated control (Figure 3.6). This common subset of seven mitochondrial N termini may indicate a core set of conserved early apoptotic events, including crucial steps committing cells to death. When investigated further, these seven core N termini and supporting MS-TAILS data provide insight into mitochondrial pathways affected during the induction of intrinsic apoptosis, including mitochondrial protein import, which typically decreases during cell stress[51]. These core N termini may indicate very early regulatory events that occur within mitochondria and propel cells toward committed cell death or are an attempt to rescue viability during stress.

Overall, few N terminome changes were common to both apoptosis inducers (11% in mitochondria; 18% in the whole cell), perhaps indicating either discrepancies between the early

cytoplasmic effects of these chemicals, chemical-specific events (such as the nonspecific consequences of STS-mediated kinase activation), or a 'calm before the storm' of caspase-3-mediated late-stage apoptosis. From the remaining 89% of mitochondrial events, MS-TAILS identified chemical-specific trends across the mitochondrial N terminome indicative of differential protein import, fission, and iron homeostasis. These included differential proteolysis of core mitochondrial N termini, such as MTS removal in the mitochondrial RNA polymerase POLRMT and proteolytic processing of MFF (Figure 3.7). If a non-quantitative technique had been used, these differences would not have been detectable, highlighting the value of the quantitative capability of MS-TAILS.

In this study, I observed different proteolytic profiles in the cytoplasmic tail of MFF during early apoptosis; BAM7 decreased proteolysis and STS increased proteolysis at two sites, including a novel site at ↓Gly273 under both conditions, corresponding to the membrane-adjacent end of the cytoplasmic tail (Figure 3.7B). MFF is an outer mitochondrial membrane protein and its long cytoplasmic tail is required for its association with dynamin-related protein 1 (Drp1). MFF co-localizes with Drp1 at fission sites[223] and is required for optimal association of Drp1 at the outer mitochondrial membrane and for mitochondrial fission[224]. The specific roles of MFF in Drp1-mediated fission are unclear[225], although fission does occur during intrinsic apoptosis, following $\Delta\Psi_m$ depolarization[226]; during STS treatment, Drp1 is dephosphorylated[227], resulting in Drp1 localization to the outer mitochondrial membrane[228] and increased mitochondrial fission[227]. Increased proteolysis at ↓Gly273 – as seen during STS treatment – would cause 84% of this domain to be shed into the cytoplasm, possibly preventing Drp1 association and inhibiting mitochondrial fission; decreased proteolysis – as seen during BAM7 treatment – may protect

fission. This further depends on the fraction of MFF protein that is proteolytically processed in this way. BAM7 directly activates Bax to induce apoptosis at the outer mitochondrial membrane, and Bax may itself be involved in mitochondrial fission[223,229], suggesting that MFF with its cytoplasmic tail may be involved in Bax-dependent fission. Together, this differential proteolytic event in a core mitochondrial protein may help uncover the elusive connection between mitochondrial fission processes and apoptosis.

Mitochondria from BAM7-treated cells were also enriched (2.6-fold) in proteins involved in the biosynthesis of porphyrin-containing compounds, such as iron-containing compounds, *e.g.* heme. Mitochondria are central regulators of iron metabolism, including heme and iron-sulfur clusters[221], iron itself may be involved in apoptosis[222]. MS-TAILS identified novel neo N termini in two proteins involved in heme biosynthesis: mitochondrial ferrochelatase (which catalyzes iron insertion into protoporphyrin IX to form protoheme) and COX15 (which is involved in the conversion of protoheme to heme A[230]; Figure 3.7C). This suggests that proteolytic processing plays a key role in regulating heme A biosynthesis during early apoptosis following BAM7 treatment.

Collectively, MS-TAILS is a powerful approach to study both the mitochondrial and cellular N terminomes in parallel to comprehensively study mitochondrial events and processes as well as their cell-wide consequences. This information is vital to understand not only diseases in which mitochondrial dysfunction plays a crucial role – such as cancer and drug-mediated toxicity – but also infectious diseases such as enterohemorrhagic and enteropathogenic *Escherichia coli*, where mitochondrial manipulation of apoptosis is vital to infection.

Chapter 4: EPEC type III secretion system-secreted effectors alter the mitochondrial and cellular N terminomes of infected human cells

4.1 Summary

Mitochondria control the induction of intrinsic apoptosis and therefore are frequent targets of invading pathogens. Enteropathogenic *E.coli* (EPEC) uses a type III secretion system (T3SS) to inject its effectors into human cells, target mitochondria, and modulate host apoptosis, among many cellular processes. However, the mechanisms by which EPEC T3SS effectors control apoptosis from within mitochondria are unknown. In this Chapter, MS-TAILS is applied to study the effects of early-stage EPEC infection and the presence of T3SS effectors on the human mitochondrial N terminome and is the first terminomics study of microbial infection. EPEC infection altered N termini in 31 mitochondrial proteins, and T3SS effectors altered N termini in 17 mitochondrial proteins, including 15 previously unknown mitochondrial proteolytic events in voltage-dependent anion-selective channel protein 1, mtHsp60, and other proteins with known roles in apoptosis. In addition, 89% of mitochondrial N terminome changes during EPEC infection and T3SS effectors were not observed during the canonical induction of intrinsic apoptosis, and 60% have not been observed in any apoptosis terminomics experiment to date. Therefore, this study suggests that the majority of EPEC-mediated mitochondrial changes correspond to infection- or T3SS effector-dependent mechanisms of apoptosis: a non-canonical, infection-specific mitochondrial apoptotic pathway that occurs through different means than the canonical apoptotic pathway.

4.2 Introduction

Apoptosis is an important function to clear damaged cells and prevent further damage to nearby cells. Intrinsic apoptosis is regulated by mitochondria, which decide the fate of their host cell. Accordingly, several human pathogens target mitochondria to manipulate host cell death during infection. EPEC accomplishes this by encoding several T3SS-secreted effectors that localize to host mitochondria and affect the induction of intrinsic apoptosis (*e.g.* $\Delta\Psi_m$, cytochrome *c* release, and caspase-9 and -3/-7 activation), namely EspF and EspZ. EspF and EspZ are essential for bacterial colonization[94–96,231], though their mechanisms are unclear. EspF promotes the induction of intrinsic apoptosis[94] and its mitochondrial localization has profound implications on the course of disease: mice infected with *C. rodentium* mutants where EspF is intact but unable to target mitochondria display reduced *C. rodentium* colonization, reduced intestinal inflammation, reduced host cell death, and increased rates of survival[95]. In contrast, EspZ protects the host cell, localizing to mitochondria, where it interacts with the inner mitochondrial membrane protein import complex and stabilizes $\Delta\Psi_m$, thereby delaying apoptosis[96]. Exogenous EspZ also protects human intestinal epithelial cells from staurosporine-mediated apoptosis[97].

Although these effectors have clear and contrasting roles in apoptosis during infection, it is unknown how they induce or delay apoptosis, respectively, and no study to date has examined the possible interplay between these mitochondria-localized T3SS effectors. Such a study would require mitochondrial techniques able to provide unbiased results with enough depth to generate testable hypotheses on how EPEC alters mitochondrial function.

Previously, mitochondrial N terminomics has enabled great insights into the mitochondrial proteome and how import and proteolysis sculpt the mitochondrial proteome, providing insights

into mitochondrial protein functions. In Chapter 2, I developed MS-TAILS: a novel mitochondrial N terminomics technique that comprehensively profiles changes in the mitochondrial and cellular terminomes between conditions. In Chapter 3, I demonstrated the value of this technique in studying quantitative changes between apoptotic and untreated mitochondria. In Chapter 4, I will apply MS-TAILS to characterize EPEC- and T3SS-mediated changes across the human mitochondrial N terminome to identify mitochondrial events that are uniquely mediated by EPEC infection and the T3SS. Studying how EPEC infection alters the mitochondrial N terminome may provide molecular-level insights into the mechanisms by which T3SS effectors control human cell death.

4.3 Methods

4.3.1 Cell culture and SILAC labeling

Cell culture and SILAC labeling were performed as described in Chapter 2.

4.3.2 Infection of cultured cells

HeLa cells were seeded into 15 cm tissue culture plates and allowed to grow to ~70% confluence. Two hours prior to infection, HeLa cells were rinsed twice with phosphate-buffered saline with calcium and magnesium (HyClone) and the culture medium was replaced with serum-free DMEM. Wild-type EPEC O127:H6 E2348/69 and EPEC *espZ* deletion mutant colonies were picked from freshly streaked plates and overnight cultures were prepared in lysogeny broth the day before infection. T3SS effector secretion was pre-induced by sub-culturing the overnight culture 1:20 in DMEM without phenol red (G.E.) and incubated at 37°C in 5% CO_2 for 3.5 h, and HeLa cells were synchronized in serum-free DMEM for 3 h. OD_{600} was

used to calculate the volume of culture needed to obtain sufficient bacteria to achieve a multiplicity of infection (MOI) of 20, *i.e.* an average of 20 bacteria per human cell. Pre-induced bacteria were added to 15 mL of serum-free DMEM and HeLa cell medium was replaced with inoculated culture medium; HeLa cells were infected for the indicated time points once cells reached 75% confluence.

4.3.3 Lactate dehydrogenase (LDH) assay

Extracellular lactate dehydrogenase activity was measured using the CytoTox 96 Non-Radioactive Cytotoxicity Assay kit (Promega). The day before, 1.5 x 10^5 HeLa cells were seeded in 500 µL DMEM per well in a 24-well plate. Cells were infected or left uninfected. Forty-five minutes prior to the end of infection time points, 50 µL of 10X lysis buffer was added to separate lysis positive control and volume control wells. At the end of infection time points, plates were spun at 250 x *g* for 4 min and 150 µL of each cell supernatant was harvested and transferred into a 96-well plate. Samples were centrifuged at 1,800 rpm for 10 min and 50 µL of supernatant was transferred to a new plate. An equal volume of reconstituted Substrate Mix was added to each supernatant and incubated in the dark for 30 min. Stop Solution (50 µL) was added to each well and absorbance at 490 nm was read immediately.

4.3.4 Cell harvesting and mitochondrial enrichments

Performed as described in Chapter 2. Prior to trypsin detachment, HeLa cells were gently rinsed with ice-cold phosphate-buffered-saline without calcium and magnesium (HyClone) three times to wash away non-adherent bacteria.

4.3.5 SDS-PAGE and western blotting

Performed as described in Chapter 2. Membranes were immunoblotted overnight at 4 °C using anti-herpes simplex virus (HSV) epitope tag (1:1,000, Abcam), anti-hemagglutinin (1:1,000, Roche), anti-ACAA2 (1:1,000, Abcam), anti-COX6C (1:1,000, Abcam), anti-DNAJA3 (1:500, Abcam), or anti-endonuclease G (1:500, Abcam) primary antibodies overnight at 4 °C.

4.3.6 Mitochondrial SILAC (MS)-TAILS N terminomics and N terminome analysis

Performed as described in Chapter 2 on an Orbitrap Velos tandem mass spectrometer. Enrichment of Biological Processes was conducted using DAVID v. 6.8 (https://david.ncifcrf.gov)[217,218], comparing the query dataset with all proteins identified using MS-TAILS, or with all mitochondrial proteins, as appropriate. Refinement and visualization of enriched processes were conducted using REVIGO[232].

4.3.7 Transfection/knockdown

HeLa cells were transfected using Lipofectamine 3000 (Thermo) and assayed 72 h later. Targeted gene knockdowns were performed with the MISSION shRNA library (Sigma), including a transfection control expressing *turboGFP* and a knockdown control expressing *turboGFP* and the corresponding shRNA for each control (SHC001-4), *ACAA2* (TRCN0000036098), *COX6C* (TRCN0000046297), *DNAJA3* (TRCN0000008775), and *ENDOG* (TRCN0000010330). Transfection and knockdown efficiency was determined using flow cytometry. Knockdown efficiency for individual target genes was determined using western blotting of cell lysates post-transfection.

4.4 T3SS effectors localize to human mitochondria before the induction of cell death

To analyze how EPEC T3SS effectors affect mitochondria during early apoptosis, EPEC infection conditions were first optimized to capture the T3SS-mediated events of early apoptosis, before late-stage cell death characterized by caspase activation and cell membrane permeability. Permeable cell membranes allow the leakage of cytoplasmic contents into the extracellular environment and, therefore, can be assessed by measuring the extracellular activity of the cytoplasmic enzyme lactate dehydrogenase (LDH). Human epithelial cells were infected with wild-type EPEC or a Δ*escN* mutant for up to three hours post-infection (h.p.i.). EPEC Δ*escN* lacks the EscN ATPase that powers type III secretion and therefore can neither secrete T3SS effectors nor translocate them into host cells. Extracellular LDH activity was consistently higher during infection with EPEC wild-type compared to the Δ*escN* strain, as expected. After 2 h of wild-type infection, extracellular LDH activity increased from 1.30% at 2 h.p.i. to 30.98% at 3 h.p.i.; extracellular LDH activity also significantly increased from 2 to 3 h.p.i. during EPEC Δ*escN* infection (Figure 4.1). Therefore, to avoid confounding results of late-stage cell death, all future experiments used infection time points before 3 h.p.i.

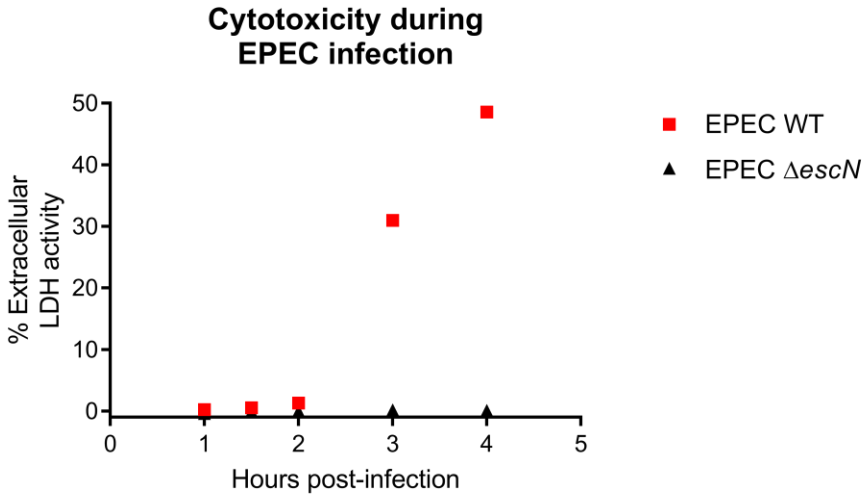

Figure 4.1 EPEC significantly increases HeLa cell membrane permeability throughout infection. HeLa cells were infected with EPEC wild-type or the EPEC Δ*escN* strain unable to secrete T3SS effectors, each at an MOI 20 and extracellular lactate dehydrogenase (LDH) activity was measured to represent membrane permeability during cell death. Data is reported as the mean percent of extracellular LDH activity relative to uninfected (0%) and detergent lysed (100%) HeLa cells from $N = 3$ biological replicates.

To confirm the occurrence of characteristic T3SS-mediated processes, epithelial cells were infected at an MOI of 20 for 1.5 h.p.i. with an EPEC strain expressing Green Fluorescent Protein (GFP) and stained for actin by immunofluorescence. Infected cells displayed actin-dense regions that co-localized with adhered bacteria, which was expected and is typical of the characteristic pedestals formed by A/E pathogens and mediated by the T3SS effector Tir[73] (Figure 4.2). Therefore, EPEC T3SS-mediated processes were underway by 1.5 h.p.i.

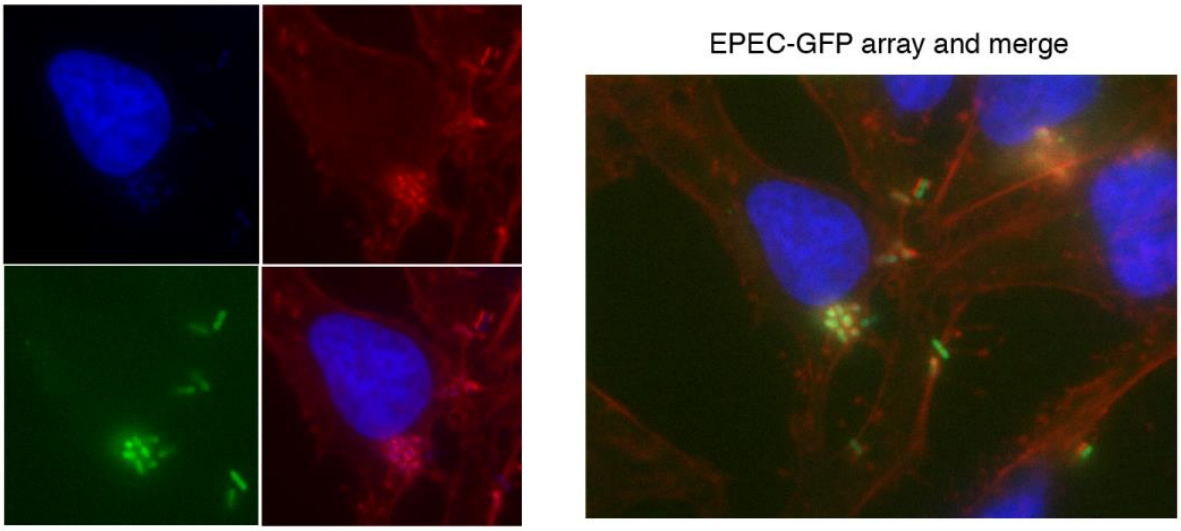

Figure 4.2 EPEC infection results in characteristic T3SS-mediated processes. HeLa cells were infected with EPEC-GFP at an MOI of 20 for 1.5 h.p.i. Cells were rinsed and immunofluorescence microscopy for actin (red) was performed on infected cells to identify actin clustering beneath infecting bacteria, as is typical of pedestal formation, a pathognomonic sign of EPEC infection that is mediated by the T3SS. Red: antibody-conjugated phalloidin binding actin; Blue: DAPI binding DNA; Green: Green Fluorescent Protein (GFP) expressed by EPEC-GFP.

To confirm whether EPEC T3SS effectors localized to mitochondria under these conditions, epithelial cells were infected with EPEC strains encoding epitope-tagged T3SS effectors that traffic to host mitochondria: EspZ and EspF (MOI 20, 2 h.p.i.). Mitochondria were enriched from infected cells (Figure 4.3A) and analyzed by western blot to detect epitope tags on each mitochondria-targeting effector. Western blot analysis showed each tagged effector within the mitochondrial sample at the expected mass (Figure 4.3B); for EspF, which encodes an N-terminal MTS and a C-terminal epitope tag, bands corresponding to both the mature and the MTS-cleaved mass were observed, suggesting successful import of epitope-tagged EspF into mitochondria.

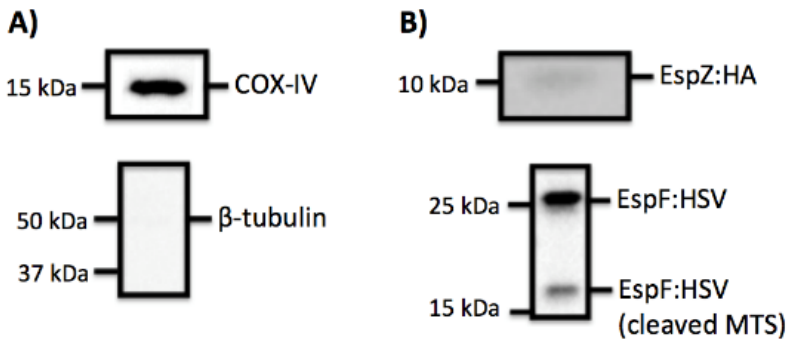

Figure 4.3 EspZ and EspF are detected within enriched human mitochondria during EPEC infection. HeLa cells were infected with EPEC containing C-terminally tagged T3SS effectors that localize to mitochondria (EspZ:HA; EspF:HSV) and mitochondria were enriched from infected cells. *A,* Mitochondria-enriched cell fractions were analyzed by western blotting using antibodies specific to the proteins as indicated following 12% SDS-PAGE. Mitochondria-enriched samples demonstrated high abundance of the mitochondrial marker (cytochrome *c* oxidase subunit IV, COX-IV) and low abundance of the cytoplasmic marker (β-tubulin). *B,* To detect EspZ:HA and EspF:HSV in mitochondrial samples, α-hemagglutinin (HA) and α-HSV primary antibodies were used. EspF:HSV was detected with its N-terminal mitochondrial targeting sequence non-cleaved and cleaved, indicating mitochondrial import into the matrix.

Because T3SS-mediated cellular processes had already occurred, mitochondria-targeted effectors were identified within enriched mitochondria, and LDH activity was <5% under these conditions, an MOI of 20 for 2 h.p.i. was used for all future experiments.

4.5 The human mitochondrial N terminome is altered upon EPEC infection

To identify how EPEC and its T3SS effectors alter the human mitochondrial and cellular N terminomes, two complementary MS-TAILS experiments were conducted: one comparing wild-type infection *vs.* no infection (to identify global consequences of EPEC infection, including both T3SS and non-T3SS effects) and another comparing wild-type *vs.* Δ*esc*N infection (to identify global consequences of T3SS effectors; Figure 4.4). MS-TAILS identified 1,150 proteins, including 228 mitochondrial proteins, and 1,363 unique N-terminal peptides, including 325 from mitochondrial proteins (Figure 4.4; Table 4.1; Supplemental File 3). As described in

Chapters 2 and 3, high-confidence, infection-dependent changes in protein mature and neo N termini were identified by filtering MS-TAILS data for N-terminal peptides with an absolute fold change > 1.5 between wild-type infection and uninfected cells or EPEC Δ*escN* infection with a *p*-value of identification < 0.05. In total, 223 N-terminal peptides were significantly affected during infection or T3SS effectors within cells or mitochondria (Figure 4.5).

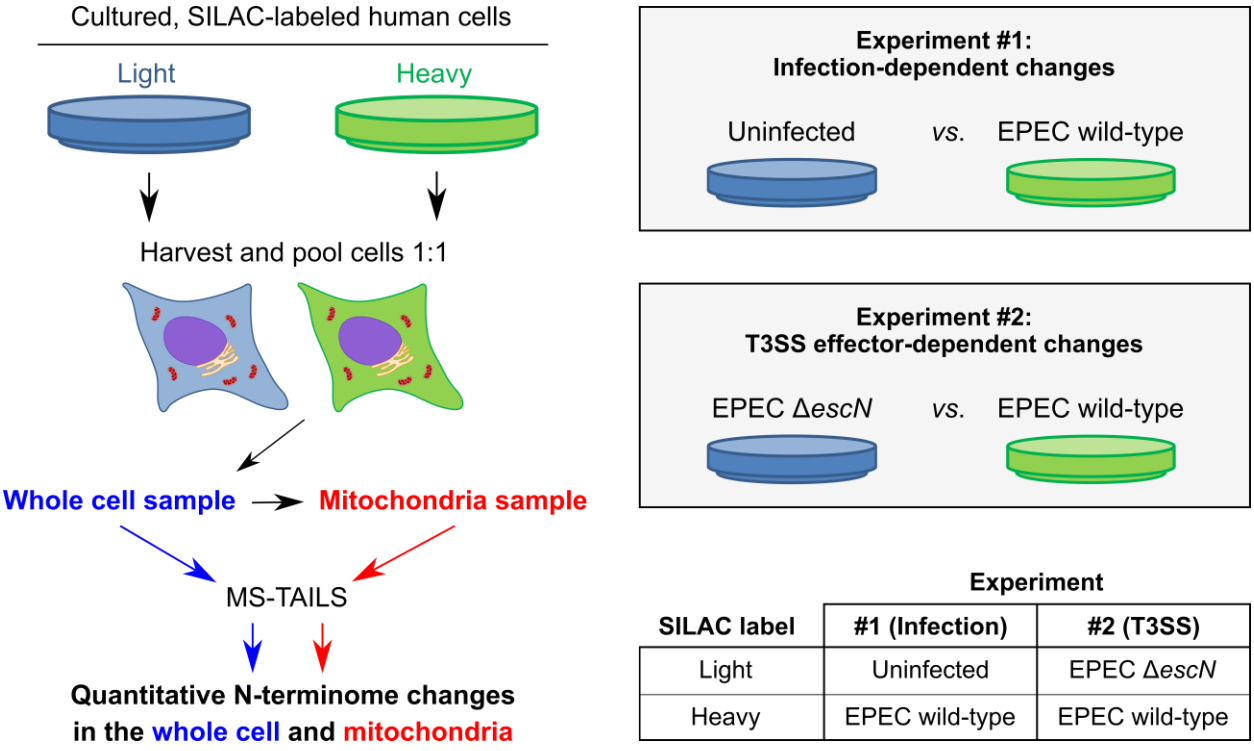

	Experiment	
SILAC label	**#1 (Infection)**	**#2 (T3SS)**
Light	Uninfected	EPEC Δ*escN*
Heavy	EPEC wild-type	EPEC wild-type

Figure 4.4 EPEC MS-TAILS experimental layout.
Isotope-labeled HeLa cells were prepared using SILAC. Cells were treated, pooled 1:1, and homogenized. Whole cell protein and enriched mitochondrial protein (1 mg each) were analyzed in parallel using MS-TAILS, MaxQuant, TAP, Center•Point, and TopFINDer as described in Figure 2.3. Two complementary experiments were performed to distinguish between infection- and T3SS effector-dependent changes in mitochondrial and cellular N terminomes. To distinguish between N terminomes of uninfected, EPEC wild-type, and EPEC Δ*escN* infected mitochondria and cells, SILAC labeling was applied between $N = 3$ biological replicates for each experiment.

Table 4.1 Summary of MS-TAILS mass spectrometry data. The number of unique proteins, peptides, and N-terminal peptides identified from $N = 3$ biological replicates of MS-TAILS of mitochondria and whole cells during both separate EPEC infection experiments.

	Total	**Mitochondria**	**Whole cell**
Unique proteins	1,150	536	821
Unique peptides	2,138	966	1,250
Unique N-terminal peptides	1,363	1,159	1,178
Proteins identified by N-terminal peptides	955	416	650
Unique peptides from mitochondrial proteins	508	387	135
Unique mitochondrial proteins	228	183	97
Coverage of the mitochondrial proteome	19.7%	15.8%	8.4%
Unique mitochondrial proteins from N-terminal peptides	194	153	74
Unique N-terminal peptides from mitochondrial proteins	325	250	84

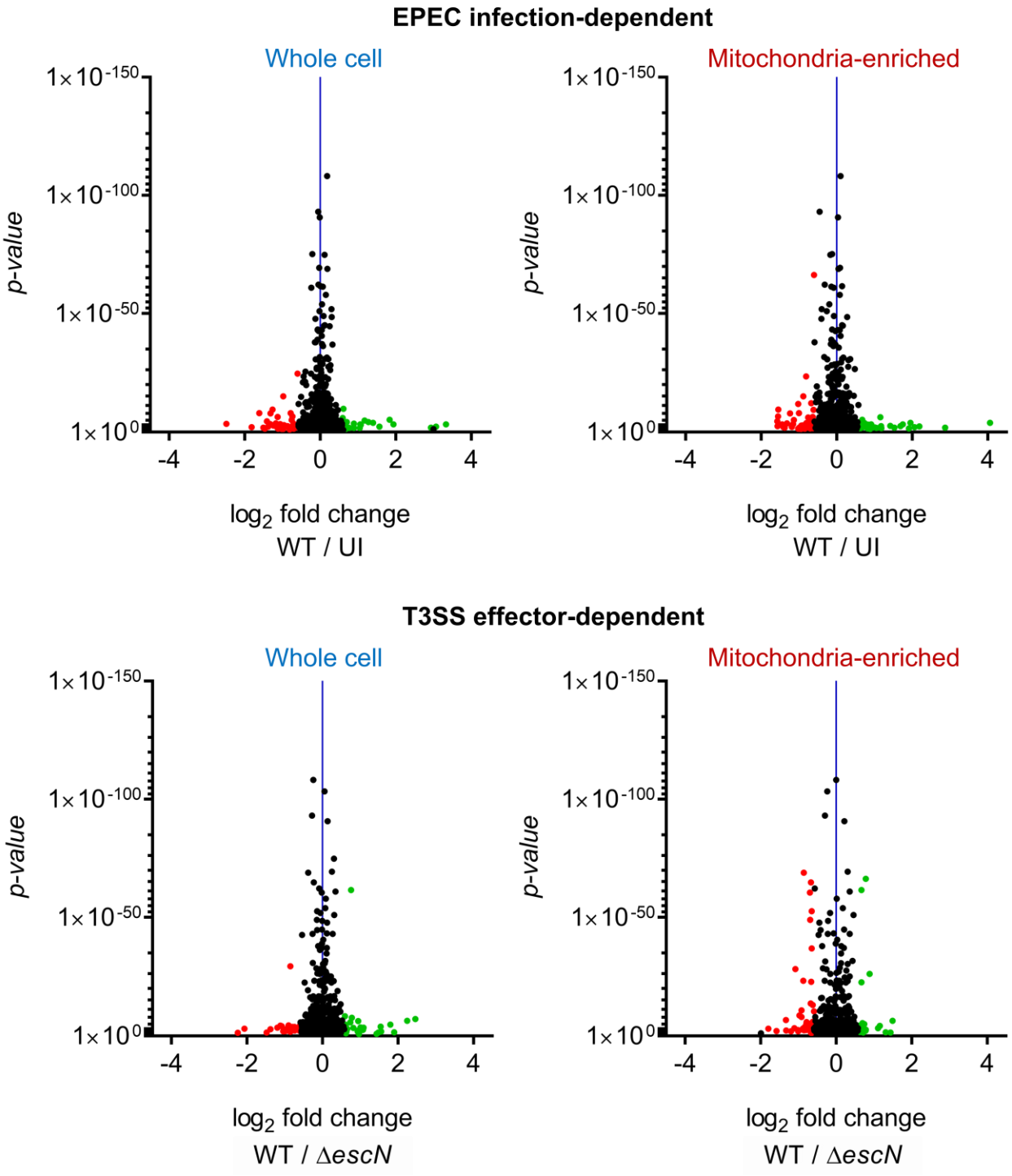

Figure 4.5 EPEC infection resulted in quantitative changes in high-confidence N-terminal peptides from mitochondria and whole cells. N-terminal peptides identified by MS-TAILS in EPEC wild-type (WT) infection *vs.* EPEC Δ*escN* infection or uninfected (UI) cells and mitochondria were assessed as volcano plots depicting the relative abundance of each N-terminal peptide to the EPEC wild-type infection condition against the posterior error probability (PEP), or *p* value of identification.

To identify key mitochondrial events that were altered during EPEC infection, I compared the relative abundance of mitochondrial N-terminal peptides identified in EPEC-infected mitochondria and cells *vs.* those identified in the uninfected control. EPEC infection altered the abundance of 22 mitochondrial N-terminal peptides from 21 proteins, including 13 neo N termini from proteolytic processing events, seven of which are novel to this study and not observed during prior apoptosis studies, as indicated by an asterisk in Table 4.2. These N termini represent a baseline effect of EPEC infection on mitochondria, including the response to bacterial infection as well as EPEC-specific and T3SS-mediated events that trigger or suppress the induction of intrinsic apoptosis.

Table 4.2 EPEC altered human mitochondrial N termini during infection. The relative fold change of each mitochondrial N-terminal peptide within the mitochondrial MS-TAILS fraction is shown comparing peptide abundance from EPEC WT *vs.* uninfected (UI) cells. Significantly up- and down-regulated N-terminal peptides are shown at ratios in green and red, respectively. '↓' notes the site of proteolysis indicated by each N-terminal peptide, within the surrounding amino acids in each protein. '*' indicates a site of proteolytic processing that was not previously identified.

Type of N terminus	Gene	Protein name	Cleavage site	Fold change WT:UI
Original	*NDUFB6*	NADH dehydrogenase [ubiquinone] 1 beta subcomplex subunit 6	N/A	**0.50**
Met1 removed	*ACOX3*	Peroxisomal acyl-coenzyme A oxidase 3	M↓A2	**1.78**
	HINT1	Histidine triad nucleotide-binding protein 1	M↓A2	**0.66**
	IDH1	Isocitrate dehydrogenase [NADP] cytoplasmic	M↓S2	**0.63**
	TFB1M	Dimethyladenosine transferase 1, mitochondrial	M↓A2	**0.58**
	ALDH9A1	4-trimethylaminobutyraldehyde dehydrogenase	M↓S2	**0.37**
	QTRT1	Queuine tRNA-ribosyltransferase catalytic subunit 1	M↓A2	**0.34**
MTS removed	*NDUFAB1*	Acyl carrier protein, mitochondrial	QLCRQY↓S69	**1.72**
	ENDOG	Endonuclease G, mitochondrial	LPVAAA↓A49	**0.64**
Proteolytic processing	*CPS1*	Carbamoyl-phosphate synthase [ammonia], mitochondrial	YPVMIR↓S588*	**16.80**
	VDAC1	Voltage-dependent anion-selective channel protein 1	TDNTLG↓T83*	**3.36**
	CPS1	Carbamoyl-phosphate synthase [ammonia], mitochondrial	FLVKGN↓D1250*	**2.28**
	HSPA9	Stress-70 protein, mitochondrial	FNDSQR↓Q203*	**1.67**
	ACAA1	3-ketoacyl-CoA thiolase, peroxisomal	PQAAPC↓L27	**1.60**
	ACAA2	3-ketoacyl-CoA thiolase, mitochondrial	KHKISR↓E177	**1.55**
	PDHB	Pyruvate dehydrogenase E1 component subunit beta, mitochondrial	LQVTVR↓D37*	**1.54**
	MRPS30	39S ribosomal protein S30, mitochondrial	TAANAA↓A26	**0.66**
	GPT2	Alanine aminotransferase 2	SWGRSQ↓S25	**0.66**
	IDE	Insulin-degrading enzyme	KKTYSK↓M42*	**0.62**
	TBRG4	Protein TBRG4	VAHKTL↓T40	**0.59**
	MRPL49	39S ribosomal protein L49, mitochondrial	CGLRLL↓S27	**0.53**
	DUT	Deoxyuridine 5'-triphosphate nucleotidohydrolase, mitochondrial	MPC↓S4*	**0.34**

To identify mitochondrial processes altered during early EPEC infection, I analyzed mitochondrial proteins with altered N termini using DAVID, as before. Mitochondrial changes were enriched in proteins in 'oxidation-reduction process,' 'nucleobase-containing small

molecule metabolism', and 'mitochondrion organization' (Figure 4.6).

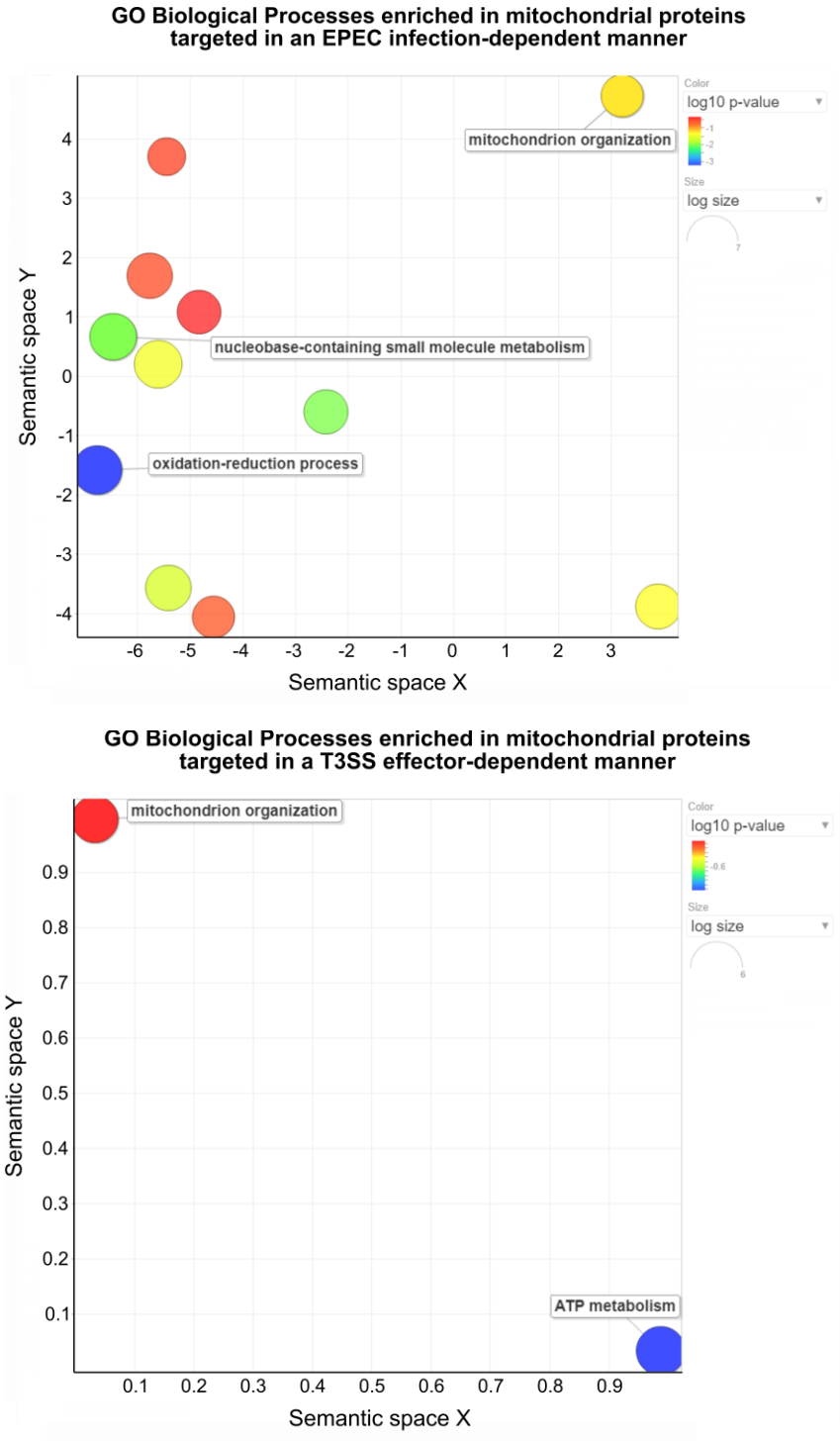

Figure 4.6 EPEC infection and T3SS effectors resulted in global changes in the mitochondrial N terminome. Mitochondrial proteins containing EPEC infection- or T3SS effector-dependent N termini were analyzed using DAVID to identify Biological Processes that were enriched in the mitochondrial N terminome in an

infection-dependent (top) or T3SS effector-dependent (bottom) manner. Enriched Biological Processes were refined and visualized using REVIGO to demonstrate clusters of the most related Biological Processes along semantic spaces on the *x*- and *y*-axes.

4.6 EPEC T3SS effectors specifically alter the mitochondrial N terminome

To specifically examine the effects of T3SS effectors on mitochondrial proteins and processes, I compared the relative abundance of mitochondrial N-terminal peptides that were identified by MS-TAILS from EPEC wild-type *vs.* Δ*escN* infection. The presence *vs.* absence of T3SS effectors altered the abundance of 12 N-terminal peptides from 12 mitochondrial proteins, including five with a known role in apoptosis and five previously unknown proteolytic events (Table 4.3). Because both conditions contained EPEC bacteria during infection, these N termini represent specific consequences of T3SS effectors and therefore provide a more exact view of T3SS effector consequences within mitochondria and infected cells.

Table 4.3 The presence of T3SS effectors altered human mitochondrial N termini during infection.
Mitochondrial proteins containing N-terminal peptides that were significantly altered within the mitochondrial samples during EPEC wild-type (WT) *vs.* EPEC Δ*escN* infection. The relative fold change of each N-terminal peptide is shown comparing peptide abundance from EPEC WT *vs.* Δ*escN* infection, lacking T3SS effectors. Significantly up- and down-regulated N-terminal peptides are shown at ratios in green and red, respectively. '↓' notes the site of proteolysis indicated by each N-terminal peptide, within the surrounding amino acids in each protein. '*' indicates a site of proteolytic processing that was not previously identified.

Type of N terminus	Gene	Protein name	Cleavage site	Fold change WT:Δ*escN*
Original	*COX6C*	Cytochrome *c* oxidase subunit 6C	N/A	**1.72**
	AK2	Adenylate kinase 2, mitochondrial	N/A	**1.53**
Met1 removed	*NDUFB4*	NADH dehydrogenase [ubiquinone] 1 beta subcomplex subunit 4	M↓S2	**1.59**
Proteolytic processing	*HSPA9*	Stress-70 protein, mitochondrial	NAEGAR↓T86*	**2.16**
	MRPS18A	39S ribosomal protein S18a, mitochondrial	RLPARG↓F35	**1.85**
	MRPS30	39S ribosomal protein S30, mitochondrial	TAANAA↓A26*	**1.73**
	ATP5A1	ATP synthase subunit alpha, mitochondrial	SILEER↓I59*	**1.68**
	HSPD1	60 kDa heat shock protein, mitochondrial	ALNATR↓A430*	**1.62**
	HINT2	Histidine triad nucleotide-binding protein 2, mitochondrial	GGQVRG↓A31	**1.59**
	OAT	Ornithine aminotransferase, mitochondrial	SSVASA↓T26	**0.63**
	VDAC1	Voltage-dependent anion-selective channel protein 1	TDNTLG↓T83*	**0.59**
	NIPSNAP1	Protein NipSnap homolog 1	AAAARF↓Y35	**0.50**

To identify proteolytic events in mitochondrial proteins known to interact with – or be functionally linked to – EPEC effectors, we compared the few known human interaction partners of mitochondria-targeting EPEC T3SS effectors from yeast two-hybrid[199] and co-immunoprecipitation[200] of tagged effectors with the list of mitochondrial proteins containing EPEC- and T3SS-mediated N termini (Figure 4.7; Table 4.4; Table 4.5). Very few mitochondrial proteins are known to interact with EPEC effectors, and none were found in common (data not shown). The lack of overlap between these lists – and the small number of known mitochondrial interaction partners – may highlight the need for mitochondrial enrichment-based protocols MS-

TAILS to identify low-abundance events within mitochondria that provide further insight into EPEC virulence mechanisms.

To examine the global effects of T3SS effectors on mitochondrial pathways, I analyzed these mitochondrial proteins as before. Mitochondrial changes were enriched in proteins in 'ATP metabolism' and 'mitochondrion organization' (Figure 4.6). Notably, both infection and effectors affected proteins involved in mitochondrion organization and ATP metabolism (a type of nucleobase-containing small molecule metabolism), corroborating these mitochondrial processes affected during wild-type EPEC infection and identifying them more specifically as T3SS-mediated.

4.7 EPEC infection and T3SS effectors mediate previously unknown proteolytic processing events in mitochondrial proteins

To identify novel mitochondrial proteolytic processing events during EPEC infection, all N termini that were significantly altered during either EPEC infection or with the T3SS were compared against BAM7- and STS-mediated mitochondrial N terminome changes from Chapter 3 and the DegraBase database of known apoptotic changes in cellular N termini. Several previously unknown proteolytic processing events were detected exclusively during EPEC infection and in a T3SS-mediated manner, including mitochondrial stress-70 protein (mtHsp70; HSPA9) at ↓Thr86, mitochondrial 60 kDa heat shock protein (mtHsp60; HSPD1) at ↓Ala430, and the voltage-dependent anion-selective channel protein 1 (VDAC1) at ↓Thr83. mtHsp60 proteolysis at ↓Ala430 cleaves 25% of the full protein length at the C terminus and therefore could abrogate the function of this mitochondrial chaperone. These previously unknown

proteolytic events could demonstrate the alternative mechanisms by which EPEC manipulates mitochondrial processes during disease. Overall, 106 novel proteolytic processing events were identified in 52 mitochondrial proteins, including 15 previously unknown proteolytic events that were significantly altered during EPEC infection and/or the presence of T3SS effectors in ten mitochondrial proteins (Table 4.2; Table 4.3).

4.8 EPEC alters the whole cell N terminome during infection

MS-TAILS was also used to identify EPEC- and T3SS-mediated changes across the whole cell. In total, EPEC infection altered the abundance of 66 N-terminal peptides (Table 4.4), and T3SS effectors altered the abundance of 51 N-terminal peptides (Table 4.5), including N termini in proteins from the 'response to oxidative stress' pathway. Of these, 40 EPEC infection-mediated and 25 T3SS-mediated proteolytic events have not been observed before in the DegraBase or in the MS-TAILS study of apoptosis in Chapter 3.

Table 4.4 EPEC altered human cellular N termini during infection. Cellular proteins containing N-terminal peptides that were significantly altered within the whole cell samples during EPEC wild-type (WT) infection. The relative fold change of each N-terminal peptide is shown comparing peptide abundance from EPEC WT *vs*. uninfected (UI) cells. Significantly up- and down-regulated N-terminal peptides are shown at ratios in green and red, respectively. '↓' notes the site of proteolysis indicated by each N-terminal peptide, within the surrounding amino acids in each protein. '*' indicates a site of proteolytic processing that was not previously identified.

Type of N terminus	Gene	Protein name	Cleavage site	Fold change WT:UI
Original	*GEMIN7*	Gem-associated protein 7	↓M1	**7.65**
	THOC1	THO complex subunit 1	↓M1	**0.66**
	GSTP1	Glutathione S-transferase P	↓M1	**0.64**
	HNRNPA1	Heterogeneous nuclear ribonucleoprotein A1	↓M1	**0.62**
Met1 removed	*UQCRB*	Cytochrome b-c1 complex subunit 7	M↓A2	**3.84**
	CAPN2	Calpain-2 catalytic subunit	M↓A2	**2.26**
	TAGLN	Transgelin	M↓A2	**2.07**
	PALM2	Paralemmin-2	MEM↓A4	**1.86**

Type of N terminus	Gene	Protein name	Cleavage site	Fold change WT:UI
	ANXA6	Annexin A6	M↓A2	**1.51**
	BLOC1S2	Biogenesis of lysosome-related organelles complex 1 subunit 2	M↓A2	**1.51**
	CPSF3	Cleavage and polyadenylation specificity factor subunit 3	M↓S2	**0.67**
	CDIP1	Cell death-inducing p53-target protein 1	M↓S2	**0.58**
	TRIP6	Thyroid receptor-interacting protein 6	M↓S2	**0.45**
	VAMP2	Vesicle-associated membrane protein 2	M↓S2	**0.33**
	TFB1M	Dimethyladenosine transferase 1, mitochondrial	M↓A2	**0.18**
MTS removed	*NDUFAB1*	Acyl carrier protein, mitochondrial	QLCRQY↓S69	**2.09**
	CPT2	Carnitine O-palmitoyltransferase 2, mitochondrial	APSRPL↓S26	**0.59**
Signal peptide removed	*HSP90B1*	Endoplasmin	SVRADD↓E24*	**0.62**
	CYR61	Protein CYR61	TRLALS↓T25*	**2.65**
	RCN2	Reticulocalbin-2	CAAAAG↓A22	**0.59**
Proteolytic processing	*VDAC1*	Voltage-dependent anion-selective channel protein 1	TDNTLG↓T83*	**10.10**
	CUBN	Cubilin	RSPENP↓M1475*	**8.41**
	ACAA1	3-ketoacyl-CoA thiolase, peroxisomal	PQAAPC↓L27	**3.58**
	HNRNPU	Heterogeneous nuclear ribonucleoprotein U	AARKKR↓N576	**2.97**
	KRT18	Keratin, type I cytoskeletal 18	FSTNYR↓S15*	**2.43**
	CCDC109B	Calcium uniporter regulatory subunit MCUb, mitochondrial	YQSHHY↓S52	**2.12**
	NDUFAF3	NADH dehydrogenase [ubiquinone] 1 alpha subcomplex assembly factor 3	WAPRRG↓H32*	**1.86**
	ALDOA	Fructose-bisphosphate aldolase A	SDIAHR↓I23*	**1.71**
	HNRNPA2B1	Heterogeneous nuclear ribonucleoprotein A1	TVKKIF↓V109*	**1.67**
	EEF1A1P5	Elongation factor 1-alpha 1	TDKPLR↓L248*	**1.63**
	PLEC	Plectin	GERSVR↓D3146*	**1.60**
	KRT18	Keratin, type I cytoskeletal 18	DIHGLR↓K187*	**1.58**
	ACTG1	Actin, cytoplasmic 1	DNGSGM↓C17*	**1.54**
	ATP5A1	ATP synthase subunit alpha, mitochondrial	RILGAD↓T64*	**1.53**
	SLC7A5	Large neutral amino acids transporter small subunit 1	KMLAAK↓S31	**1.53**
	CANX	Calnexin	QEEEDR↓K571*	**1.53**
	MECR	Enoyl-[acyl-carrier-protein] reductase, mitochondrial	GCHGPA↓A31	**1.53**
	HYPK	Huntingtin-interacting protein K	RGEIDM↓A10*	**0.66**
	RPL6	60S ribosomal protein L6	LRKMPR↓Y115	**0.66**
	PGM2	Phosphoglucomutase-2	PDADRL↓A329*	**0.62**
	SLC7A5	Large neutral amino acids transporter small subunit 1	AGPKRR↓A10	**0.61**
	DUT	Deoxyuridine 5'-triphosphate nucleotidohydrolase, mitochondrial	MPC↓S4*	**0.60**
	FLNA	Filamin-A	FMADIR↓D665*	**0.59**
	TUBB	Tubulin beta chain	GAELVD↓S115*	**0.57**

Type of N terminus	Gene	Protein name	Cleavage site	Fold change WT:UI
	FBLL1	rRNA/tRNA 2'-O-methyltransferase fibrillarin-like protein 1	NVAKKR↓T220*	**0.55**
	PLEC	Plectin	GRDALD↓G2772	**0.52**
	VIM	Vimentin	LQDSVD↓F86	**0.51**
	PLEC	Plectin	WEVMQS↓D3731*	**0.51**
	USP5	Ubiquitin carboxyl-terminal hydrolase 5	HIDDLD↓A768	**0.50**
	ATP5A1	ATP synthase subunit alpha, mitochondrial	HLQKTG↓T48*	**0.49**
	DNAJA2	DnaJ homolog subfamily A member 2	SDCNGE↓G193*	**0.49**
	HSP90B1	Endoplasmin	DEVDVD↓G29	**0.48**
	TUFM	Elongation factor Tu, mitochondrial	LLDAVD↓T245	**0.46**
	ACTG1	Actin, cytoplasmic 1	SYELPD↓G245*	**0.46**
	ACTG1	POTE ankyrin domain family member I	HPILLT↓E807*	**0.46**
	PLEC	Plectin	DALDGP↓A2774	**0.44**
	TUBA1A	Tubulin alpha-1B chain	PRAVFV↓D69*	**0.44**
	MRPL49	39S ribosomal protein L49, mitochondrial	CGLRLL↓S27	**0.42**
	NAP1L1	Nucleosome assembly protein 1-like 1	LQERLD↓G58	**0.42**
	HTRA1	Serine protease HTRA1	LSRAGR↓S30*	**0.40**
	PTBP1	Polypyrimidine tract-binding protein 1	SAAAVD↓A173	**0.40**
	DDX49	Probable ATP-dependent RNA helicase DDX49	KRKQLI↓L418*	**0.38**
	RTN4	Reticulon-4	VPPAPR↓G92*	**0.38**
	GTF2I	General transcription factor II-I	NRMSVD↓A106*	**0.36**
	SIPA1L2	Signal-induced proliferation-associated 1-like protein 2	LVEICK↓V997*	**0.35**
	PKLR	Pyruvate kinase PKM	YRPVAV↓A111*	**0.28**

Table 4.5 T3SS effectors altered cellular N termini during EPEC infection. Cellular proteins containing N-terminal peptides that were significantly altered within the whole cell samples during EPEC wild-type (WT) *vs*. Δ*escN* infection. The relative fold change of each N-terminal peptide is shown comparing peptide abundance from EPEC WT *vs*. Δ*escN* infection, lacking T3SS effectors. Significantly up- and down-regulated N-terminal peptides are shown at ratios in green and red, respectively. '↓' notes the site of proteolysis indicated by each N-terminal peptide, within the surrounding amino acids in each protein. '*' indicates a site of proteolytic processing that was not previously identified.

Type of N terminus	Gene	Protein name	Cleavage site	Fold change WT:Δ*escN*
Original	*NDUFA12*	NADH dehydrogenase [ubiquinone] 1 alpha subcomplex subunit 12	↓M1	**1.96**
	BTF3L4	Transcription factor BTF3	QMKETI↓M50*	**1.58**
	DFFA	DNA fragmentation factor subunit alpha	↓M1	**1.56**
	EEF2	Elongation factor 2	↓M1	**0.60**
	NUBP2	Cytosolic Fe-S cluster assembly factor NUBP2	↓M1	**0.54**
	MTHFD1	C-1-tetrahydrofolate synthase,	↓M1	**0.46**

Type of N terminus	Gene	Protein name	Cleavage site	Fold change WT:Δ*escN*
		cytoplasmic		
	EEF2	Elongation factor 2	↓M1	**0.36**
	RTN4	Reticulon-4	↓M1	**0.21**
Met1 removed	*TRIM32*	E3 ubiquitin-protein ligase TRIM32	M↓A2	**5.51**
	CCT5	T-complex protein 1 subunit epsilon	M↓A2	**3.48**
	PLK1	Serine/threonine-protein kinase PLK1	M↓S2	**1.94**
	PTER	Phosphotriesterase-related protein	M↓S2	**1.77**
	MSH2	DNA mismatch repair protein Msh2	M↓A2	**1.53**
	NDUFB4	NADH dehydrogenase [ubiquinone] 1 beta subcomplex subunit 4	M↓S2	**1.50**
	TGM2	Protein-glutamine gamma-glutamyltransferase 2	M↓A2	**0.66**
	TBCE	Tubulin-specific chaperone E	M↓S2	**0.65**
	METTL2B	Methyltransferase-like protein 2B	M↓A2	**0.60**
	SNX5	Sorting nexin-5	M↓A2	**0.56**
	GCLC	Glutamate--cysteine ligase catalytic subunit	M↓G2	**0.55**
	TPM1	Tropomyosin alpha-1 chain	M↓A2	**0.55**
	FADS1	Fatty acid desaturase 1	M↓A2	**0.54**
	HECTD3	E3 ubiquitin-protein ligase HECTD3	M↓A2	**0.53**
	IRF2BP2	Interferon regulatory factor 2-binding protein 2	M↓A2	**0.51**
	GTF2I	General transcription factor II-I	M↓A2	**0.47**
MTS removed	*ENDOG*	Endonuclease G, mitochondrial	LPVAAA↓A49	**0.24**
Signal peptide removed	*PSAP*	Prosaposin	LGAALA↓G17*	**1.57**
	CTSA	Lysosomal protective protein	ASRGEA↓A29	**0.50**
Pro-peptide removed	*CTSZ*	Cathepsin Z	EYLSPA↓D61*	**0.50**
Proteolytic processing	*ACTG1*	Actin, cytoplasmic 1	SYELPD↓G245*	**4.74**
	DNAJA2	DnaJ homolog subfamily A member 2	SDCNGE↓G193*	**3.73**
	CUBN	Cubilin	RSPENP↓M1475*	**2.94**
	ACTG1	Actin, cytoplasmic 1	SSSLEK↓S239*	**2.91**
	TUBB	Tubulin beta chain	GAELVD↓S115*	**2.80**
	SDC4	Syndecan-4	FVGGVA↓E19*	**2.14**
	GUK1	Guanylate kinase	MLRRPL↓A7*	**2.11**
	MERTK	Tyrosine-protein kinase Mer	TSAPSA↓A948*	**2.09**
	SLC7A5	Large neutral amino acids transporter small subunit 1	AGPKRR↓A10	**2.02**
	TOMM34	Mitochondrial import receptor subunit TOM34	MAP↓K4	**1.91**
	IPO11	Importin-11	SLERTL↓L213*	**1.72**
	HINT2	Histidine triad nucleotide-binding protein 2, mitochondrial	GGQVRG↓A31	**1.69**
	HSPD1	60 kDa heat shock protein, mitochondrial	RALMLQ↓G43*	**1.67**
	TUBA1A	Tubulin alpha-1B chain	GKHVPR↓A65*	**1.52**
	SLC39A14	Zinc transporter ZIP14	TPEAHA↓S31	**1.51**
	ALDOA	Fructose-bisphosphate aldolase A	PLAGTN↓G121	**0.66**
	ENG	Endoglin	SPTSLA↓E26	**0.61**

Type of N terminus	Gene	Protein name	Cleavage site	Fold change WT:Δ*escN*
	ACTG1	Actin, cytoplasmic 1	MATAAS↓S233*	**0.58**
	VDAC1	Voltage-dependent anion-selective channel protein 1	TDNTLG↓T83*	**0.57**
	COL16A1	Collagen alpha-1(XVI) chain	PGQPGP↓A1305*	**0.51**
	NIPSNAP1	Protein NipSnap homolog 1	AAAARF↓Y35	**0.49**
	DDX31	Probable ATP-dependent RNA helicase DDX31	SPTQTM↓A107	**0.44**
	FKBP11	Peptidyl-prolyl cis-trans isomerase FKBP11	VCRAEA↓G28	**0.38**

4.9 EPEC infection and the T3SS affected a shared subset of mitochondrial protein neo N termini.

In total, EPEC infection altered N termini in 31 mitochondrial proteins, and T3SS effectors altered N termini in 17 mitochondrial proteins. When significant mitochondrial changes were compared between EPEC-dependent and T3SS-dependent events, three events were observed in both an EPEC infection- and T3SS-dependent manner: MTS removal of endonuclease G at ↓Ala49, proteolysis in mitochondrial 39S ribosomal protein S30 (MRPS30) at ↓Ala26, and proteolysis in VDAC1 at ↓Thr83 (Figure 4.7).

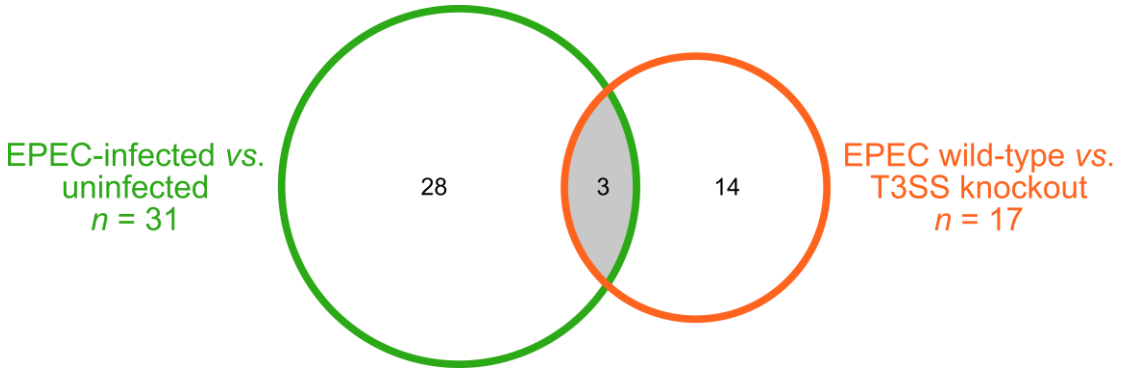

Figure 4.7 EPEC infection significantly altered the abundance of mitochondrial N-terminal peptides in an infection-and effector-dependent manner. Mitochondrial N termini that were significantly altered in enriched mitochondria and whole cells during EPEC wild-type infection (*vs.* no infection) were compared in the absence of T3SS effectors (*v.s.* EPEC wild-type infection).

The N-terminal peptide identified in endonuclease G occurs at ↓Ala49 and corresponds to the removal of this protein's MTS, which occurs during import into the mitochondrial matrix. This event is also reported in the DegraBase, suggesting that this proteolytic event occurs during apoptosis (although it was not observed during BAM7 or STS treatments in Chapter 3). Because this N-terminal peptide is observed less during wild-type EPEC infection compared to uninfected cells, it suggests either decreased endonuclease G trafficking to mitochondria during infection, increased degradation of endonuclease G within mitochondria, or increased trafficking out of mitochondria. Since the abundance of this peptide was not significantly changed in the whole cell sample, and no "ragging" was detected (*i.e.* single amino acid shearing at a peptide terminus), it is most likely that infection decreases endonuclease import to mitochondria. In contrast, this peptide was not detected in mitochondria during EPEC Δ*escN* infection and was observed more in the whole cell fraction during Δ*escN* infection compared to wild-type infection, suggesting that endonuclease G was primarily trafficked out of mitochondria, into the cytoplasm, and perhaps to its late apoptotic target: the cell nucleus. The release of endonuclease G from mitochondria occurs after the point-of-no-return in intrinsic apoptosis (*i.e.* MOMP); therefore this event suggests a later stage of apoptotic cell death occurring during infection with EPEC Δ*escN*.

A proteolytic event at ↓Ala26 in MRPS30 was detected only within mitochondrial samples and never in the whole cell. In Chapter 3, this peptide was also observed during BAM7 treatment, where it was also only detected within mitochondria; otherwise, this N terminus is novel to this work and has not been reported in the DegraBase or the MEROPS database of protease substrates. This proteolytic event occurs within the expected region for an MTS within a

mitochondrial protein; however, MRPS30 does not encode a known MTS and the cleavage motif (TAANAA↓ATATET) does not correlate with the known MPP cleavage motif identified by Vögtle *et al*.[53]; therefore it is more likely to represent proteolytic processing. During BAM7-mediated apoptosis, this N terminus was identified *more* during BAM7 treatment compared to the DMSO vehicle control. During EPEC infection, this N-terminal peptide was identified *less* during wild-type infection (*vs*. uninfected) and *less* during Δ*escN* infection compared to wild-type (UI > WT > Δ*escN*).

VDAC1 forms a channel in the OMM and is the OMM component of the mitochondrial permeability transition pore complex (mPTPC) through which $\Delta\Psi_m$ dissipates at the point-of-no-return in intrinsic apoptosis[61]; VDAC1 is therefore very important during apoptosis and to maintain mitochondrial membrane impermeability. In mitochondria during EPEC wild-type and Δ*escN* infection, a proteolytic event was identified in VDAC1 at ↓Thr83, within one of the many OMM transmembrane domains (at amino acids 80 – 89; Figure 4.8). The ↓Thr83 cleavage occurs *more* during wild-type infection than in uninfected cells and *less* during wild-type infection than Δ*escN* infection (UI < WT < Δ*escN*). This cleavage pattern may indicate that infection activates a host protease (or introduces an EPEC protease) to cleave VDAC – resulting in MOMP and inducing apoptosis – and that EspZ or another T3SS effector down-regulates this during wild-type infection. This proteolytic event at ↓Thr83 has not been observed in prior terminomics studies or in the MEROPS database of protease substrates[233,234], nor was it identified during the induction of canonical apoptosis using BAM7 or STS in Chapter 3. Therefore, this event may be related to the induction of intrinsic apoptosis during EPEC infection, such as by the mitochondrial-targeting T3SS effectors EspF and EspZ that are known to modulate apoptosis.

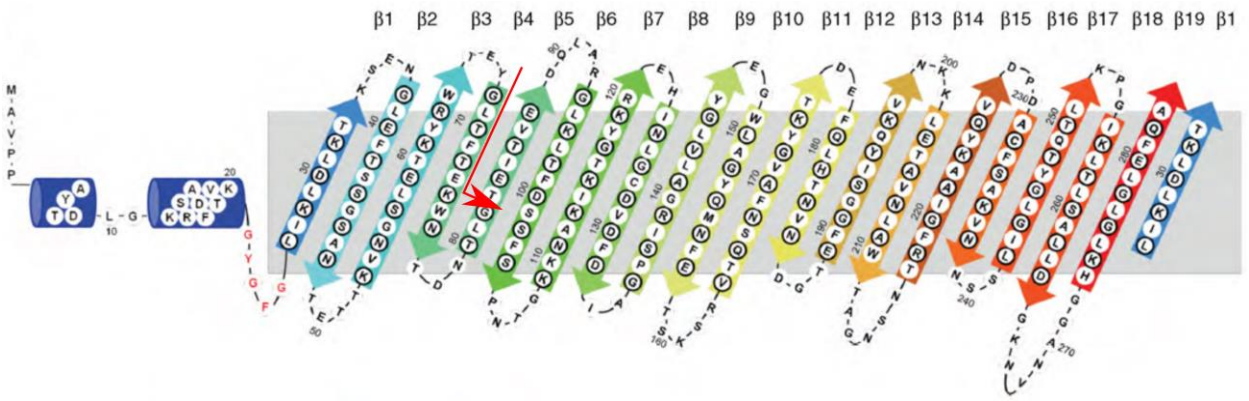

Figure 4.8 MS-TAILS revealed a neo N terminus indicating a T3SS effector-mediated proteolytic processing event in VDAC1. MS-TAILS revealed a neo N terminus at ↓Thr83 in VDAC1 that occurred in an EPEC infection- and T3SS effector-dependent manner. The 3D structure of VDAC1 shows that this proteolytic event corresponds to the fifth β-strand (site shown by middle of red arrow). Reproduced from Hiller *et al.*[235] with permission.

4.10 The majority of EPEC- and T3SS-mediated changes are unique from canonical intrinsic apoptosis

EPEC T3SS effectors are known to induce or delay intrinsic apoptosis from within mitochondria, though the mechanisms involved are not known. Changes in mitochondria that are specific to infection and distinct from canonical apoptosis by BAM7 and STS (*e.g.* VDAC1 proteolysis at ↓Thr83) may indicate T3SS effector-targeted pathways to induce and control apoptosis. Therefore, to identify mitochondrial proteins targeted by T3SS effectors, I compared all significantly-affected mitochondrial N-terminal peptides from EPEC infection and T3SS effectors with those from BAM7 and STS treatments in Chapter 3.

Early changes in canonical apoptosis from BAM7 and STS affected 66 mitochondrial N termini at 65 sites, including seven core mitochondrial early apoptotic events seen in both treatments (Figure 3.6). Only 7.6% of these (n = 5/66) were observed during EPEC infection, and none of the core mitochondrial early apoptotic events were observed; these changes accounted for only

11.1% of all EPEC- and T3SS-mediated changes in the mitochondrial N terminome (*n* = 5/45; Figure 4.9A). When compared to the DegraBase of N termini observed during apoptosis, only 16 EPEC- or T3SS-mediated mitochondrial N termini were previously observed during apoptosis (Figure 4.9C). Overall, of the 45 total changes in the mitochondrial terminome during infection, 88.9% were not observed during canonical apoptosis (*n* = 40/45), though the same cell line and experimental method was used, and 60.0% (*n* = 27/45) have not previously been associated with apoptosis in the DegraBase or previous MS-TAILS experiments (Figure 4.9C–D). Therefore, up to 40.0% of EPEC-mediated mitochondrial changes correspond to infection- or T3SS effector-dependent mechanisms of apoptosis: a non-canonical, infection-associated mitochondrial apoptotic pathway (I-MAP) that occurs through different means than the canonical apoptotic pathway.

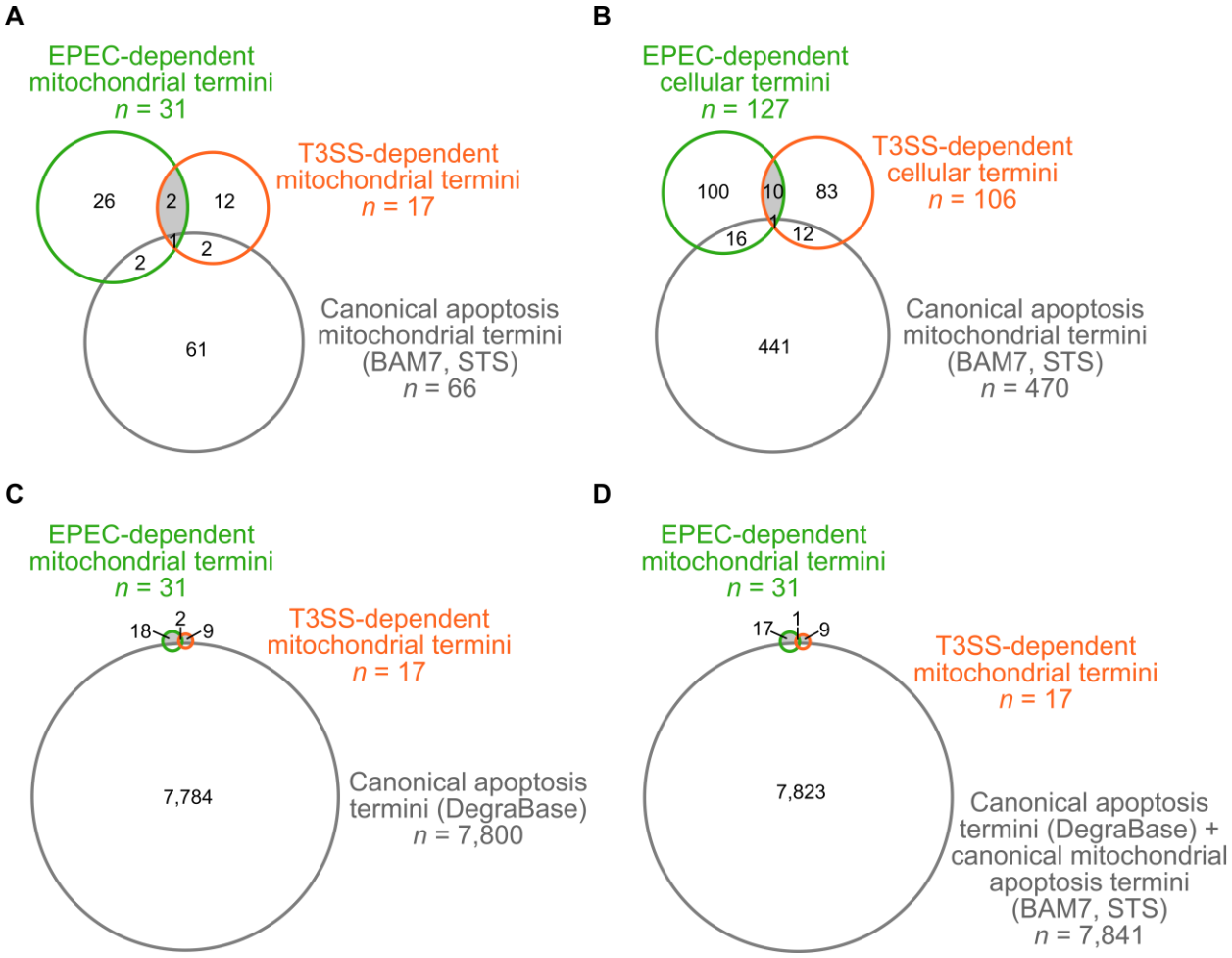

Figure 4.9 EPEC infection- and T3SS-dependent mitochondrial N termini are unique to infection and distinct from canonical apoptosis events. N-terminal peptides that were significantly up- or down-regulated during EPEC infection (*vs.* uninfected cells or *vs.* infection with a T3SS-defective strain) were compared. *A*, Mitochondrial N-terminal peptides affected in an EPEC infection- (green) and/or T3SS effector (orange)-dependent manner were compared with mitochondrial N-terminal peptides affected during canonical intrinsic apoptosis induction with BAM7 and STS in Chapter 3. *B*, Whole cell N-terminal peptides affected by EPEC infection and/or T3SS effectors were compared with those affected during canonical intrinsic apoptosis induction with BAM7 and STS in Chapter 3. *C*, Mitochondrial N-terminal peptides affected by EPEC infection and/or T3SS effectors were compared with all protein N termini in the DegraBase database of apoptotic protein termini. *D*, Mitochondrial N-terminal peptides affected by EPEC infection and/or T3SS effectors were compared with all protein N termini in the DegraBase database of apoptotic protein termini and mitochondrial N-termini affected during BAM7 and STS treatments.

Of these 40 I-MAP events in mitochondrial proteins, 23 occurred in 20 mitochondrial proteins that have no known role in apoptosis. These 20 mitochondrial proteins included those involved in mitochondrial protein import (*e.g.* TOMM34), mitochondrial translation (*e.g.* MRPL49,

MRPS18A, TUFM), and OXPHOS (*e.g.* ATP5A1, NDUFA12, NDUFAF3, NDUFB4, NDUFB6), which could be targeted by EPEC to execute a distinct mechanism of apoptosis induction.

In addition, seven I-MAP events occurred in five proteins with a known role in apoptosis (Table 4.6), which could indicate how EPEC targets existing apoptotic pathways from atypical directions. These proteins were: 3-ketoacyl-CoA thiolase, mitochondrial (ACAA2); endonuclease G (ENDOG), stress-70 protein, mitochondrial (HSPA9; mtHsp70); 60 kDa heat shock protein, mitochondrial (HSPD1; mtHsp60); and voltage-dependent anion-selective channel protein 1 (VDAC1; Table 4.6).

Table 4.6 EPEC infection- and T3SS-dependent N termini occurred in mitochondrial proteins with a known role in apoptosis. Mitochondrial proteins containing N-terminal peptides that were significantly altered within the mitochondrial samples during EPEC wild-type (WT) infection compared to uninfected (UI) and/or EPEC Δ*escN*-infected cells. The relative fold change of each N-terminal peptide is shown comparing peptide abundance from EPEC WT *vs*. UI or Δ*escN*-infected cells. Significantly up- and down-regulated N-terminal peptides are shown at ratios in green and red, respectively. '↓' notes the site of proteolysis indicated by each N-terminal peptide, within the surrounding amino acids in each protein. '*' indicates a previously unknownsite of proteolytic processing. ND, not detected.

Type of N terminus	Gene	Protein name	Cleavage site	Fold change WT:UI		Fold change WT:Δ*escN*	
				Mito	Cell	Mito	Cell
MTS removed	ENDOG	Endonuclease G, mitochondrial	LPVAAA↓A49	**0.64**	1.13	ND	**0.24**
Proteolytic processing	ACAA2	3-ketoacyl-CoA thiolase, mitochondrial	KHKISR↓E177*	**1.55**	ND	ND	ND
	HSPA9	Stress-70 protein, mitochondrial	FNDSQR↓Q203*	**1.67**	ND	ND	ND
	HSPA9	Stress-70 protein, mitochondrial	NAEGAR↓T86*	1.15	ND	**2.16**	ND
	HSPD1	60 kDa heat shock protein, mitochondrial	ALNATR↓A430*	1.02	1.27	**1.63**	1.29
	HSPD1	60 kDa heat shock protein, mitochondrial	RALMLQ↓G43*	0.95	ND	ND	**1.67**
	VDAC1	Voltage-dependent anion-selective channel protein 1	TDNTLG↓T83*	**3.37**	**10.10**	**0.59**	**0.57**

Similarly, of the 222 whole cell terminomic changes induced by EPEC infection or T3SS effectors, only 29 (13.1%) were also observed during BAM7 and/or STS treatment, explaining

only 13.1% of terminomic changes and covering only 6.2% of the changes induced during early stages of canonical intrinsic apoptosis (Figure 4.9). As observed in mitochondria, several N termini were affected during EPEC infection that were not observed during canonical apoptosis, including decreased Met1 removal in the cell death-inducing p53-target protein 1 (CDIP1) during wild-type infection *vs.* uninfected – suggesting decreased abundance of this protein that regulates TNFα-mediated apoptosis – and decreased pro-peptide removal of cathepsin Z at ↓Asp61 during wild-type infection *vs.* Δ*escN* – suggesting decreased cathepsin Z activity. These cell-wide effects may further demonstrate the altered apoptotic pathway executed during EPEC infection.

The mitochondrial heat shock protein 70 (mtHsp70) is an ATP-dependent molecular chaperone that binds to mitochondrial peptides before import, promotes their unfolding (especially on the cytoplasmic side), and helps proteins fold in the matrix. mtHsp70 N-terminal peptides were only detected within mitochondrial fractions. Within mitochondria, two previously undetected N-terminal peptides were identified at ↓Gln203 (infection-specific) and ↓Thr86 (T3SS-specific). ↓Gln203 occurs within an α-helix and was observed 1.7-fold more during wild-type *vs.* uninfected. ↓Thr86 occurred between two β-strands and was observed 2.2-fold more during wild-type *vs.* Δ*escN*. Either of these proteolytic events could abrogate the function of mtHsp70 within mitochondria and prevent proper protein folding during EPEC infection. Further study might elucidate the value of this event to the pathogen and the T3SS effector(s) responsible, or whether it is an effect of more global mitochondrial dysfunction and mitochondrial protease dysregulation.

ACAA2 plays a role in fatty acid β-oxidation for cellular energy[236]. ACAA2 binds to BCL2/adenovirus E1B 19 kDa protein-interacting protein 3 (BNIP3): a pro-apoptotic protein in the Bcl-2 family. ACAA2-BNIP3 binding abrogates BNIP3-mediated apoptosis, perhaps by preventing BNIP3 interactions with other proteins that regulate or execute apoptosis. Proteolysis in ACAA2 at ↓Glu177 occurred within an α-helix from amino acids 176 – 196 and increased during wild-type infection compared to uninfected, which would separate the two primary sequences that make up the ACAA2 active site: the N-terminal acyl-thioester intermediate from two C-terminal proton acceptor sites. Therefore, this proteolytic event may abrogate the function of this protein, and may perhaps compromise its ability to decrease apoptosis through the BNIP3 pathway.

4.11 A unique infection-mediated mitochondrial event affects the first step in the induction of apoptosis

To validate protein N-terminal events during EPEC infection and characterize I-MAP candidates, human epithelial cells were infected with EPEC wild-type or Δ*escN* or left uninfected and mitochondria were enriched from each sample and prepared for western blot. Following SDS-PAGE and western blotting against ACAA2, whole cell samples each displayed one band at the expected mass of the full-length protein (~41 kDa) that was absent from an EPEC bacteria sample with no human cells (Figure 4.10, *Left*); no band was seen at a smaller mass that might correlate with a proteolytic event at ↓Glu177, which should cause a mass shift of ~21 kDa. Western blot analysis of enriched mitochondria from uninfected and EPEC-infected cells displayed two bands: a large band at ~34 kDa and a small band at ~13 kDa (Figure 4.10, *Right*).

In these mitochondrial samples, the large band was ~8 kDa smaller than expected (and smaller than was observed in the whole cell lysate), as was the small band, although the small band was detected at the expected mass shift of ~21 kDa. It is possible that ACAA2 contains a cleavable N-terminal MTS that is unannotated; an MTS typically corresponds to 2 – 11 kDa, which might account for this ~8 kDa decrease in mass that is observed within mitochondria but not within the whole cell. This size shift is reproducible and therefore likely represents the proteolytic event identified by MS-TAILS. This small band that would arise from the MS-TAILS-predicted proteolysis occurs 2.23-fold brighter in the wild-type EPEC-infected sample compared to the uninfected sample, further corroborating the increased proteolysis observed by MS-TAILS, which was observed 1.55-fold more during wild-type infection *vs.* no infection (Table 4.2).

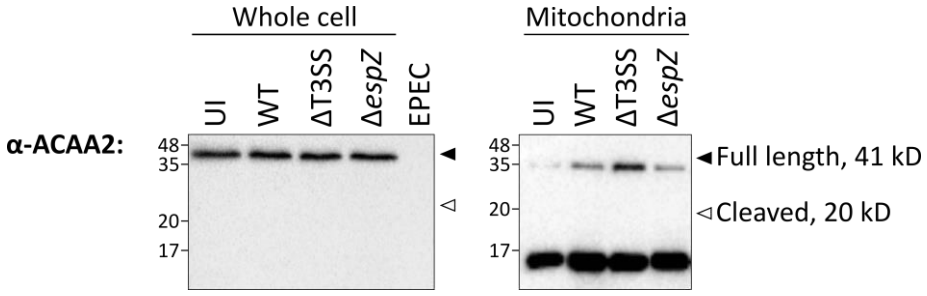

Figure 4.10 ACAA2 was detected in infected cells and in mitochondria from infected cells. *A*, HeLa cells were left uninfected (UI) or infected with EPEC wild-type (WT), a T3SS-defective strain (Δ*escN*), or a strain lacking the mitochondria-targeting T3SS effector EspZ (Δ*espZ*). Mitochondria were enriched from each cell population and analyzed by western blot with an anti-ACAA2 antibody following 15% SDS-PAGE. An EPEC bacteria-only control is shown to ensure no antibody cross-reactivity with EPEC proteins. Filled arrows mark the expected molecular weight of full-length ACAA2. Hollow arrows mark the expected molecular weight of the proteolytically cleaved fragment of ACAA2 as determined by MS-TAILS.

To characterize the impact of the I-MAP candidate ACAA2 on the induction of intrinsic apoptosis during EPEC infection, *ACAA2* gene expression was decreased by short hairpin RNA (shRNA) transfection, transfected *vs.* non-transfected cells were infected with wild-type EPEC or left uninfected, and $\Delta\Psi_m$ was measured. Gene knockdowns were optimized to 68% transfection

efficiency and 94% knockdown efficiency (Figure 4.11) and the decreased abundance of ACAA2 was confirmed at the protein level by western blot by 25.2% using densitometry (Figure 4.12A).

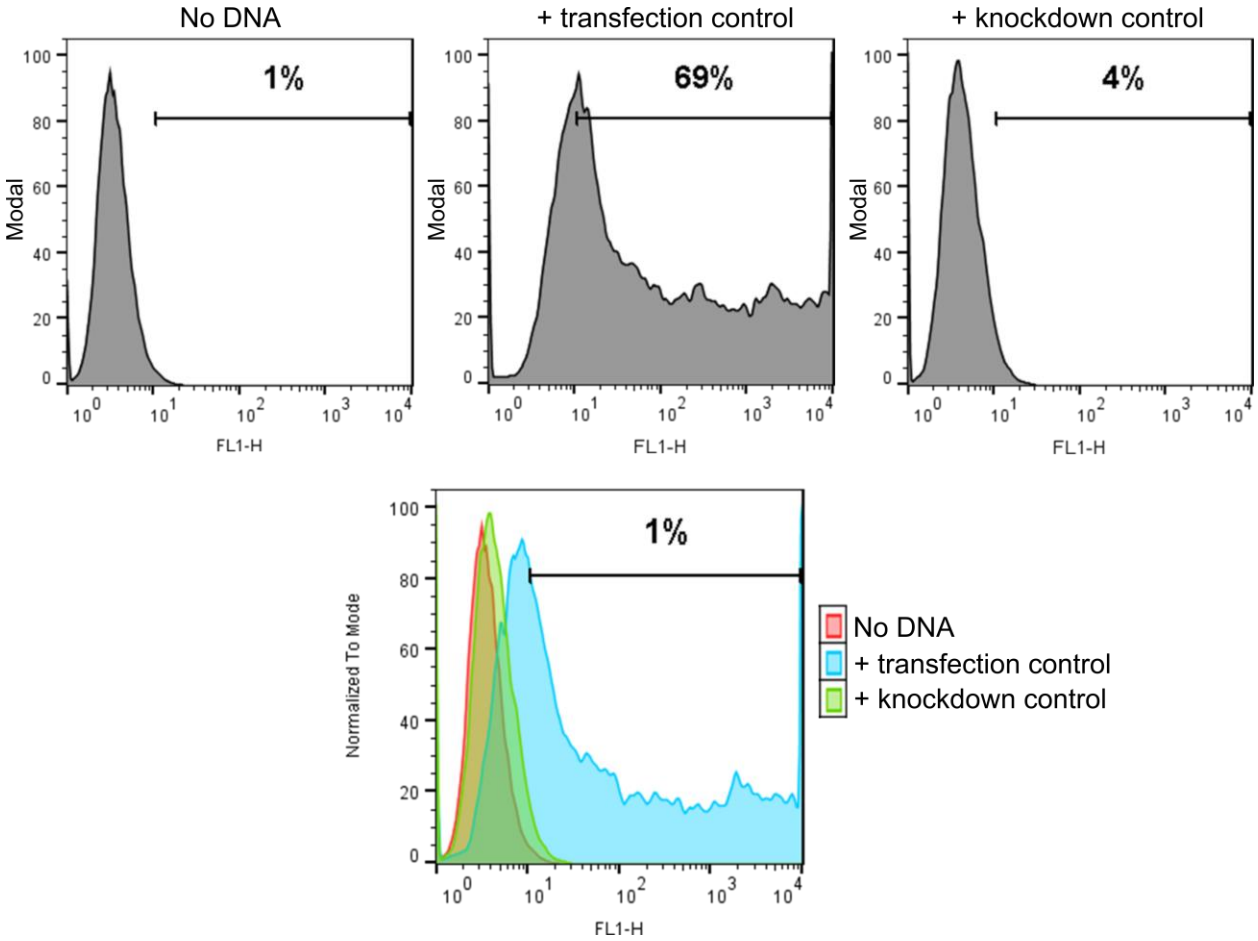

Figure 4.11 Levels of mitochondrial proteins were decreased with gene-targeted shRNA vectors transfection and knockdown by flow cytometry. HeLa cells were mock-transfected (*i.e.* with no DNA), transfected with a positive transfection control expressing TurboGFP, or transfected with a positive knockdown control expressing TurboGFP and an shRNA targeting the *turboGFP* gene. Cells were detached, rinsed, and examined using flow cytometry to identify the proportion of cells emitting green fluorescence, shown here as a histogram.

Because EPEC infection decreases $\Delta\Psi_m$, we next wanted to determine whether ACAA2 contributed to $\Delta\Psi_m$ dissipation during EPEC infection. To do this, *ACAA2* was knocked down in

HeLa cells or cells were given a non-targeting control that did not affect ACAA2 protein levels (Figure 4.12); cells were then either infected with EPEC wild-type or left uninfected. When *ACAA2* was knocked down, $\Delta\Psi_m$ decreased relative to a non-targeting control. However, EPEC infection of *ACAA2* knockdown cells resulted in a significantly smaller decrease than was seen in uninfected knockdown cells *vs.* non-targeting control cells. Overall, when *ACAA2* knockdown cells were compared with cells given a non-targeting construct (*i.e.* no knockdown), *ACAA2* knockdown resulted in a significantly smaller decrease in $\Delta\Psi_m$ during EPEC infection compared to the relatively large decrease in $\Delta\Psi_m$ in uninfected cells during *ACAA2* knockdown from serum starvation ($p = 0.0255$; Figure 4.12B), suggesting that the ACAA2 protein may be important for $\Delta\Psi_m$ regulation in mitochondria and may further contribute to EPEC-mediated modulation of $\Delta\Psi_m$. This may occur in a BNIP3-dependent manner and ACAA2 proteolysis at ↓Glu177 may be a key event in this process, though further study is required.

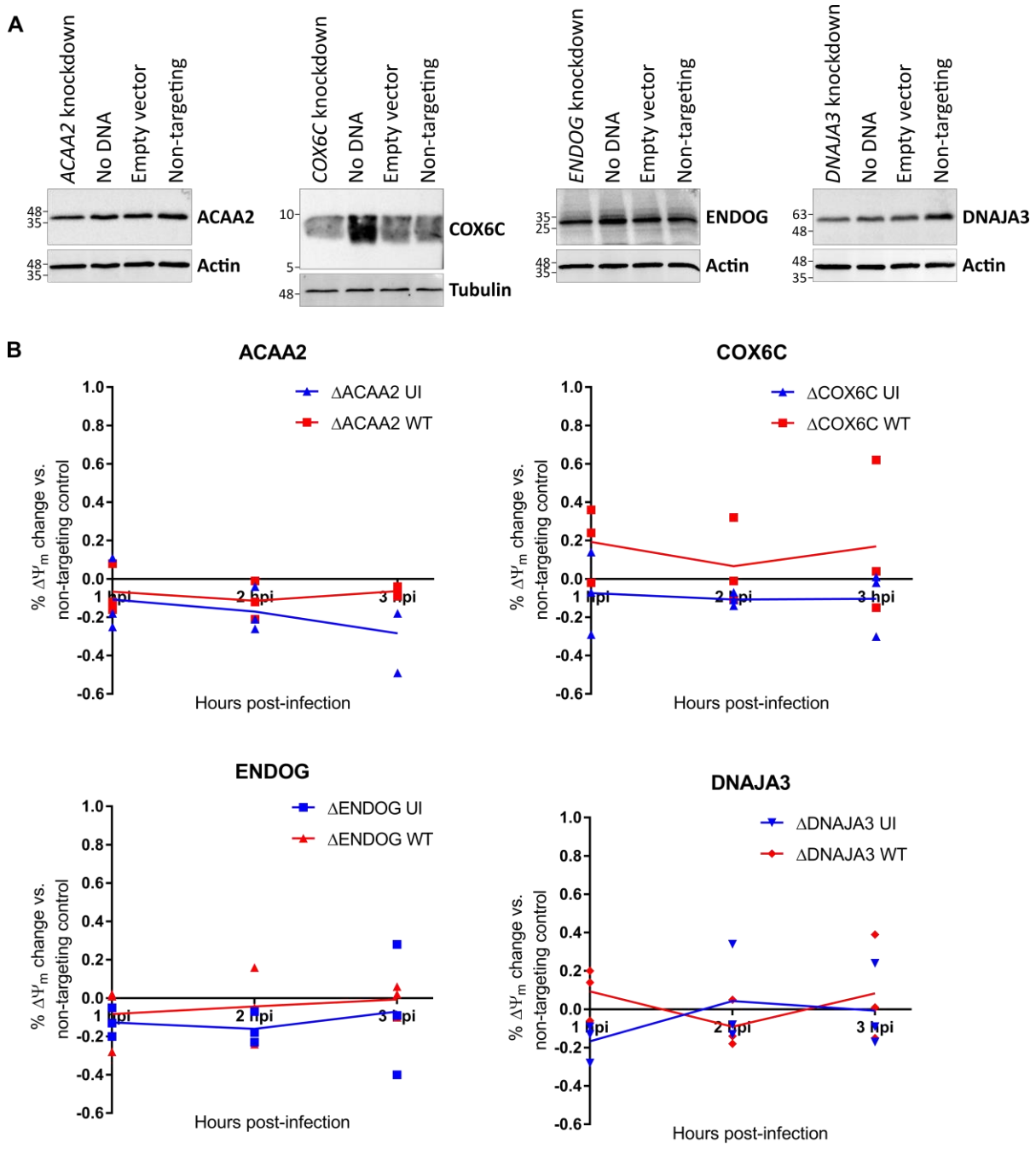

Figure 4.12 *ACAA2* knockdown altered mitochondrial membrane potential throughout EPEC infection. *A*, HeLa cells were transfected with shRNA to knock down mitochondrial genes of interest (*ACAA2*, *COX6C*, *ENDOG*, *DNAJA3*) or were transfected with no DNA, an empty vector control, or a non-targeting shRNA control against a mouse gene. Cell lysates were analyzed by western blotting using an antibody specific to each mitochondrial protein or a cytoplasmic loading control (actin or β-tubulin). *B*, HeLa cells were left untreated, treated with a non-targeting shRNA control, or treated with shRNA to knockdown the expression of mitochondrial genes with EPEC infection- and/or T3SS effector-dependent changes, including *ACAA2*, *COX6C*, *ENDOG*, and *DNAJA3*. Untreated and treated cells were left uninfected or were infected with EPEC wild-type at MOI 20 for 1, 2, or 3 h.p.i. and inner mitochondrial membrane potential ($\Delta\Psi_m$) was measured. For EPEC wild-type infection and uninfected cells, the percentage change in $\Delta\Psi_m$ during

knockdown *vs.* non-targeting control was calculated for each time point. The results of $N = 3$ biological replicates were compared by two-way ANOVA.

When *COX6C* and *ENDOG* were knocked down (Figure 4.11B), a similar trend was observed in $\Delta\Psi_m$ (Figure 4.12), however it was not statistically significant. In contrast, when *DNAJA3* was knocked down, there was no observable trend, suggesting that the presence or absence of DNAJA3 was not clearly linked with EPEC-mediated changes in the induction of intrinsic apoptosis. This may relate to the opposing pro- and anti-apoptotic activities of the two isoforms of DNAJA3, where one may be involved in EPEC infection but both are knocked down at the gene level.

Therefore, MS-TAILS identified EPEC infection-specific proteolytic events occurring in mitochondrial proteins that are involved in apoptosis: possible candidates for an infection-specific mitochondrial apoptotic pathway that occurs during infection but not during the canonical induction of intrinsic apoptosis. This work identified ACAA2, a mitochondrial protein that is important for the regulation of $\Delta\Psi_m$ in EPEC-infected human cells. ACAA2 and the other infection-specific N terminome changes in mitochondria together provide mechanistic insights into how EPEC and T3SS effectors manipulate mitochondria and apoptosis during infection.

4.12 Discussion

Several pathogens target mitochondria to prevent the induction of intrinsic apoptosis and control the host response to infection over the course of disease[21]. EPEC uses a T3SS to inject effectors directly into the host cell cytoplasm, which can traffic to host cell sub-compartments to subvert

standard cellular functions to the advantage of the pathogen. EspF and EspZ target mitochondria, where they exert a respective balance of pro- *vs.* anti-apoptotic functions that are poorly understood yet crucial for EPEC disease. In this Chapter, MS-TAILS was used to study mitochondria during EPEC infection with *vs.* without T3SS effectors. This work revealed substantial EPEC- and T3SS-mediated changes in the mitochondrial N terminome, infection-specific mitochondrial events that are distinct from canonical intrinsic apoptosis events in Chapter 3, and specific mitochondrial proteins that may involved in I-MAP.

EPEC infection altered the human mitochondrial N terminome, significantly altering the abundance of 22 mitochondrial N-terminal peptides. T3SS effectors elicited a unique subset of mitochondrial events, including previously unknown proteolytic events in key apoptosis proteins that may be targeted by T3SS effectors to trigger or suppress the induction of apoptosis. In addition to identifying specific changes in mitochondrial proteins, MS-TAILS also enabled global analyses that identified mitochondrial processes targeted by T3SS effectors: mitochondrion organization and ATP metabolism. Notably, a core set of three mitochondrial N termini were observed in both an EPEC infection- and T3SS-dependent manner: import of endonuclease G and proteolysis of MRPS30 and VDAC1. Together, MS-TAILS provided terminome-wide data on the global consequences of EPEC infection and the specific changes co-ordinated by the full repertoire of T3SS effectors, demonstrating the utility of MS-TAILS to study pathogen-encoded virulence systems and their global effects on host cell compartments.

MS-TAILS identified 15 previously unknown mitochondrial proteolytic events that were significantly altered during EPEC infection and/or the presence of T3SS effectors. These mitochondrial N termini could be caused by a T3SS effector that induces apoptosis in a way that

is distinct from host induction of apoptosis, *e.g.* by directly or indirectly controlling host mitochondrial protease activity to short-circuit a critical regulatory step. For example, proteolysis in both the N and C terminus of mtHsp60 could abrogate this protein's function. Recently, Jeong *et al.* showed that mtHsp60 up-regulates the mitogen-activated protein kinase pathway of cellular immunity and is necessary and sufficient for host resistance to *Pseudomonas aeruginosa* infection in a *Caenorhabditis elegans* model[237]. EPEC T3SS effectors may target this mitochondrial chaperone to target several pathways in cellular health and apoptosis. The remaining previously unknown proteolytic events in mitochondrial proteins may also connect T3SS effectors with mitochondrial phenotypes and processes.

Within the mitochondrial N terminome, the vast majority (89%) of EPEC- and T3SS-mediated changes were unique to infection and were not observed during early canonical apoptosis (Chapter 3), which is to say that only 11% of EPEC- and T3SS-mediated mitochondrial events identified in this study could be explained by canonical apoptosis. Moreover, none of the seven core mitochondrial events that occurred during both BAM7- and STS-mediated apoptosis were observed during EPEC infection. Although all three compared conditions were in the same cell line, used the same experimental method, and exhibited traits of early apoptosis (*e.g.* decreased $\Delta\Psi_m$), EPEC affected distinct changes in the mitochondrial terminome. These differences may indicate an infection-associated mitochondrial apoptosis pathway (I-MAP) that EPEC T3SS effectors use to induce and modulate apoptosis during infection. This highlights the importance of identifying infection-specific events with an unbiased approach, which makes it possible to detect the system-wide consequences of EPEC infection beyond the known apoptotic events expected in the canonical pathway. For example, a previously unknown EPEC- and T3SS-

dependent proteolytic event in VDAC1 could directly impact the formation of the VDAC1-containing mPTPC pore through which toxic, pro-apoptotic mitochondrial proteins are released into the cytoplasm, accelerating and inducing the cell-wide consequences of apoptosis. In addition, proteolysis in ACAA2 increased during wild-type EPEC infection compared to uninfected, cleaving apart the protein to separate the ACAA2 active site, which could interfere with its known role abrogating apoptosis through BNIP3 and mitochondrial damage. Further infection-specific events in the cellular terminome, such as increased cathepsin Z activity, may highlight the cellular effects of altered mitochondrial apoptosis induction within mitochondria.

By comparing EPEC infection- and T3SS-mediated changes in the mitochondrial N terminome, MS-TAILS identified high-confidence targets of EPEC T3SS effectors during infection, connecting these EPEC virulence factors with a small subset of mitochondrial proteins that may be specifically targeted to induce I-MAP. Ergo, this work highlights the importance of systems-level tools to study bacterial infection and virulence mechanisms rather than limiting the experimental scope to the small proportion of known canonical apoptotic events that also occur during early EPEC infection.

To my knowledge, this is the first study of the mitochondrial proteome during infection and the first proteomics study of cellular and mitochondrial changes in parallel. This work reveals previously undetected proteolytic events across the mitochondrial terminome that were not detected during canonical apoptosis and may indicate an I-MAP. This data lays the groundwork to identify the mechanisms of T3SS effectors that target mitochondria and apoptosis during infection. Further studies could identify the consequences of individual T3SS effectors by comparing infections with the wild-type *vs.* single T3SS effector knockout strains (*e.g.* Δ*espZ*) or

begin to identify host response by comparing live infection with an inoculum of heat-killed bacteria. Furthermore, these systems-level studies of microbial infections can be powerful tools to elucidate the role of mitochondria in regulating the pathway of intrinsic apoptosis.

Chapter 5: Conclusion

This thesis examines changes in the human mitochondrial N terminome, generating a better understanding of mitochondrial function and regulation by proteases. In Chapter 2, this thesis develops and introduces MS-TAILS: a new technique to characterize the N terminomes of mitochondria and whole parent cells, simultaneously. MS-TAILS also enables the quantitative comparison of mitochondrial and whole cell N terminome changes between up to three conditions; therefore, in Chapter 3, I applied MS-TAILS to compare untreated *vs.* early apoptotic cells, identifying a core set of seven mitochondrial terminome changes that occur within mitochondria during the early stages of canonical intrinsic apoptosis. In Chapter 4, this work extends the application of MS-TAILS to study mitochondrial changes during infection with the enteric pathogen EPEC and the involvement of its T3SS, identifying previously unknown sites of proteolysis within important mitochondrial regulators of apoptosis. Discussion of the results from Chapters 2 – 4 are included at the ends of the respective chapters. This chapter provides more general conclusions about the contributions of this work given current knowledge in the field.

5.1 Overall significance of this work

Because proteases are essential for the proper regulation and execution of mitochondrial functions[101], and mitochondrial proteases are essential for human health[114], it is essential to study proteolysis within mitochondria and how it changes during mitochondrial functions and mitochondrial dysregulation.

This thesis work developed a novel mitochondrial terminomics technique to profile global changes in proteolytic events across mitochondria and whole cells in up to three biological conditions. This technique, MS-TAILS, is the first capable of quantifying terminome changes within mitochondria and therefore the first to quantitatively compare mitochondrial terminomes. Furthermore, MS-TAILS enables the simultaneous analysis of both mitochondria and the whole parent cells and therefore is a valuable tool to 'zoom in' on mitochondrial events and 'zoom out' on their cell-wide consequences. Accordingly, MS-TAILS is a valuable tool to study mitochondrial proteolysis, proteases, and import, as well as how those functions are altered during mitochondrial processes and dysfunction.

When applied to study the induction of intrinsic apoptosis, MS-TAILS identified proteolytic events that were not previously identified from proteins from enriched cellular and mitochondrial pathways, uncovering possible mechanistic insights into the regulation and execution of intrinsic apoptosis, including a core set of conserved early apoptotic events that may shed light upon the earliest steps in committing cells to death. This work is the first to apply terminomics to study the early and relatively poorly-characterized events of intrinsic apoptosis, and therefore illuminates additional regulatory and mechanistic levels by which mitochondria control this crucial cellular process.

When applied to study bacterial infection, MS-TAILS identified a majority of unique and previously undetected infection-mediated proteolytic events in mitochondrial proteins, suggesting that EPEC may execute an infection-associated mitochondrial apoptosis pathway (I-MAP) rather than the canonical intrinsic apoptosis pathway. These events lay the foundation for mechanisms by which mitochondrial-targeted EPEC T3SS effectors contribute to disease. This

thesis work is the first application of a terminomics technique to study an ongoing bacterial infection; previous work has only identified substrates of individual microbial proteases within host cell lysates, marking a substantial gap in our knowledge of microbial virulence mechanisms and host immune responses that are mediated by proteolysis (reviewed by Marshall *et al.*[101]).

Overall, this thesis work provides a novel approach to study global dynamics in mitochondrial proteolysis between conditions. This approach can address a technical gap to characterize mitochondrial dynamics, processes, pathologies, and proteases, including and beyond apoptosis.

5.2 Developing a suitable mitochondrial terminomics technique

Because of the value of 'omics tools in studying mitochondria and mitochondrial processes and the suitability of terminomics to study mitochondrial import and regulation by proteases, this thesis aimed to develop a mitochondrial terminomics technique with the following criteria: (*i*) reduced experimental variability throughout the workflow (particularly the mitochondrial enrichment); (*ii*) modularity, so that this technique could be flexibly applied with the best mitochondrial (or another organelle) enrichment technique for any sample; (*iii*) robust N-terminal peptide identification; and (*iv*) substantial enrichment of mitochondria from other cellular components.

To decrease experimental variability in the MS-TAILS technique, we utilized metabolic isotopic labeling with SILAC: the gold standard of labeling in biological samples. By doing so, cell and mitochondrial samples can be pooled and processed together regardless of experimental treatments. This decreased the number of separate mitochondrial enrichments from three to one

(*i.e*. one per condition to one per biological replicate) and substantially reduced experimental variability, which streamlined the overall workflow and decreased the hands-on time at the bench while also decreasing the number of samples for TAILS, preTAILS, and mass spectrometry analysis by three-fold.

The use of SILAC also enabled a modular MS-TAILS workflow, to which any enrichment protocol could be applied, whether for superior mitochondrial purification, mitochondrial enrichment from a different cell line or organism, or enrichment of a different cellular compartment entirely. This modularity enabled the simultaneous analysis (and parallel sample processing) of a whole parent cell sample alongside enriched mitochondria from the same cell population, empowering a global view of mitochondrial consequences. MS-TAILS can even be applied *in vivo* using completely SILAC-labeled mice[238,239]. Therefore, this technique can be further applied to study enriched mitochondria from mammalian tissues while retaining these advantages of SILAC quantitation. *In vivo* work is particularly important for biologically significant research findings, particularly while studying proteolysis, which is best studied under biologically-relevant concentrations of proteases and inhibitors[101]. An additional benefit of *in vivo* studies to reduce and remove artefacts of cancer cell lines, particularly the Warburg effect: the altered metabolism of cancer cells towards lactic acid fermentation even in the presence of oxygen, suggesting altered mitochondrial function for increased resistance to hypoxia (reviewed by Potter *et al.*[240] and Zhou *et al.*[241]). However, the use of SILAC also helps to negate the Warburg effect in cancer cell lines: the consequences of the Warburg effect will be present as baseline events, altered 1:1 between biological conditions and leaving true consequences of

different biological conditions or treatments as significantly altered proteins, peptides, or N termini.

To robustly identify N-terminal peptides, TAILS N terminomics was applied. While several terminomics techniques exist, TAILS was readily available and involved minimal mass spectrometry work and instrument time, reducing the overall cost and labour of the technique. By combining SILAC and TAILS techniques, N terminome changes could be easily quantified by comparing the relative abundance of SILAC-labeled peptides originating from different treatment conditions, either heavy, medium, or light labeled. Accordingly, the label on each N-terminal peptide and the cell fraction of origin together provide information on treatment-specific changes and how these change in the cell overall or within mitochondria. A change in a SILAC ratio for a proteolytic neo N terminal peptide therefore indicates sites of altered proteolysis (provided that preTAILS or mature N termini can control for changes in the overall abundance of that protein). While MS-TAILS does not provide information on the overall proportion of the substrate protein that is cleaved, MS-TAILS identifies substrates and specific proteolytic sites as well as quantitative changes in proteolysis between conditions of interest, which is exceedingly valuable in the search for cleaved proteins. Such sites of altered proteolysis may cause a gain or loss of protein function, which could be confirmed by subsequent experiments based on MS-TAILS data.

Finally, to successfully enrich mitochondria, a well-established mitochondrial enrichment protocol was followed that enriches functional mitochondria from cultured cells[211].

When developing and validating the MS-TAILS technique, we observed all four of the selected criteria: (*i*) good reproducibility of N terminal peptides and proteins (Figure 2.5); (*ii*) the ability

to simultaneously analyze mitochondrial and whole cell changes (Figure 2.3; Figure 3.4; Figure 3.5); (*iii*) successful enrichment of 2,237 N-terminal peptides from 1,789 proteins (Table 2.1); and (*iv*) successful enrichment of mitochondria (Figure 2.4), allowing for identification of 45% of the known mitochondrial proteome (Figure 2.7). Additionally, this technique identified a characteristic mitochondrial N terminome profile distinct from the cellular N terminome (Figure 2.7C); 97 previously unknown sites of proteolysis in mitochondrial proteins, 101 known MTS sites (the most of any terminomics study to date; Figure 2.7D), and 135 previously unknown MTS sites that displayed a characteristic cleavage motif for the Mitochondrial Processing Peptidase identified in the first mitochondrial N terminomics study in yeast[53] (Figure 2.7E).

Therefore, MS-TAILS is a useful tool to study mitochondrial proteolysis and global mitochondrial dynamics, processes, pathologies, and proteases. Accordingly, MS-TAILS could be immensely valuable in characterizing the 20 mitochondrial proteases and identifying their substrates across the mitochondrial and whole cellular proteomes – few of which are known (reviewed by Quirós *et al.*[114]). Thus far, mitochondrial proteases have been characterized by studying single proteases knockouts and recombinant proteases[114]; unbiased 'omics approaches have not been applied to study mitochondrial proteases, with one exception where COFRADIC terminomics was used to identify substrates of the Mitochondrial Processing Peptidase[53]. Similarly, MS-TAILS can be applied as a valuable tool to identify the substrates of the 20 known mitochondrial proteases by comparing mitochondria with a functional protease *vs.* an active site mutant (if known) or *vs.* a protease knockout. While MS-TAILS does not provide information on the overall proportion of the substrate protein is cleaved, MS-TAILS identifies substrates and specific proteolytic sites as well as quantitative changes in proteolysis between conditions of

interest, which is exceedingly valuable in the search for the substrates of these proteases. In addition to the COFRADIC technique applied to study the Mitochondrial Processing Peptidase, MS-TAILS provides the benefits of quantitation, decreased experimental error, decreased labour and instrument time, and a parallel whole cell sample where further substrates can be identified, as well as the global consequences of protease dysfunction. Given the important roles of mitochondrial proteases on human health and disease, as well as protein quality control, mitochondrial fusion and fission, stress responses, mitophagy, and apoptosis (reviewed by Quirós *et al.*[114]), it is important to study mitochondrial proteases and important to have the tools to do so effectively.

This thesis has developed a novel tool to conduct quantitative and comparative analyses of the mitochondrial N terminome. Therefore, MS-TAILS enabled analyses that could not be done in the few previous mitochondrial terminomics studies. MS-TAILS identified more unique MTS sites than Calvo *et al.* and Vaca-Jacome *et al.*, who used COFRADIC and doublet N-terminal oriented proteomics (dN-TOP), respectively[179,182]; because each of these studies analyzed multiple samples where this thesis work analyzed only two, this demonstrates the superior value of MS-TAILS in studying mitochondrial protein targeting and import. Furthermore, the MS-TAILS workflow is less labour-intensive and involves less mass spectrometer instrument time (which is expensive) because SILAC metabolic labeling dramatically decreases the number of samples for TAILS processing and mass spectrometry analysis. In contrast, COFRADIC requires repeated analyses to identify N-terminal peptides, and dN-TOP requires redundant analyses to identify both N-terminal and internal peptides[242]. While requiring far fewer samples, MS-TAILS is also a flexible and modular workflow to which parallel analyses can be added easily. Here,

shotgun proteomics (*a.k.a.* preTAILS) and whole cell sample analyses were added; a different mitochondrial enrichment or purification technique could be added easily, or a technique to enrich a different organelle entirely. This additional whole cell sample is novel to this study and has not been done in previous terminomics applications in the literature, yet it easily allows the observation of whole cell changes and a broader context for mitochondrial N terminome changes. This is valuable given the constant cross-talk between mitochondria and the cytoplasm, nucleus, and endoplasmic reticulum, in particular, and to identify cellular substrates of mitochondrial proteases outside of mitochondria. MS-TAILS also includes an improved bioinformatics pipeline to validate and study identified mitochondrial N termini. Whereas Vögtle *et al.* validated hits individually by searching the literature and comparing SDS-PAGE mobility of radiolabeled peptides *in organello*, this thesis introduces two new software programs (TAP and Center•Point) to assist the proteomics, positional proteomics, and terminomics research communities. TAP and TopFINDer together can directly and automatically compare each N-terminal peptide identified by MS-TAILS by the thousands with UniProt, MEROPS, and TopFIND (which includes previously published terminomics data from other groups) to determine whether any of the N termini from MS-TAILS have been identified before.

By far, the most significant contribution of this thesis work to the field is the quantitative capability of MS-TAILS, which can compare up to three biological conditions within a single experiment. Therefore, MS-TAILS experiments can be strategically designed to directly compare terminomes from samples containing a functional *vs*. non-functional *vs.* knocked out protease to identify the biological consequences and direct substrates of a protease of interest. All previous mitochondrial terminomics applications have aimed to characterize mitochondrial proteolysis

during untreated conditions: in addition to this, MS-TAILS allows the quantitative comparison of mitochondrial proteolysis between different biological conditions to understand how mitochondria change during a condition of interest and infer biological consequences.

5.3 Disturbing mitochondrial homeostasis to study mitochondrial regulation through proteolysis

After successfully applying MS-TAILS to enrich mitochondria proteins, identifying known sites of proteolysis and MTS removal, and identifying putative proteolytic processing sites that were previously undetected, I applied MS-TAILS to determine how mitochondria changed when a single mitochondrial function was underway. Therefore, MS-TAILS was next applied to study quantitative N terminome changes during a fundamental mitochondrial process: intrinsic apoptosis.

By treating cells with two different inducers of apoptosis (BAM7 and STS) and applying MS-TAILS to study mitochondrial and whole cell changes before caspase-3 activation, I aimed to identify a core set of events involved in the earliest steps of the induction of intrinsic apoptosis, committing cells to death. As expected of two chemicals with different mechanisms of apoptosis induction, BAM7 and STS altered the mitochondrial N terminome in unique ways, affecting >400 N-terminal peptides (Figure 3.6). Globally, specific cellular and mitochondrial pathways were affected by each treatment, including mitochondrial protein import, fission, and iron regulation (Figure 3.7). MS-TAILS comparison of BAM7 and STS treatments revealed seven mitochondrial and 85 cellular N termini that were altered significantly during both apoptotic treatments (Figure 3.6), which may indicate a core set of conserved early apoptotic events,

including crucial steps committing cells to death. Subsequent research may determine the importance of each core event in the induction of apoptosis and may identify the proteases responsible for each proteolytic event.

Intrinsic apoptosis is essential for cellular and human health, yet little is known about how the pathway is induced (*i.e.* before caspase-3 activation). Mitochondrial proteases are known to have a role in intrinsic apoptosis[114], yet tools did not exist that could identify and quantify mitochondrial proteolysis beyond *a priori* knowledge of individual proteolytic events or proteases. Therefore, MS-TAILS provides a means to study global changes in mitochondrial proteolysis, identifying how and where proteolytic events occur and change, as well as the whole cell consequences. Here, MS-TAILS demonstrates seven putative core events within mitochondria that may be involved in the earliest steps in the induction of intrinsic apoptosis and therefore lay the groundwork to investigate these poorly characterized early steps in an otherwise well-characterized pathway to commit human cells to death. None of these seven core events have been implicated directly in apoptosis before, yet several are related to processes that have been linked with apoptosis, including mitochondrial fission and iron homeostasis. These processes have been implicated in the progression of apoptosis yet it remains unclear what role they play in apoptosis, without specific events linking them to apoptosis as either cause or effect. Therefore, by applying MS-TAILS to study enriched mitochondria and identify proteolytic events, this research provides a novel perspective and new data connecting specific proteolytic events in core mitochondrial proteins to both apoptosis and linked processes. This data will be informative in future research connecting these processes with apoptosis and separating cause and effect.

Altogether, these findings provide novel mechanistic insights into the pathway of intrinsic apoptosis and the role of proteolysis, fully supporting the earlier hypothesis that examining mitochondrial N terminome changes during the induction of intrinsic apoptosis will reveal mechanistic insights into the regulation and execution of apoptosis.

5.4 Identifying mitochondrial consequences of bacterial infection

Because MS-TAILS successfully characterized mitochondrial terminome changes during the induction of apoptosis, I next applied MS-TAILS to a context in which the mitochondrial induction of apoptosis was subverted: EPEC infection.

EPEC infection altered the abundance of N termini from 31 mitochondrial proteins (Table 4.2) and EPEC T3SS effectors (which target mitochondria and modulate apoptosis) altered the abundance of N termini from 17 mitochondrial proteins (Table 4.3). Fifteen previously undetected proteolytic events were identified in mitochondrial proteins that occurred in a T3SS-dependent manner, including several in proteins with known roles in apoptosis (*e.g.* VDAC1, mtHsp60). Furthermore, 89% of EPEC-/T3SS-mediated mitochondrial N terminome changes were not observed during the induction of canonical intrinsic apoptosis in Chapter 3, and 60% have not been observed in any apoptosis terminomics experiment to date. Therefore, most EPEC-mediated changes in mitochondria were not explained by canonical apoptosis and may rather correspond to an infection-associated mitochondrial apoptotic pathway that is regulated by T3SS effectors during infection and not previously known. Therefore, this study sheds light on the mechanisms that T3SS effectors utilize to control apoptosis during infection by identifying specific mitochondrial proteins and proteolytic events that occur when T3SS effectors are

present, thereby identifying potential proteins and pathways targeted by T3SS effectors that were not previously known. Future MS-TAILS studies with EPEC strains lacking single T3SS effectors (*e.g.* Δ*espF*, Δ*espZ*) could identify specific mitochondrial proteins targeted by individual effectors during T3SS effector-mediated subversion of apoptosis, as well as important regulatory events by mitochondrial and cellular proteases. Because terminomics has not been applied to study EPEC infection – or any ongoing bacterial infection – until this study, this work provides the first look at global protease dysregulation during infection: a novel perspective of EPEC infection and T3SS-mediated disease.

Altogether, these findings identify the global and mitochondrial consequences of T3SS-mediated disease as well as individual proteins that are important for the first step of intrinsic apoptosis during EPEC infection (*i.e.* $\Delta\Psi_m$), supporting the hypothesis that identifying changes in the human mitochondrial N terminome during EPEC infection will uncover mechanisms by which T3SS effectors contribute to disease.

Understanding how EPEC regulates human cellular apoptosis is essential to understand the virulence mechanisms of this pathogen, which causes significant morbidity and mortality worldwide. In particular, T3SS effectors that target mitochondria have a significant impact on host cell death during infection[94–96,231] and highly-conserved T3SS effectors possess both pro- and anti-apoptotic activities. This raises the question why two effectors with opposing functions exist.

During infection, EPEC is strongly attached to the apical face of a human intestinal epithelial cell. Intestinal epithelial cells typically mature along intestinal villi and eventually undergo apoptosis when they are shed after reaching the top of the villus (reviewed by Günther *et al.*[60]

and Yen and Wright[243]). Accordingly, it may be to EPEC's benefit to modulate apoptosis for long enough to multiply or prepare for effective transmission to its next host, all while suppressing host immune processes. Therefore, the pro- and anti-apoptotic EPEC T3SS effectors may carefully and temporally modulate apoptosis from within mitochondria throughout infection to extend the life of the host cell until it is no longer required. Current research on these effectors is unable to address this question because of the lack of standardization of infection methods (*e.g.* T3SS pre-inductions, cell lines) or multiplicity of infection. Future research would benefit from the use of more biologically relevant models, particularly intestinal cell lines, such as TC7 cells, in which EPEC T3SS-mediated processes were recently characterized[244]. Furthermore, longitudinal experiments with a standardized infection might capture this dynamic interplay between the functions of mitochondria- and apoptosis-targeting effectors, particularly those using techniques such as MS-TAILS, immunofluorescence microscopy, and interactomics techniques using tagged effectors. To this end, this thesis provides an overall view of the consequences of all EPEC T3SS effectors under their native regulatory systems and therefore is a valuable reference for single effector studies to characterize the complex and dynamic process of T3SS-mediated EPEC disease.

5.5 Value of studying microbial infection and the host-pathogen interface with terminomics

In infectious disease the distinction between causation and association is invaluable. The first tools to address this were Koch's Postulates, a set of three criteria proposed by Robert Koch in the late 1800s to assess a causative link between the presence of bacterial species during disease

and the cause of disease itself[245,246]. Koch's Postulates have many weaknesses, and have since been reviewed[247] and ultimately replaced with more rigorous standards, such as Hill's criteria for causation[248]. Hill's criteria help evaluate the strength of an association between a pathogen or compound and a particular disease. Hill's nine criteria for causation are strength, consistency, specificity, temporality, biological gradient, plausibility, coherence, experiment, and analogy. It has been argued that 'omics tools allow for "a systems approach to extract causation from association"[249]. Indeed, 'omics tools do provide some advantages in examining Hill's criteria. With proper experimental design, 'omics datasets can be mined for the strength and consistency of the association within the same datasets, and between technical replicates. Due to the advances of multiplexing several experimental conditions within a single mass spectrometry run[105], and the alternate possibility of employing metabolic labeling strategies, such as SILAC, modern terminomics techniques allow for the minimization of technical variability while considering relevant controls (*e.g.* protease-null, uninfected, non-cleavable substrate). Similarly, unbiased tools such as 'omics tools provide a wealth of data that can lead to multiple approaches to more easily identify the plausibility of associations. Thus, future research in infectious diseases would be substantially increased by the new insights gained by further endeavors using terminomics. These applications may shed light on the global effects of microbial proteases, including identifying their full substrate repertoire and cleavage motifs and would be valuable to study the dysregulation of host pathways that are significant during infection and disease. And finally, in conducting 'omics work with the appropriate biological question and experimental design, one can satisfy the experiment and the biological gradient (*e.g.* higher infecting dose, higher protease concentration), including the temporality of the association (*e.g.* early and late

time points). It is therefore reasonable that techniques like terminomics can serve as a more high-throughput way by which to address Hill's criteria, at the very least.

Terminomics studies of infected human cells can identify cellular pathways that are important to infection. For example, TAILS has identified previously unknown substrates of microbial proteases within human cell lysates. Jagdeo *et al.* incubated poliovirus and coxsackievirus 3C proteases with a human cell lysate and performed TAILS to identify known 3C substrates, as well as novel substrates, one of which was validated: heterogeneous nuclear ribonucleoprotein M[250,251]. Heterogeneous nuclear ribonucleoprotein M was shown to be cleaved by both viral 3C proteases, resulting in a nuclear to cytoplasmic re-localization, and was important for optimal poliovirus and coxsackievirus infection.

TAILS has also identified surprising roles of human proteases during viral infection. Marchant *et al.* identified substrates of human matrix metalloproteinase (MMP) 12, which is essential for antiviral defense[252]. TAILS identified multiple nuclear substrates, which was unexpected for an extracellular matrix protein. However, during infection with coxsackievirus B3 and respiratory syncytial virus, MMP12 was found to localize to the nucleus and bind to DNA, affecting the transcription of IκBα and interferon α secretion for antiviral immunity[252].

These studies demonstrate the value of terminomics to study the involvement of host- and pathogen-encoded proteases on the host-pathogen interface and the potential of terminomics techniques to study the pathogen effects and cellular response to infection, particularly to generate testable hypotheses for the mechanisms of virulence and host immunity.

The application of terminomics to study the bacterium-host interface – *i.e.* an ongoing infection rather than a cell lysate with a recombinant protease added – could generate a wealth of knowledge on infectious diseases, yet, to our knowledge, no other applications have been reported. For example, host substrates of microbial proteases could be identified through simple *in vitro* terminomics studies in cell culture models. Furthermore, whether or not pathogens employ proteases as virulence factors, virulence processes can substantially affect infected cells. Therefore, by studying the impact of infection on the host proteome, global changes across the entire cell may be viewed more comprehensively. Moreover, these studies will be inherently less biased than the classical approach of studying a targeted subset of host proteins or pathways and will require less *a priori* knowledge of pathogenic mechanisms. This is particularly valuable for the study of non-model organisms and pathogens without tractable genomes, such as *Chlamydia* species, where the lack of molecular tools obstruct further research[79,101].

Finally, terminomics can identify proteolytic signatures of infection, which can be used to generate clinically-relevant knowledge including infection biomarkers for rapid diagnostics and early treatment[253,254]. This knowledge and subsequent diagnostic tests can improve the speed of diagnosis and outcome of treatments with antimicrobial clinical interventions.

5.6 Future directions

This thesis work examines the mitochondrial and whole cell N terminomes of human epithelial cells *in vitro* and examines how these terminomes change during the induction of apoptosis using chemicals as well as the manipulation of apoptosis during bacterial infection. Specific directions of future research are provided within Chapters 5.3 and 5.4 and are extended more broadly here.

One of the advantages of the MS-TAILS workflow is the ability to assess both mitochondria and whole parent cells simultaneously. The work in Chapters 2 – 4 heavily focused on mitochondrial changes to capitalize on the technique's sensitivity to mitochondrial proteins and N-terminal events. However, future research using this data or applying the MS-TAILS technique should examine both mitochondrial and whole cell changes to a greater degree in order to more fully examine the whole cell consequences of mitochondrial events and the treatments being studied.

Similarly, MS-TAILS provides data on co- and post-translational modifications beyond proteolysis, which were identified but not pursued in this work. For example, MS-TAILS identifies methionine oxidation and N-terminal acetylation events within N-terminal peptides, which are important during the induction and execution of apoptosis (*e.g.* N-terminal acetylation impacts Bax translocation to mitochondria[255]). Therefore, this MS-TAILS data holds an even more considerable wealth of biological information that future studies could use to pursue further insights into apoptosis and other applications of MS-TAILS.

The data provided in this thesis provides many clear avenues forward to characterize the induction of apoptosis further. Subsequent research to identify the importance of each core mitochondrial event from Chapter 2 in the induction of apoptosis would be valuable to validate these events, and may also identify the proteases responsible for each proteolytic event, including perhaps new mitochondrial and cellular proteases involved in the induction of apoptosis. Furthermore, MS-TAILS is equipped to study the temporal regulation of apoptosis by comparing untreated *vs.* early apoptotic *vs.* late apoptotic events in the mitochondrial and cellular N terminomes or to compare the caspase-dependent *vs.* caspase-independent stages of apoptosis

by comparing late apoptosis with an identical sample that also contains a pan-caspase inhibitor, such as zVAD-FMK[256].

Finally, future research would benefit from the use of more biologically relevant models. In the case of EPEC infection, human intestinal epithelial cells would be a valuable model to study, potentially revealing essential T3SS effector-mediated changes in proteins that are only expressed in intestinal cells. This study used HeLa cells because of their widespread use in various applications, not limited to mitochondrial protein import[257], mitochondrial proteases[258], mitochondrial proteomics[259,260], apoptosis[41,261–264], and microbial infection[96,265,266]. HeLa cells were used throughout this thesis so that mitochondrial and cellular terminome changes would be directly compared between health, apoptosis, and infection. However, in future studies, the most biologically relevant cell sources should be selected. For EPEC, this could be polarized human intestinal epithelial cells (*e.g.* TC7, as used by Dean *et al.*[244]), intestinal tissues from SILAC-labeled mice, or intestinal tissues from unlabeled mice with a spike-in SILAC standard, as developed by the Mann group[267] and later applied to study hepatitis C infections[268].

References

1. Milane, L., Trivedi, M., Singh, A., Talekar, M. & Amiji, M. Mitochondrial biology, targets, and drug delivery. *J Control Release* **207,** 40–58 (2015).
2. Naviaux, R. K. Metabolic features of the cell danger response. *Mitochondrion* **16,** 7–17 (2014).
3. West, A. P., Shadel, G. S. & Ghosh, S. Mitochondria in innate immune responses. *Nat. Rev. Immunol.* **11,** 389–402 (2011).
4. Bhosale, G., Sharpe, J. A., Sundier, S. Y. & Duchen, M. R. Calcium signaling as a mediator of cell energy demand and a trigger to cell death. *Ann. N. Y. Acad. Sci.* **1350,** 107–116 (2015).
5. Chikando, A. C., Kettlewell, S., Williams, G. S., Smith, G. & Lederer, W. J. Ca2+ dynamics in the mitochondria - state of the art. *J. Mol. Cell. Cardiol.* **51,** 627–31 (2011).
6. Denton, R. M. & McCormack, J. G. The role of calcium in the regulation of mitochondrial metabolism. *Biochem. Soc. Trans.* **8,** 266–268 (1980).
7. Bhola, P. D. & Letai, A. Mitochondria-Judges and Executioners of Cell Death Sentences. *Mol. Cell* **61,** 695–704 (2016).
8. Tait, S. W. G. & Green, D. R. Mitochondrial regulation of cell death. *Cold Spring Harb Perspect Biol* **5,** (2013).
9. Ugarte-Uribe, B. & García-Sáez, A. J. Membranes in motion: Mitochondrial dynamics and their role in apoptosis. *Biol. Chem.* **395,** 297–311 (2014).
10. Kroemer, G. & Reed, J. Mitochondrial control of cell death. *Nat. Med.* **6,** 513–519 (2000).
11. Cooper, G. M. Mitochondria. (2000). at <http://www.ncbi.nlm.nih.gov/books/NBK9896/>
12. Parsons, D. F. & Yano, Y. The cholesterol content of the outer and inner membranes of

guinea-pig liver mitochondria. *Biochim. Biophys. Acta* **135,** 362–364 (1967).

13. Daniele, T. & Schiaffino, M. V. Organelle biogenesis and interorganellar connections. *Commun. Integr. Biol.* **7,** e29587 (2014).

14. Hoppins, S. & Nunnari, J. Mitochondrial Dynamics and Apoptosis—the ER Connection. *Science (80-.).* **337,** 1052–1054 (2012).

15. Kornmann, B., Currie, E., Collins, S. R., Schuldiner, M., Nunnari, J., Weissman, J. S. & Walter, P. An ER-mitochondria tethering complex revealed by a synthetic biology screen. *Science (80-.).* **325,** 477–481 (2009).

16. Youle, R. J. & Bliek, A. M. van der. Mitochondrial Fission, Fusion, and Stress. *Science (80-.).* **337,** 1062–1065 (2012).

17. Ruan, L., Zhou, C., Jin, E., Kucharavy, A., Zhang, Y., Wen, Z., Florens, L. & Li, R. Cytosolic proteostasis through importing of misfolded proteins into mitochondria. *Nature* **543,** 443–446 (2017).

18. Chacinska, A. Cell biology: Sort and destroy. *Nature* **543,** 324–325 (2017).

19. Quinlan, C. L., Perevoshchikova, I. V, Hey-Mogensen, M., Orr, A. L. & Brand, M. D. Sites of reactive oxygen species generation by mitochondria oxidizing different substrates. *Redox Biol.* **1,** 304–312 (2013).

20. Shadel, G. S. & Horvath, T. L. Mitochondrial ROS signaling in organismal homeostasis. *Cell* **163,** 560–569 (2015).

21. Rudel, T., Kepp, O. & Kozjak-Pavlovic, V. Interactions between bacterial pathogens and mitochondrial cell death pathways. *Nat Rev Micro* **8,** 693–705 (2010).

22. Cagin, U. & Enriquez, J. A. The complex crosstalk between mitochondria and the nucleus: What goes in between? *Int. J. Biochem. Cell Biol.* **63,** 10–15 (2015).

23. Huynen, M. A., de Hollander, M. & Szklarczyk, R. Mitochondrial proteome evolution and genetic disease. *Biochim. Biophys. Acta* **1792,** 1122–1129 (2009).

24. Schapira, A. H. V. Mitochondrial diseases. *Lancet* **379,** 1825–1834 (2012).

25. Hang, L., Thundyil, J. & Lim, K.-L. Mitochondrial dysfunction and Parkinson disease: a Parkin-AMPK alliance in neuroprotection. *Ann. N. Y. Acad. Sci.* **1350,** 37–47 (2015).

26. Ryan, B. J., Hoek, S., Fon, E. A. & Wade-Martins, R. Mitochondrial dysfunction and mitophagy in Parkinson's: from familial to sporadic disease. *Trends Biochem. Sci.* **40,** 200–210 (2015).

27. Bayeva, M., Gheorghiade, M. & Ardehali, H. Mitochondria as a therapeutic target in heart failure. *J. Am. Coll. Cardiol.* **61,** 599–610 (2013).

28. Dominic, E. A., Ramezani, A., Anker, S. D., Verma, M., Mehta, N. & Rao, M. Mitochondrial cytopathies and cardiovascular disease. *Heart* **100,** 611–618 (2014).

29. Sun, N. & Finkel, T. Cardiac mitochondria: a surprise about size. *J. Mol. Cell. Cardiol.* **82,** 213–215 (2015).

30. van der Burgh, R. & Boes, M. Mitochondria in autoinflammation: cause, mediator or bystander? *Trends Endocrinol. Metab.* **26,** 263–271 (2015).

31. Bratic, A. & Larsson, N.-G. The role of mitochondria in aging. *J. Clin. Invest.* **123,** 951–957 (2013).

32. Hamon, M.-P., Bulteau, A.-L. & Friguet, B. Mitochondrial proteases and protein quality control in ageing and longevity. *Ageing Res. Rev.* **23,** 56–66 (2015).

33. Senft, D. & Ronai, Z. A. Regulators of mitochondrial dynamics in cancer. *Curr. Opin. Cell Biol.* **39,** 43–52 (2016).

34. Schwarz, K., Siddiqi, N., Singh, S., Neil, C. J., Dawson, D. K. & Frenneaux, M. P. The

breathing heart - mitochondrial respiratory chain dysfunction in cardiac disease. *Int. J. Cardiol.* **171,** 134–143 (2014).

35. Hollander, J. M., Thapa, D. & Shepherd, D. L. Physiological and structural differences in spatially distinct subpopulations of cardiac mitochondria: influence of cardiac pathologies. *Am. J. Physiol. Heart Circ. Physiol.* **307,** H1-14 (2014).

36. Schumacker, P. T. Lung cell hypoxia: role of mitochondrial reactive oxygen species signaling in triggering responses. *Proc. Am. Thorac. Soc.* **8,** 477–484 (2011).

37. Tan, A. S., Baty, J. W. & Berridge, M. V. The role of mitochondrial electron transport in tumorigenesis and metastasis. *Biochim. Biophys. Acta* **1840,** 1454–1463 (2014).

38. Hsu, C.-C., Lee, H.-C. & Wei, Y.-H. Mitochondrial DNA alterations and mitochondrial dysfunction in the progression of hepatocellular carcinoma. *World J. Gastroenterol. WJG* **19,** 8880–8886 (2013).

39. Urra, F. A., Cordova-Delgado, M., Pessoa-Mahana, H., Ramírez-Rodríguez, O., Weiss-Lopez, B., Ferreira, J. & Araya-Maturana, R. Mitochondria: a promising target for anticancer alkaloids. *Curr. Top. Med. Chem.* **13,** 2171–2183 (2013).

40. Bao, R., Shu, Y., Wu, X., Weng, H., Ding, Q., Cao, Y., Li, M., Mu, J., Wu, W., Ding, Q., Tan, Z., Liu, T., Jiang, L., Hu, Y., Gu, J. & Liu, Y. Oridonin induces apoptosis and cell cycle arrest of gallbladder cancer cells via the mitochondrial pathway. *BMC Cancer* **14,** 217 (2014).

41. Kim, E. Y., Shin, J. Y., Park, Y.-J. & Kim, A. K. Equol induces mitochondria-mediated apoptosis of human cervical cancer cells. *Anticancer Res.* **34,** 4985–4992 (2014).

42. Brinkmann, K. & Kashkar, H. Targeting the mitochondrial apoptotic pathway: a preferred approach in hematologic malignancies? *Cell Death Dis.* **5,** e1098 (2014).

43. Chromosome MT. *NeXtProt* (2017).

44. Anderson, S., Bankier, A. T., Barrell, B. G., de Bruijn, M. H., Coulson, A. R., Drouin, J., Eperon, I. C., Nierlich, D. P., Roe, B. A., Sanger, F., Schreier, P. H., Smith, A. J., Staden, R. & Young, I. G. Sequence and organization of the human mitochondrial genome. *Nature* **290,** 457–65 (1981).

45. Meisinger, C., Sickmann, A. & Pfanner, N. The mitochondrial proteome: from inventory to function. *Cell* **134,** 22–24 (2008).

46. Hollander, J. M., Baseler, W. A. & Dabkowski, E. R. Proteomic remodeling of mitochondria in heart failure. *Congest Hear. Fail* **17,** 262–268 (2011).

47. Pagliarini, D. J., Calvo, S. E., Chang, B., Sheth, S. A., Vafai, S. B., Ong, S.-E., Walford, G. A., Sugiana, C., Boneh, A., Chen, W. K., Hill, D. E., Vidal, M., Evans, J. G., Thorburn, D. R., Carr, S. A. & Mootha, V. K. A mitochondrial protein compendium elucidates complex I disease biology. *Cell* **134,** 112–123 (2008).

48. Calvo, S. E., Clauser, K. R. & Mootha, V. K. MitoCarta2.0: an updated inventory of mammalian mitochondrial proteins. *Nucleic Acids Res.* **44,** D1251-7 (2016).

49. Mackenzie, J. A., Mark Payne, R. & Payne, R. M. Mitochondrial Protein Import and Human Health and Disease. *Biochim Biophys Acta* **1772,** 509–523 (2007).

50. Opalińska, M. & Meisinger, C. Metabolic control via the mitochondrial protein import machinery. *Curr. Opin. Cell Biol.* **33,** 42–48 (2015).

51. Harbauer, A. B., Zahedi, R. P., Sickmann, A., Pfanner, N. & Meisinger, C. The protein import machinery of mitochondria - A regulatory hub in metabolism, stress, and disease. *Cell Metab.* **19,** 357–372 (2014).

52. Paschen, S. & Neupert, W. Protein import into mitochondria. *IUBMB Life* **52,** 101–112

(2001).

53. Vögtle, F.-N. N., Wortelkamp, S., Zahedi, R. P., Becker, D., Leidhold, C., Gevaert, K., Kellermann, J., Voos, W., Sickmann, A., Pfanner, N. & Meisinger, C. Global Analysis of the Mitochondrial N-Proteome Identifies a Processing Peptidase Critical for Protein Stability. *Cell* **139,** 428–439 (2009).

54. Lee, C. M., Neupert W. & Stuart, R. A. in *Protein, Lipid Membr. Traffic Pathways Target.* (ed. Op den Kamp, J. A. F.) **322,** 151–159 (IOS Press [u.a.], 2000).

55. von Heijne, G. Mitochondrial targeting sequences may form amphiphilic helices. *EMBO J.* **5,** 1335–42 (1986).

56. Roise, D., Theiler, F., Horvath, S. J., Tomich, J. M., Richards, J. H., Allison, D. S. & Schatz, G. Amphiphilicity is essential for mitochondrial presequence function. *EMBO J.* **7,** 649–53 (1988).

57. Rehling, P., Brandner, K. & Pfanner, N. Mitochondrial import and the twin-pore translocase. *Nat. Rev. Mol. Cell Biol.* **5,** 519–530 (2004).

58. Wu, C.-C. & Bratton, S. B. Regulation of the intrinsic apoptosis pathway by reactive oxygen species. *Antioxid. Redox Signal.* **19,** 546–558 (2013).

59. Green, D. R. & Llambi, F. Cell Death Signaling. *Cold Spring Harb. Perspect. Biol.* **7,** (2015).

60. Günther, C., Neumann, H., Neurath, M. F. & Becker, C. Apoptosis, necrosis and necroptosis: cell death regulation in the intestinal epithelium. *Gut* **62,** 1062–1071 (2013).

61. Galluzzi, L., Vitale, I., Abrams, J. M., Alnemri, E. S., Baehrecke, E. H., Blagosklonny, M. V., Dawson, T. M., Dawson, V. L., El-Deiry, W. S., Fulda, S., Gottlieb, E., Green, D. R., Hengartner, M. O., Kepp, O., Knight, R. A., Kumar, S., Lipton, S. A., Lu, X., Madeo, F.,

Malorni, W., Mehlen, P., Nuñez, G., Peter, M. E., Piacentini, M., Rubinsztein, D. C., Shi, Y., Simon, H.-U., Vandenabeele, P., White, E., Yuan, J., Zhivotovsky, B., Melino, G. & Kroemer, G. Molecular definitions of cell death subroutines: recommendations of the Nomenclature Committee on Cell Death 2012. *Cell Death Differ.* **19,** 107–120 (2012).

62. Jeong, S.-Y. & Seol, D.-W. The role of mitochondria in apoptosis. *BMB Rep* **41,** 11–22 (2008).

63. Galluzzi, L., Kepp, O. & Kroemer, G. Mitochondria: master regulators of danger signalling. *Nat. Rev. Mol. Cell Biol.* **13,** 780–788 (2012).

64. Fischer Walker, C. L., Rudan, I., Liu, L., Nair, H., Theodoratou, E., Bhutta, Z. A., O'Brien, K. L., Campbell, H., Black, R. E., Walker, C. L. F., Rudan, I., Liu, L., Nair, H., Theodoratou, E., Bhutta, Z. A., O'Brien, K. L., Campbell, H. & Black, R. E. Global burden of childhood pneumonia and diarrhoea. *Lancet* **381,** 1405–1416 (2013).

65. Majowicz, S., W, M., Sockett, P., Henson, T., Doré, K., Edge, V., Buffett, M., Fazil, A., Read, S., S, M., Stacey, D. & Wilson, J. Burden and cost of gastroenteritis in a Canadian community. *J. Food Prot.* **69,** 651–659 (2006).

66. Thomas, M., Majowicz, S., Sockett, P., Fazil, A., Pollari, F., Doré, K., Flint, J. & Edge, V. Estimated Numbers of Community Cases of Illness Due to Salmonella, Campylobacter and Verotoxigenic Escherichia coli: Pathogen-specific Community Rates. *Can. J. Infect. Dis. Med. Microbiol. = J. Can. des Mal. Infect. la Microbiol. médicale / AMMI Canada* **17,** 229–234 (2006).

67. Croxen, M. A., Law, R. J., Scholz, R., Keeney, K. M., Wlodarska, M. & Finlay, B. B. Recent Advances in Understanding Enteric Pathogenic Escherichia coli. *Clin. Microbiol. Rev.* **26,** 822–880 (2013).

68. Goosney, D. L., Gruenheid, S. & Finlay, B. B. Gut feelings: enteropathogenic E. coli (EPEC) interactions with the host. *Annu. Rev. Cell Dev. Biol.* **16,** 173–189 (2000).

69. Croxen, M. & Finlay, B. Molecular mechanisms of Escherichia coli pathogenicity. *Nat. Rev. Microbiol.* **8,** 26–38 (2010).

70. Yerushalmi, G., Nadler, C., Berdichevski, T. & Rosenshine, I. Mutational analysis of the locus of enterocyte effacement-encoded regulator (Ler) of enteropathogenic Escherichia coli. *J. Bacteriol.* **190,** 7808–7818 (2008).

71. Deng, W., Yu, H. B., De Hoog, C. L., Stoynov, N., Li, Y., Foster, L. J. & Finlay, B. B. Quantitative proteomic analysis of type III secretome of enteropathogenic Escherichia coli reveals an expanded effector repertoire for attaching/effacing bacterial pathogens. *Mol. Cell. Proteomics* **11,** 692–709 (2012).

72. Iguchi, A., Thomson, N., Ogura, Y., Saunders, D., Ooka, T., Henderson, I., Harris, D., Asadulghani, M., Kurokawa, K., Dean, P., Kenny, B., Quail, M., Thurston, S., Dougan, G., Hayashi, T., Parkhill, J. & Frankel, G. Complete genome sequence and comparative genome analysis of enteropathogenic Escherichia coli O127:H6 strain E2348/69. *J. Bacteriol.* **191,** 347–354 (2009).

73. Kenny, B., DeVinney, R., Stein, M., Reinscheid, D. J., Frey, E. A. & Finlay, B. B. Enteropathogenic E. coli (EPEC) transfers its receptor for intimate adherence into mammalian cells. *Cell* **91,** 511–520 (1997).

74. Rosenshine, I., Ruschkowski, S., Stein, M., Reinscheid, D. J., Mills, S. D. & Finlay, B. B. A pathogenic bacterium triggers epithelial signals to form a functional bacterial receptor that mediates actin pseudopod formation. *EMBO J.* **15,** 2613–2624 (1996).

75. Kenny, B. & Jepson, M. Targeting of an enteropathogenic Escherichia coli (EPEC)

effector protein to host mitochondria. *Cell. Microbiol.* **2,** 579–590 (2000).

76. Ma, C., Wickham, M. E., Guttman, J. A., Deng, W., Walker, J., Madsen, K. L., Jacobson, K., Vogl, W. A., Finlay, B. B. & Vallance, B. A. Citrobacter rodentium infection causes both mitochondrial dysfunction and intestinal epithelial barrier disruption in vivo: role of mitochondrial associated protein (Map). *Cell. Microbiol.* **8,** 1669–1686 (2006).

77. Dean, P. & Kenny, B. Intestinal barrier dysfunction by enteropathogenic Escherichia coli is mediated by two effector molecules and a bacterial surface protein. *Mol. Microbiol.* **54,** 665–675 (2004).

78. Holmes, A., Mühlen, S., Roe, A. J. & Dean, P. The EspF effector, a bacterial pathogen's Swiss army knife. *Infect. Immun.* **78,** 4445–4453 (2010).

79. Marshall, N. C. & Finlay, B. B. Targeting the type III secretion system to treat bacterial infections. *Expert Opin. Ther. Targets* **18,** 137–152 (2014).

80. Crepin, V. F., Collins, J. W., Habibzay, M. & Frankel, G. Citrobacter rodentium mouse model of bacterial infection. *Nat. Protoc.* **11,** 1851–1876 (2016).

81. Shames, S. Elucidating the function of the type-III secreted effector proteins EspZ and NleC of the attaching and effacing bacterial pathogens. (2011). at <https://circle.ubc.ca/handle/2429/39770>

82. Crane, J., Majumdar, S. & Pickhardt, D. Host cell death due to enteropathogenic Escherichia coli has features of apoptosis. *Infect. Immun.* **67,** 2575–2584 (1999).

83. Crane, J. K., McNamara, B. P., Donnenberg, M. S., B, M., Donnenberg, M. S., McNamara, B. P. & Donnenberg, M. S. Role of EspF in host cell death induced by enteropathogenic Escherichia coli. *Cell. Microbiol.* **3,** 197–211 (2001).

84. Anand, S. K. & Tikoo, S. K. Viruses as modulators of mitochondrial functions. *Adv. Virol.*

2013, 738794 (2013).

85. Arnoult, D., Carneiro, L., Tattoli, I. & Girardin, S. E. The role of mitochondria in cellular defense against microbial infection. *Semin. Immunol.* **21,** 223–232 (2009).

86. Best, S. M. Viral subversion of apoptotic enzymes: escape from death row. *Annu. Rev. Microbiol.* **62,** 171–192 (2008).

87. Kozjak-Pavlovic, V., Ross, K. & Rudel, T. Import of bacterial pathogenicity factors into mitochondria. *Curr. Opin. Microbiol.* **11,** 9–14 (2008).

88. Lee, G.-C., Lee, J. H., Kim, B. Y. & Lee, C. H. Mitochondria-targeted apoptosis in human cytomegalovirus-infected cells. *J. Microbiol. Biotechnol.* **23,** 1627–1635 (2013).

89. Blasche, S., Mötl, M., Steuber, H., Siszler, G., Nisa, S., Schwarz, F., Lavrik, I., Gronewold, T. M. A., Maskos, K., Donnenberg, M. S., Ullmann, D., Uetz, P. & Kögl, M. The E. coli effector protein NleF is a caspase inhibitor. *PLoS One* **8,** e58937 (2013).

90. Baruch, K., Gur-Arie, L., Nadler, C., Koby, S., Yerushalmi, G., Ben-Neriah, Y., Yogev, O., Shaulian, E., Guttman, C., Zarivach, R. & Rosenshine, I. Metalloprotease type III effectors that specifically cleave JNK and NF-κB. *EMBO J.* **30,** 221–231 (2011).

91. Barkett, M. & Gilmore, T. D. Control of apoptosis by Rel/NF-κB transcription factors. *Oncogene* **18,** 6910–6924 (1999).

92. Kaltschmidt, B., Kaltschmidt, C., Hofmann, T. G., Hehner, S. P., Dröge, W. & Schmitz, M. L. The pro- or anti-apoptotic function of NF-kappaB is determined by the nature of the apoptotic stimulus. *Eur. J. Biochem.* **267,** 3828–35 (2000).

93. Garmendia, J., Frankel, G. & Crepin, V. Enteropathogenic and enterohemorrhagic Escherichia coli infections: translocation, translocation, translocation. *Infect. Immun.* **73,** 2573–2585 (2005).

94. Nougayrède, J.-P. P. & Donnenberg, M. S. Enteropathogenic Escherichia coli EspF is targeted to mitochondria and is required to initiate the mitochondrial death pathway. *Cell. Microbiol.* **6,** 1097–1111 (2004).

95. Nagai, T., Abe, A. & Sasakawa, C. Targeting of enteropathogenic Escherichia coli EspF to host mitochondria is essential for bacterial pathogenesis: critical role of the 16th leucine residue in EspF. *J. Biol. Chem.* **280,** 2998–3011 (2005).

96. Shames, S. R., Croxen, M. A., Deng, W. & Finlay, B. B. The type III system-secreted effector EspZ localizes to host mitochondria and interacts with the translocase of inner mitochondrial membrane 17b. *Infect. Immun.* **79,** 4784–4790 (2011).

97. Roxas, J. L., Wilbur, J. S., Zhang, X., Martinez, G., Vedantam, G. & Viswanathan, V. K. The enteropathogenic Escherichia coli-secreted protein EspZ inhibits host cell apoptosis. *Infect. Immun.* **80,** 3850–3857 (2012).

98. Shames, S. R., Deng, W., Guttman, J. A., de Hoog, C. L., Li, Y., Hardwidge, P. R., Sham, H. P., Vallance, B. A., Foster, L. J. & Finlay, B. B. The pathogenic E. coli type III effector EspZ interacts with host CD98 and facilitates host cell prosurvival signalling. *Cell. Microbiol.* **12,** 1322–1339 (2010).

99. Bömer, U., Rassow, J., Zufall, N., Pfanner, N., Meijer, M. & Maarse, A. The preprotein translocase of the inner mitochondrial membrane: evolutionary conservation of targeting and assembly of Tim17. *J. Mol. Biol.* **262,** 389–395 (1996).

100. Martinez-Caballero, S., Grigoriev, S., Herrmann, J., Campo, M. & Kinnally, K. Tim17p regulates the twin pore structure and voltage gating of the mitochondrial protein import complex TIM23. *J. Biol. Chem.* **282,** 3584–3593 (2007).

101. Marshall, N. C., Finlay, B. B. & Overall, C. M. Sharpening host defenses during infection:

Proteases cut to the chase. *Mol. Cell. Proteomics* **16,** S161–S171 (2017).

102. Puente, X. S., Sánchez, L. M., Overall, C. M., Carlos, L.-O. & López-Otín, C. Human and mouse proteases: a comparative genomic approach. *Nat. Rev. Genet.* **4,** 544–558 (2003).

103. Dean, R. A., Cox, J. H., Bellac, C. L., Doucet, A., Starr, A. E. & Overall, C. M. Macrophage-specific metalloelastase (MMP-12) truncates and inactivates ELR+ CXC chemokines and generates CCL2, -7, -8, and -13 antagonists: potential role of the macrophage in terminating polymorphonuclear leukocyte influx. *Blood* **112,** 3455–3464 (2008).

104. Cox, J. H. & Overall, C. M. in *Cancer Degrad. Proteases Cancer Biol.* 519–539 (Springer New York, 2008). at <http://download.springer.com/static/pdf/415/bok%253A978-0-387-69057-5.pdf?originUrl=http%3A%2F%2Flink.springer.com%2Fbook%2F10.1007%2F978-0-387-69057-5&token2=exp=1481839760~acl=%2Fstatic%2Fpdf%2F415%2Fbok%25253A978-0-387-69057-5.pdf%3ForiginUrl%3Dhttp%25>

105. Klein, T., Fung, S.-Y., Renner, F., Blank, M. A., Dufour, A., Kang, S., Bolger-Munro, M., Scurll, J. M., Priatel, J. J., Schweigler, P., Melkko, S., Gold, M. R., Viner, R. I., Régnier, C. H., Turvey, S. E. & Overall, C. M. The paracaspase MALT1 cleaves HOIL1 reducing linear ubiquitination by LUBAC to dampen lymphocyte NF-κB signalling. *Nat Commun* **6,** 8777 (2015).

106. Hajishengallis, G. & Lambris, J. D. Microbial manipulation of receptor crosstalk in innate immunity. *Nat. Rev. Immunol.* **11,** 187–200 (2011).

107. Ricklin, D., Hajishengallis, G., Yang, K. & Lambris, J. D. Complement: a key system for

immune surveillance and homeostasis. *Nat. Immunol.* **11,** 785–797 (2010).

108. auf dem Keller, U., Prudova, A., Eckhard, U., Fingleton, B. & Overall, C. M. Systems-level analysis of proteolytic events in increased vascular permeability and complement activation in skin inflammation. *Sci Signal* **6,** rs2 (2013).

109. Bellac, C. L., Dufour, A., Krisinger, M. J., Loonchanta, A., Starr, A. E., dem Keller, U., Lange, P. F., Goebeler, V., Kappelhoff, R., Butler, G. S., Burtnick, L. D., Conway, E. M., Roberts, C. R. & Overall, C. M. Macrophage matrix metalloproteinase-12 dampens inflammation and neutrophil influx in arthritis. *Cell Rep.* **9,** 618–632 (2014).

110. Bhuiyan, M. S. & Fukunaga, K. Activation of HtrA2, a mitochondrial serine protease mediates apoptosis: current knowledge on HtrA2 mediated myocardial ischemia/reperfusion injury. *Cardiovasc Ther* **26,** 224–232 (2008).

111. Byun, Y., Chen, F., Chang, R., Trivedi, M., Green, K. J. & Cryns, V. L. Caspase cleavage of vimentin disrupts intermediate filaments and promotes apoptosis. *Publ. online 02 May 2001; - doi10.1038/sj.cdd.4400840* **8,** 443–450 (2001).

112. Pfanner, N. & Geissler, A. Versatility of the mitochondrial protein import machinery. *Nat. Rev. Mol. Cell Biol.* **2,** 339–349 (2001).

113. Schmidt, O., Pfanner, N. & Meisinger, C. Mitochondrial protein import: from proteomics to functional mechanisms. *Nat. Rev. Mol. Cell Biol.* **11,** 655–667 (2010).

114. Quirós, P. M., Langer, T. & López-Otín, C. New roles for mitochondrial proteases in health, ageing and disease. *Nat. Rev. Mol. Cell Biol.* **16,** 345–359 (2015).

115. Bota, D. A., Ngo, J. K. & Davies, K. J. A. Downregulation of the human Lon protease impairs mitochondrial structure and function and causes cell death. *Free Radic. Biol. Med.* **38,** 665–677 (2005).

116. Pinti, M., Gibellini, L., Nasi, M., De Biasi, S., Bortolotti, C. A., Iannone, A. & Cossarizza, A. Emerging role of Lon protease as a master regulator of mitochondrial functions. *Biochim. Biophys. Acta* **1857,** 1300–1306 (2016).

117. Goard, C. A. & Schimmer, A. D. Mitochondrial matrix proteases as novel therapeutic targets in malignancy. *Oncogene* **33,** 2690–2699 (2014).

118. Taylor, A. B., Smith, B. S., Kitada, S., Kojima, K., Miyaura, H., Otwinowski, Z., Ito, A. & Deisenhofer, J. Crystal structures of mitochondrial processing peptidase reveal the mode for specific cleavage of import signal sequences. *Structure* **9,** 615–25 (2001).

119. Neupert, W. & Herrmann, J. M. Translocation of proteins into mitochondria. *Annu. Rev. Biochem.* **76,** 723–749 (2007).

120. Gakh, O., Cavadini, P. & Isaya, G. Mitochondrial processing peptidases. *Biochim. Biophys. Acta* **1592,** 63–77 (2002).

121. Kalousek, F., Hendrick, J. P. & Rosenberg, L. E. Two mitochondrial matrix proteases act sequentially in the processing of mammalian matrix enzymes. *Proc. Natl. Acad. Sci. U. S. A.* **85,** 7536–40 (1988).

122. Esser, K., Tursun, B., Ingenhoven, M., Michaelis, G. & Pratje, E. A novel two-step mechanism for removal of a mitochondrial signal sequence involves the mAAA complex and the putative rhomboid protease Pcp1. *J. Mol. Biol.* **323,** 835–43 (2002).

123. Nolden, M., Ehses, S., Koppen, M., Bernacchia, A., Rugarli, E. I. & Langer, T. The m-AAA protease defective in hereditary spastic paraplegia controls ribosome assembly in mitochondria. *Cell* **123,** 277–89 (2005).

124. Rabilloud, T., Kieffer, S., Procaccio, V., Louwagie, M., Courchesne, P. L., Patterson, S. D., Martinez, P., Garin, J. & Lunardi, J. Two-dimensional electrophoresis of human

placental mitochondria and protein identification by mass spectrometry: toward a human mitochondrial proteome. *Electrophoresis* **19,** 1006–1014 (1998).

125. Lefort, N., Yi, Z., Bowen, B., Glancy, B., De Filippis, E. A., Mapes, R., Hwang, H., Flynn, C. R., Willis, W. T., Civitarese, A., Højlund, K. & Mandarino, L. J. Proteome profile of functional mitochondria from human skeletal muscle using one-dimensional gel electrophoresis and HPLC-ESI-MS/MS. *J Proteomics* **72,** 1046–1060 (2009).

126. Taylor, S. W., Fahy, E., Zhang, B., Glenn, G. M., Warnock, D. E., Wiley, S., Murphy, A. N., Gaucher, S. P., Capaldi, R. A., Gibson, B. W. & Ghosh, S. S. Characterization of the human heart mitochondrial proteome. *Nat. Biotechnol.* **21,** 281–286 (2003).

127. Forner, F., Foster, L. J., Campanaro, S., Valle, G. & Mann, M. Quantitative proteomic comparison of rat mitochondria from muscle, heart, and liver. *Mol. Cell. Proteomics* **5,** 608–619 (2006).

128. Fountoulakis, M., Berndt, P., Langen, H. & Suter, L. The rat liver mitochondrial proteins. *Electrophoresis* **23,** 311–328 (2002).

129. Zhang, J., Li, X., Mueller, M., Wang, Y., Zong, C., Deng, N., Vondriska, T. M., Liem, D. A., Yang, J.-I., Korge, P., Honda, H., Weiss, J. N., Apweiler, R. & Ping, P. Systematic characterization of the murine mitochondrial proteome using functionally validated cardiac mitochondria. *Proteomics* **8,** 1564–1575 (2008).

130. Prokisch, H., Scharfe, C., Camp, D. G., Xiao, W., David, L., Andreoli, C., Monroe, M. E., Moore, R. J., Gritsenko, M. A., Kozany, C., Hixson, K. K., Mottaz, H. M., Zischka, H., Ueffing, M., Herman, Z. S., Davis, R. W., Meitinger, T., Oefner, P. J., Smith, R. D. & Steinmetz, L. M. Integrative analysis of the mitochondrial proteome in yeast. *PLoS Biol.* **2,** e160 (2004).

131. Sickmann, A., Reinders, J., Wagner, Y., Joppich, C., Zahedi, R., Meyer, H. E., Schönfisch, B., Perschil, I., Chacinska, A., Guiard, B., Rehling, P., Pfanner, N. & Meisinger, C. The proteome of Saccharomyces cerevisiae mitochondria. *Proc. Natl. Acad. Sci. U.S.A.* **100,** 13207–13212 (2003).

132. Fountoulakis, M. & Schlaeger, E.-J. The mitochondrial proteins of the neuroblastoma cell line IMR-32. *Electrophoresis* **24,** 260–275 (2003).

133. Chen, X., Li, J., Hou, J., Xie, Z. & Yang, F. Mammalian mitochondrial proteomics: insights into mitochondrial functions and mitochondria-related diseases. *Expert Rev Proteomics* **7,** 333–345 (2010).

134. Gaucher, S. P., Taylor, S. W., Fahy, E., Zhang, B., Warnock, D. E., Ghosh, S. S. & Gibson, B. W. Expanded coverage of the human heart mitochondrial proteome using multidimensional liquid chromatography coupled with tandem mass spectrometry. *J. Proteome Res.* **3,** 495–505 (2004).

135. Mootha, V. K., Bunkenborg, J., Olsen, J. V, Hjerrild, M., Wisniewski, J. R., Stahl, E., Bolouri, M. S., Ray, H. N., Sihag, S., Kamal, M., Patterson, N., Lander, E. S. & Mann, M. Integrated analysis of protein composition, tissue diversity, and gene regulation in mouse mitochondria. *Cell* **115,** 629–640 (2003).

136. Johnson, D. T., Harris, R. A., French, S., Blair, P. V, You, J., Bemis, K. G., Wang, M. & Balaban, R. S. Tissue heterogeneity of the mammalian mitochondrial proteome. *Am. J. Physiol., Cell Physiol.* **292,** C689--697 (2007).

137. Distler, A. M., Kerner, J. & Hoppel, C. L. Proteomics of mitochondrial inner and outer membranes. *Proteomics* **8,** 4066–4082 (2008).

138. Caslavka Zempel, K. E., Vashisht, A. A., Barshop, W. D., Wohlschlegel, J. A. & Clarke,

S. G. Determining the Mitochondrial Methyl Proteome in Saccharomyces cerevisiae using Heavy Methyl SILAC. *J. Proteome Res.* **15,** 4436–4451 (2016).

139. Koc, E. C., Burkhart, W., Blackburn, K., Moseley, A., Koc, H. & Spremulli, L. L. A proteomics approach to the identification of mammalian mitochondrial small subunit ribosomal proteins. *J. Biol. Chem.* **275,** 32585–32591 (2000).

140. Koc, E. C., Burkhart, W., Blackburn, K., Koc, H., Moseley, A. & Spremulli, L. L. Identification of four proteins from the small subunit of the mammalian mitochondrial ribosome using a proteomics approach. *Protein Sci.* **10,** 471–481 (2001).

141. Suzuki, T., Terasaki, M., Takemoto-Hori, C., Hanada, T., Ueda, T., Wada, A. & Watanabe, K. Proteomic analysis of the mammalian mitochondrial ribosome. Identification of protein components in the 28 S small subunit. *J. Biol. Chem.* **276,** 33181–33195 (2001).

142. Suzuki, T., Terasaki, M., Takemoto-Hori, C., Hanada, T., Ueda, T., Wada, A. & Watanabe, K. Structural compensation for the deficit of rRNA with proteins in the mammalian mitochondrial ribosome. Systematic analysis of protein components of the large ribosomal subunit from mammalian mitochondria. *J. Biol. Chem.* **276,** 21724–21736 (2001).

143. Alberio, T., Pieroni, L., Ronci, M., Banfi, C., Bongarzone, I., Bottoni, P., Brioschi, M., Caterino, M., Chinello, C., Cormio, A., Cozzolino, F., Cunsolo, V., Fontana, S., Garavaglia, B., Giusti, L., Greco, V., Lucacchini, A., Maffioli, E., Magni, F., Monteleone, F., Monti, M., Monti, V., Musicco, C., Petrosillo, G., Porcelli, V., Saletti, R., Scatena, R., Soggiu, A., Tedeschi, G., Zilocchi, M., Roncada, P., Urbani, A. & Fasano, M. Toward the Standardization of Mitochondrial Proteomics: The Italian Mitochondrial Human Proteome

Project Initiative. *J. Proteome Res.* (2017). doi:10.1021/acs.jproteome.7b00350

144. Chan, X. C. Y., Black, C. M., Lin, A. J., Ping, P. & Lau, E. Mitochondrial protein turnover: methods to measure turnover rates on a large scale. *J. Mol. Cell. Cardiol.* **78,** 54–61 (2015).

145. Venkatraman, A., Landar, A., Davis, A. J., Chamlee, L., Sanderson, T., Kim, H., Page, G., Pompilius, M., Ballinger, S., Darley-Usmar, V. & Bailey, S. M. Modification of the mitochondrial proteome in response to the stress of ethanol-dependent hepatotoxicity. *J. Biol. Chem.* **279,** 22092–22101 (2004).

146. Shi, L., Wang, Y., Tu, S., Li, X., Sun, M., Srivastava, S., Xu, N., Bhatnagar, A. & Liu, S. The responses of mitochondrial proteome in rat liver to the consumption of moderate ethanol: the possible roles of aldo-keto reductases. *J. Proteome Res.* **7,** 3137–3145 (2008).

147. Jin, J., Davis, J., Zhu, D., Kashima, D. T., Leroueil, M., Pan, C., Montine, K. S. & Zhang, J. Identification of novel proteins affected by rotenone in mitochondria of dopaminergic cells. *BMC Neurosci.* **8,** 67 (2007).

148. Amado, F. M., Barros, A., Azevedo, A. L., Vitorino, R. & Ferreira, R. An integrated perspective and functional impact of the mitochondrial acetylome. *Expert Rev Proteomics* **11,** 383–394 (2014).

149. Padrão, A. I., Vitorino, R., Duarte, J. A., Ferreira, R. & Amado, F. Unraveling the phosphoproteome dynamics in mammal mitochondria from a network perspective. *J. Proteome Res.* **12,** 4257–4267 (2013).

150. Peinado, J. R., Diaz-Ruiz, A., Frühbeck, G. & Malagon, M. M. Mitochondria in metabolic disease: getting clues from proteomic studies. *Proteomics* **14,** 452–466 (2014).

151. Brandon, M. C., Lott, M. T., Nguyen, K. C., Spolim, S., Navathe, S. B., Baldi, P. &

Wallace, D. C. MITOMAP: A human mitochondrial genome database - 2004 update. *Nucleic Acids Res.* **33,** D611–D613 (2005).

152. Lau, E., Huang, D., Cao, Q., Dincer, T. U., Black, C. M., Lin, A. J., Lee, J. M., Wang, D., Liem, D. A., Lam, M. P. Y. & Ping, P. Spatial and temporal dynamics of the cardiac mitochondrial proteome. *Expert Rev Proteomics* **12,** 133–146 (2015).

153. Jazwinski, S. M. The retrograde response: When mitochondrial quality control is not enough. *Biochim. Biophys. Acta - Mol. Cell Res.* **1833,** 400–409 (2013).

154. Weinberg, S. E., Sena, L. A. & Chandel, N. S. Mitochondria in the regulation of innate and adaptive immunity. *Immunity* **42,** 406–417 (2015).

155. Schulz, C., Schendzielorz, A. & Rehling, P. Unlocking the presequence import pathway. *Trends Cell Biol.* **25,** 265–275 (2015).

156. Jovaisaite, V. & Auwerx, J. The mitochondrial unfolded protein response—synchronizing genomes. *Curr. Opin. Cell Biol.* **33,** 74–81 (2015).

157. Rizzuto, R., De Stefani, D., Raffaello, A. & Mammucari, C. Mitochondria as sensors and regulators of calcium signalling. *Nat. Rev. Mol. Cell Biol.* **13,** 566–578 (2012).

158. Kleifeld, O., Doucet, A., auf dem Keller, U., Prudova, A., Schilling, O., Kainthan, R. K., Starr, A. E., Foster, L. J., Kizhakkedathu, J. N. & Overall, C. M. Isotopic labeling of terminal amines in complex samples identifies protein N-termini and protease cleavage products. *Nat. Biotechnol.* **28,** 281–288 (2010).

159. Kleifeld, O., Doucet, A., Prudova, A., auf dem Keller, U., Gioia, M., Kizhakkedathu, J. N. & Overall, C. M. Identifying and quantifying proteolytic events and the natural N terminome by terminal amine isotopic labeling of substrates. *Nat Protoc* **6,** 1578–1611 (2011).

160. Gevaert, K., Goethals, M., Martens, L., Van Damme, J., Staes, A., Thomas, G. R. & Vandekerckhove, J. Exploring proteomes and analyzing protein processing by mass spectrometric identification of sorted N-terminal peptides. *Nat. Biotechnol.* **21,** 566–569 (2003).

161. Dix, M. M., Simon, G. M. & Cravatt, B. F. Global identification of caspase substrates using PROTOMAP (protein topography and migration analysis platform). *Methods Mol. Biol.* **1133,** 61–70 (2014).

162. Mahrus, S., Trinidad, J. C., Barkan, D. T., Sali, A., Burlingame, A. L. & Wells, J. A. Global sequencing of proteolytic cleavage sites in apoptosis by specific labeling of protein N termini. *Cell* **134,** 866–876 (2008).

163. Pham, V. C., Pitti, R., Anania, V. G., Bakalarski, C. E., Bustos, D., Jhunjhunwala, S., Phung, Q. T., Yu, K., Forrest, W. F., Kirkpatrick, D. S., Ashkenazi, A. & Lill, J. R. Complementary proteomic tools for the dissection of apoptotic proteolysis events. *J. Proteome Res.* **11,** 2947–2954 (2012).

164. Becker-Pauly, C., Barré, O., Schilling, O., Auf Dem Keller, U., Ohler, A., Broder, C., Schü, A., Kappelhoff, R., Stö, W. & Overall, C. M. Proteomic Analyses Reveal an Acidic Prime Side Specificity for the Astacin Metalloprotease Family Reflected by Physiological Substrates* □ S. **1,** 1–19 (2011).

165. Van Damme, P., Lasa, M., Polevoda, B., Gazquez, C., Elosegui-Artola, A., Kim, D. S., De Juan-Pardo, E., Demeyer, K., Hole, K., Larrea, E., Timmerman, E., Prieto, J., Arnesen, T., Sherman, F., Gevaert, K. & Aldabe, R. N-terminal acetylome analyses and functional insights of the N-terminal acetyltransferase NatB. *Proc. Natl. Acad. Sci. U. S. A.* **109,** 12449–12454 (2012).

166. Prudova, A., auf dem Keller, U., Butler, G. S. & Overall, C. M. Multiplex N-terminome analysis of MMP-2 and MMP-9 substrate degradomes by iTRAQ-TAILS quantitative proteomics. *Mol. Cell. Proteomics* **9,** 894–911 (2010).

167. Vande Walle, L., Van Damme, P., Lamkanfi, M., Saelens, X., Vandekerckhove, J., Gevaert, K. & Vandenabeele, P. Proteome-wide Identification of HtrA2/Omi Substrates. *J. Proteome Res.* **6,** 1006–1015 (2007).

168. Wilson, C. H., Indarto, D., Doucet, A., Pogson, L. D., Pitman, M. R., McNicholas, K., Menz, R. I., Overall, C. M. & Abbott, C. A. Identifying natural substrates for dipeptidyl peptidases 8 and 9 using terminal amine isotopic labeling of substrates (TAILS) reveals in vivo roles in cellular homeostasis and energy metabolism. *J. Biol. Chem.* **288,** 13936–13949 (2013).

169. Staes, A., Van Damme, P., Timmerman, E., Ruttens, B., Stes, E., Gevaert, K. & Impens, F. Protease Substrate Profiling by N-Terminal COFRADIC. *Methods Mol. Biol.* **1574,** 51–76 (2017).

170. Starr, A. E., Bellac, C. L., Dufour, A., Goebeler, V. & Overall, C. M. Biochemical characterization and N-terminomics analysis of leukolysin, the membrane-type 6 matrix metalloprotease (MMP25): chemokine and vimentin cleavages enhance cell migration and macrophage phagocytic activities. *J. Biol. Chem.* **287,** 13382–13395 (2012).

171. Scott, N. E., Rogers, L. D., Prudova, A., Brown, N. F., Fortelny, N., Overall, C. M. & Foster, L. J. Interactome disassembly during apoptosis occurs independent of caspase cleavage. *Mol. Syst. Biol.* **13,** 906 (2017).

172. Van Damme, P., Martens, L., Van Damme, J., Hugelier, K., Staes, A., Vandekerckhove, J. & Gevaert, K. Caspase-specific and nonspecific in vivo protein processing during Fas-

induced apoptosis. *Nat. Methods* **2,** 771–777 (2005).

173. Fortelny, N., Cox, J. H., Kappelhoff, R., Starr, A. E., Lange, P. F., Pavlidis, P. & Overall, C. M. Network analyses reveal pervasive functional regulation between proteases in the human protease web. *PLoS Biol.* **12,** e1001869 (2014).

174. Wiita, A. P., Hsu, G. W., Lu, C. M., Esensten, J. H. & Wells, J. A. Circulating proteolytic signatures of chemotherapy-induced cell death in humans discovered by N-terminal labeling. *PNAS* **111,** 7594–7599 (2014).

175. Prudova, A., Serrano, K., Eckhard, U., Fortelny, N., Devine, D. V & Overall, C. M. TAILS N-terminomics of human platelets reveals pervasive metalloproteinase-dependent proteolytic processing in storage. *Blood* **124,** e49--60 (2014).

176. Eckhard, U., Marino, G., Butler, G. S. & Overall, C. M. Positional proteomics in the era of the human proteome project on the doorstep of precision medicine. *Biochimie* **122,** 110–118 (2016).

177. Schilling, O., auf dem Keller, U. & Overall, C. M. Protease specificity profiling by tandem mass spectrometry using proteome-derived peptide libraries. *Methods Mol. Biol.* **753,** 257–272 (2011).

178. Van Damme, P. & Gevaert, K. OMICS views on protein N-terminal biology. *Proteomics* **15,** 2383–2384 (2015).

179. Vaca Jacome, A. S., Rabilloud, T., Schaeffer-Reiss, C., Rompais, M., Ayoub, D., Lane, L., Bairoch, A., Van Dorsselaer, A. & Carapito, C. N-terminome analysis of the human mitochondrial proteome. *Proteomics* **15,** 2519–2524 (2015).

180. Vögtle, F.-N., Burkhart, J. M., Rao, S., Gerbeth, C., Hinrichs, J., Martinou, J.-C., Chacinska, A., Sickmann, A., Zahedi, R. P. & Meisinger, C. Intermembrane Space

Proteome of Yeast Mitochondria. *Mol. Cell. Proteomics* **11,** 1840–1852 (2012).

181. Huesgen, P. F., Alami, M., Lange, P. F., Foster, L. J., Schröder, W. P., Overall, C. M. & Green, B. R. Proteomic amino-termini profiling reveals targeting information for protein import into complex plastids. *PLoS One* **8,** e74483 (2013).

182. Calvo, S. E., Julien, O., Clauser, K. R., Shen, H., Kamer, K. J., Wells, J. A. & Mootha, V. K. Comparative Analysis of Mitochondrial N-Termini from Mouse, Human, and Yeast. *Mol. Cell. Proteomics* **16,** 512–523 (2017).

183. Escobar-Alvarez, S., Gardner, J., Sheth, A., Manfredi, G., Yang, G., Ouerfelli, O., Heaney, M. L. & Scheinberg, D. A. Inhibition of human peptide deformylase disrupts mitochondrial function. *Mol. Cell. Biol.* **30,** 5099–5109 (2010).

184. Lee, M. D., She, Y., Soskis, M. J., Borella, C. P., Gardner, J. R., Hayes, P. A., Dy, B. M., Heaney, M. L., Philips, M. R., Bornmann, W. G., Sirotnak, F. M. & Scheinberg, D. A. Human mitochondrial peptide deformylase, a new anticancer target of actinonin-based antibiotics. *J. Clin. Invest.* **114,** 1107–1116 (2004).

185. Ren, X., Bai, X., Zhang, X., Li, Z. Z., Tang, L., Zhao, X., Li, Z. Z., Ren, Y., Wei, S., Wang, Q., Liu, C. & Ji, J. Quantitative nuclear proteomics identifies that miR-137-mediated EZH2 reduction regulates resveratrol-induced apoptosis of neuroblastoma cells. *Mol. Cell. Proteomics* **14,** 316–328 (2015).

186. Short, D. M., Heron, I. D., Birse-Archbold, J.-L. A., Kerr, L. E., Sharkey, J. & McCulloch, J. Apoptosis induced by staurosporine alters chaperone and endoplasmic reticulum proteins: Identification by quantitative proteomics. *Proteomics* **7,** 3085–3096 (2007).

187. Duan, W., Chen, S. S., Zhang, Y., Li, D., Wang, R., Chen, S. S., Li, J., Qiu, X. & Xu, G.

Protein C-terminal enzymatic labeling identifies novel caspase cleavages during the apoptosis of multiple myeloma cells induced by kinase inhibition. *Proteomics* **16,** 60–69 (2016).

188. Crawford, E. D., Seaman, J. E., Agard, N., Hsu, G. W., Julien, O., Mahrus, S., Nguyen, H., Shimbo, K., Yoshihara, H. A. I., Zhuang, M., Chalkley, R. J. & Wells, J. A. The DegraBase: a database of proteolysis in healthy and apoptotic human cells. *Mol. Cell. Proteomics* **12,** 813–24 (2013).
189. Bhavsar, A. P., Auweter, S. D. & Finlay, B. B. Proteomics as a probe of microbial pathogenesis and its molecular boundaries. *Futur. Microbiol* **5,** 253–265 (2010).
190. Malmström, L., Malmström, J. & Aebersold, R. Quantitative proteomics of microbes: Principles and applications to virulence. *Proteomics* **11,** 2947–2956 (2011).
191. Walduck, A., Rudel, T. & Meyer, T. F. Proteomic and gene profiling approaches to study host responses to bacterial infection. *Curr. Opin. Microbiol.* **7,** 33–38 (2004).
192. Fels, U., Gevaert, K. & Van Damme, P. Proteogenomics in Aid of Host-Pathogen Interaction Studies: A Bacterial Perspective. *Proteomes* **5,** (2017).
193. Altindis, E., Dong, T., Catalano, C. & Mekalanos, J. Secretome analysis of Vibrio cholerae type VI secretion system reveals a new effector-immunity pair. *MBio* **6,** e00075 (2015).
194. Boetzkes, A., Felkel, K. W., Zeiser, J., Jochim, N., Just, I. & Pich, A. Secretome analysis of Clostridium difficile strains. *Arch. Microbiol.* **194,** 675–687 (2012).
195. Clair, G., Roussi, S., Armengaud, J. & Duport, C. Expanding the known repertoire of virulence factors produced by Bacillus cereus through early secretome profiling in three redox conditions. *Mol. Cell. Proteomics* **9,** 1486–1498 (2010).

196. Enany, S., Yoshida, Y., Magdeldin, S., Zhang, Y., Bo, X. & Yamamoto, T. Extensive proteomic profiling of the secretome of European community acquired methicillin resistant Staphylococcus aureus clone. *Peptides* **37,** 128–137 (2012).

197. Vargas-Romero, F., Guitierrez-Najera, N., Mendoza-Hernández, G., Ortega-Bernal, D., Hernández-Pando, R. & Castañón-Arreola, M. Secretome profile analysis of hypervirulent Mycobacterium tuberculosis CPT31 reveals increased production of EsxB and proteins involved in adaptation to intracellular lifestyle. *Pathog Dis* **74,** (2016).

198. Friedel, C. C. & Haas, J. Virus-host interactomes and global models of virus-infected cells. *Trends Microbiol.* **19,** 501–508 (2011).

199. Hardwidge, P. R., Donohoe, S., Aebersold, R. & Finlay, B. B. Proteomic analysis of the binding partners to enteropathogenic Escherichia coli virulence proteins expressed in Saccharomyces cerevisiae. *Proteomics* **6,** 2174–2179 (2006).

200. Law, R. J., Law, H. T., Scurll, J. M., Scholz, R., Santos, A. S., Shames, S. R., Deng, W., Croxen, M. A., Li, Y., de Hoog, C. L., van der Heijden, J., Foster, L. J., Guttman, J. A. & Finlay, B. B. Quantitative Mass Spectrometry Identifies Novel Host Binding Partners for Pathogenic Escherichia coli Type III Secretion System Effectors. *J. Proteome Res.* **15,** 1613–1622 (2016).

201. Georges, A. A. & Frappier, L. Proteomics methods for discovering viral-host interactions. *Methods* **90,** 21–27 (2015).

202. Hardwidge, P. R., Rodriguez-Escudero, I., Goode, D., Donohoe, S., Eng, J., Goodlett, D. R., Aebersold, R. & Finlay, B. B. Proteomic analysis of the intestinal epithelial cell response to enteropathogenic Escherichia coli. *J. Biol. Chem.* **279,** 20127–20136 (2004).

203. Munday, D. C., Surtees, R., Emmott, E., Dove, B. K., Digard, P., Barr, J. N., Whitehouse,

A., Matthews, D. & Hiscox, J. A. Using SILAC and quantitative proteomics to investigate the interactions between viral and host proteomes. *Proteomics* **12,** 666–672 (2012).

204. Ge, R. & Shan, W. Bacterial phosphoproteomic analysis reveals the correlation between protein phosphorylation and bacterial pathogenicity. *Genomics Proteomics Bioinforma.* **9,** 119–127 (2011).

205. Schmidt, F. & Völker, U. Proteome analysis of host-pathogen interactions: Investigation of pathogen responses to the host cell environment. *Proteomics* **11,** 3203–3211 (2011).

206. Scholz, R., Imami, K., Scott, N. E., Trimble, W. S., Foster, L. J. & Finlay, B. B. Novel Host Proteins and Signaling Pathways in Enteropathogenic E. coli Pathogenesis Identified by Global Phosphoproteome Analysis. *Mol. Cell. Proteomics* **14,** 1927–1945 (2015).

207. Eckhard, U., Huesgen, P. F., Brandstetter, H. & Overall, C. M. Proteomic protease specificity profiling of clostridial collagenases reveals their intrinsic nature as dedicated degraders of collagen. *J Proteomics* **100,** 102–114 (2014).

208. Woof, J. M. & Russell, M. W. Structure and function relationships in IgA. *Mucosal Immunol* **4,** 590–597 (2011).

209. Gill, N., Ferreira, R. B. R., Antunes, L. C. M., Willing, B. P., Sekirov, I., Al-Zahrani, F., Hartmann, M. & Finlay, B. B. Neutrophil elastase alters the murine gut microbiota resulting in enhanced Salmonella colonization. *PLoS One* **7,** e49646 (2012).

210. Ong, S.-E. & Mann, M. A practical recipe for stable isotope labeling by amino acids in cell culture (SILAC). *Nat Protoc* **1,** 2650–60 (2006).

211. Frezza, C., Cipolat, S. & Scorrano, L. Organelle isolation: functional mitochondria from mouse liver, muscle and cultured fibroblasts. *Nat Protoc* **2,** 287–295 (2007).

212. Poulsen, J. W., Madsen, C. T., Poulsen, F. M., Nielsen, M. L., Young, C., Poulsen, F. M.

& Nielsen, M. L. Using guanidine-hydrochloride for fast and efficient protein digestion and single-step affinity-purification mass spectrometry. *J. Proteome Res.* **12,** 1020–1030 (2013).

213. Cox, J. J. & Mann, M. MaxQuant enables high peptide identification rates, individualized p.p.b.-range mass accuracies and proteome-wide protein quantification. *Nat. Biotechnol.* **26,** 1367–1372 (2008).

214. Csordas, A., Ovelleiro, D., Wang, R., Foster, J. M., Ríos, D., Vizcaíno, J. A. & Hermjakob, H. PRIDE: quality control in a proteomics data repository. *Database J. Biol. Databases Curation* **2012,** bas004 (2012).

215. Fortelny, N., Yang, S., Pavlidis, P., Lange, P. F. & Overall, C. M. Proteome TopFIND 3.0 with TopFINDer and PathFINDer: database and analysis tools for the association of protein termini to pre- and post-translational events. *Nucleic Acids Res.* **43,** D290-7 (2015).

216. Crooks, G. E., Hon, G., Chandonia, J.-M. & Brenner, S. E. WebLogo: a sequence logo generator. *Genome Res.* **14,** 1188–1190 (2004).

217. Huang, D. W., Sherman, B. T. & Lempicki, R. A. Bioinformatics enrichment tools: paths toward the comprehensive functional analysis of large gene lists. *Nucleic Acids Res.* **37,** 1–13 (2009).

218. Huang, D. W., Lempicki, R. a & Sherman, B. T. Systematic and integrative analysis of large gene lists using DAVID bioinformatics resources. *Nat. Protoc.* **4,** 44–57 (2009).

219. Gavathiotis, E., Reyna, D. E., Bellairs, J. a, Leshchiner, E. S. & Walensky, L. D. Direct and selective small-molecule activation of proapoptotic BAX. *Nat Chem Biol* **8,** 639–645 (2012).

220. Smith, A. C. & Robinson, A. J. MitoMiner, an integrated database for the storage and analysis of mitochondrial proteomics data. *Mol. Cell. Proteomics* **8,** 1324–1337 (2009).

221. Richardson, D. R., Lane, D. J. R., Becker, E. M., Huang, M. L.-H., Whitnall, M., Rahmanto, Y. S., Sheftel, A. D., Ponka, P., R Lane, D. J., Becker, E. M., L-H Huang, M., Whitnall, M., Suryo Rahmanto, Y., Sheftel, A. D. & Ponka, P. Mitochondrial iron trafficking and the integration of iron metabolism between the mitochondrion and cytosol. *Proc. Natl. Acad. Sci. U. S. A.* **107,** 10775–10782 (2010).

222. Koc, M., Nad'ová, Z., Truksa, J., Ehrlichová, M. & Kovář, J. Iron deprivation induces apoptosis via mitochondrial changes related to Bax translocation. *Apoptosis* **10,** 381–393 (2005).

223. Karbowski, M., Lee, Y. J., Gaume, B., Jeong, S. Y., Frank, S., Nechushtan, A., Santel, A., Fuller, M., Smith, C. L. & Youle, R. J. Spatial and temporal association of Bax with mitochondrial fission sites, Drp1, and Mfn2 during apoptosis. *J. Cell Biol.* **159,** 931–938 (2002).

224. Wasiak, S., Zunino, R. & McBride, H. M. Bax/Bak promote sumoylation of DRP1 and its stable association with mitochondria during apoptotic cell death. *J. Cell Biol.* **177,** 439–450 (2007).

225. Koirala, S., Guo, Q., Kalia, R., Bui, H. T., Eckert, D. M., Frost, A. & Shaw, J. M. Interchangeable adaptors regulate mitochondrial dynamin assembly for membrane scission. *Proc. Natl. Acad. Sci. U. S. A.* **110,** E1342-51 (2013).

226. Sheridan, C. & Martin, S. J. Mitochondrial fission/fusion dynamics and apoptosis. *Mitochondrion* **10,** 640–648 (2010).

227. Cribbs, J. T. & Strack, S. Reversible phosphorylation of Drp1 by cyclic AMP-dependent

protein kinase and calcineurin regulates mitochondrial fission and cell death. *EMBO Rep.* **8,** 939–944 (2007).

228. Cereghetti, G. M., Stangherlin, A., Martins de Brito, O., Chang, C. R., Blackstone, C., Bernardi, P. & Scorrano, L. Dephosphorylation by calcineurin regulates translocation of Drp1 to mitochondria. *Proc. Natl. Acad. Sci. U. S. A.* **105,** 15803–15808 (2008).

229. Parone, P. A., James, D. I., Da Cruz, S., Mattenberger, Y., Donze, O., Barja, F. & Martinou, J.-C. Inhibiting the Mitochondrial Fission Machinery Does Not Prevent Bax/Bak-Dependent Apoptosis. *Mol. Cell. Biol.* **26,** 7397–7408 (2006).

230. Antonicka, H., Mattman, A., Carlson, C. G., Glerum, D. M., Hoffbuhr, K. C., Leary, S. C., Kennaway, N. G. & Shoubridge, E. A. Mutations in COX15 Produce a Defect in the Mitochondrial Heme Biosynthetic Pathway, Causing Early-Onset Fatal Hypertrophic Cardiomyopathy. *Am. J. Hum. Genet* **72,** 101–114 (2003).

231. Papatheodorou, P., Domańska, G., Oxle, M., Mathieu, J., Selchow, O., Kenny, B., Rassow, J., Öxle, M., Mathieu, J., Selchow, O., Kenny, B., Rassow, J., Oxle, M., Mathieu, J., Selchow, O., Kenny, B. & Rassow, J. The enteropathogenic Escherichia coli (EPEC) Map effector is imported into the mitochondrial matrix by the TOM/Hsp70 system and alters organelle morphology. *Cell. Microbiol.* **8,** 677–689 (2006).

232. Supek, F., Bošnjak, M., Škunca, N. & Šmuc, T. REVIGO summarizes and visualizes long lists of gene ontology terms. *PLoS One* **6,** e21800 (2011).

233. Lange, P., Huesgen, P. & Overall, C. TopFIND 2.0--linking protein termini with proteolytic processing and modifications altering protein function. *Nucleic Acids Res.* **40,** D351–D361 (2012).

234. Rawlings, N. D., Barrett, A. J. & Bateman, A. MEROPS: the peptidase database. *Nucleic*

Acids Res. **38,** D227–D233 (2010).

235. Hiller, S., Abramson, J., Mannella, C., Wagner, G. & Zeth, K. The 3D structures of VDAC represent a native conformation. *Trends Biochem. Sci.* **35,** 514–521 (2010).

236. Cao, W., Liu, N., Tang, S., Bao, L., Shen, L., Yuan, H., Zhao, X. & Lu, H. Acetyl-Coenzyme A acyltransferase 2 attenuates the apoptotic effects of BNIP3 in two human cell lines. *Biochim. Biophys. Acta* **1780,** 873–880 (2008).

237. Jeong, D., Lee, D., Hwang, S., Lee, Y., Lee, J., Seo, M., Hwang, W., Seo, K., Hwang, A. B., Artan, M., Son, H. G., Jo, J., Baek, H., Oh, Y. M., Ryu, Y., Kim, H., Ha, C. M., Yoo, J. & Lee, S. V. Mitochondrial chaperone HSP-60 regulates anti-bacterial immunity via p38 MAP kinase signaling. *EMBO J.* e201694781 (2017). doi:10.15252/embj.201694781

238. Krüger, M., Moser, M., Ussar, S., Thievessen, I., Luber, C. A., Forner, F., Schmidt, S., Zanivan, S., Fässler, R. & Mann, M. SILAC mouse for quantitative proteomics uncovers kindlin-3 as an essential factor for red blood cell function. *Cell* **134,** 353–364 (2008).

239. Zanivan, S., Krueger, M. & Mann, M. In vivo quantitative proteomics: the SILAC mouse. *Methods Mol. Biol.* **757,** 435–450 (2012).

240. Potter, M., Newport, E. & Morten, K. J. The Warburg effect: 80 years on. *Biochem. Soc. Trans.* **44,** 1499–1505 (2016).

241. Zhou, W., Liotta, L. A. & Petricoin, E. F. The Warburg Effect and Mass Spectrometry-based Proteomic Analysis. *Cancer Genomics Proteomics* **14,** 211–218 (2017).

242. Bertaccini, D., Vaca, S., Carapito, C., Arsène-Ploetze, F., Van Dorsselaer, A. & Schaeffer-Reiss, C. An improved stable isotope N-terminal labeling approach with light/heavy TMPP to automate proteogenomics data validation: DN-TOP. *J. Proteome Res.* **12,** 3063–3070 (2013).

243. Yen, T.-H. & Wright, N. A. The gastrointestinal tract stem cell niche. *Stem Cell Rev.* **2,** 203–212 (2006).

244. Dean, P., Young, L., Quitard, S. & Kenny, B. Insights into the pathogenesis of enteropathogenic E. coli using an improved intestinal enterocyte model. *PLoS One* **8,** e55284 (2013).

245. Koch, R. *Aetiology of Tuberculosis*. (William R. Jenkins, 1890). at <https://books.google.ca/books?id=i8Q1AQAAMAAJ&ots=f5EfRK5sJ-&dq= tuberculosis OR tuberculose OR aetiology OR aetiologie r koch&lr&pg=PA1#v=onepage&q=tuberculosis OR tuberculose OR aetiology OR aetiologie r koch&f=false>

246. Koch, R. An Address on Bacteriological Research. *Br Med J* **2,** 380–383 (1890).

247. Fredricks, D. N. & Relman, D. A. Sequence-based identification of microbial pathogens: a reconsideration of Koch's postulates. *Clin. Microbiol. Rev.* **9,** 18–33 (1996).

248. Bradford-Hill, A. & Hill, A. B. The environment and disease: association or causation? *Proc. R. Soc. Med.* **58,** 295–300 (1965).

249. Santamaría, R., Rizzetto, L., Bromley, M., Zelante, T., Lee, W., Cavalieri, D., Romani, L., Miller, B., Gut, I., Santos, M., Pierre, P., Bowyer, P. & Kapushesky, M. Systems biology of infectious diseases: a focus on fungal infections. *Immunobiology* **216,** 1212–1227 (2011).

250. Jagdeo, J. M., Dufour, A., Fung, G., Luo, H., Kleifeld, O., Overall, C. M. & Jan, E. Heterogeneous Nuclear Ribonucleoprotein M Facilitates Enterovirus Infection. *J. Virol.* **89,** 7064–7078 (2015).

251. Jagdeo, J. M., Dufour, A., Klein, T., Solis, N., Kleifeld, O., Kizhakkedathu, J., Luo, H.,

Overall, C. M. & Jan, E. N-Terminomics TAILS identifies host cell substrates of poliovirus and coxsackievirus B3 3C proteinases that modulate virus infection. *J. Virol.* JVI.02211-17 (2018). doi:10.1128/JVI.02211-17

252. Marchant, D. J., Bellac, C. L., Moraes, T. J., Wadsworth, S. J., Dufour, A., Butler, G. S., Bilawchuk, L. M., Hendry, R. G., Robertson, A. G., Cheung, C. T., Ng, J., Ang, L., Luo, Z., Heilbron, K., Norris, M. J., Duan, W., Bucyk, T., Karpov, A., Devel, L., Georgiadis, D., Hegele, R. G., Luo, H., Granville, D. J., Dive, V., McManus, B. M. & Overall, C. M. A new transcriptional role for matrix metalloproteinase-12 in antiviral immunity. *Nat. Med.* **20,** 493–502 (2014).

253. Huesgen, P. F., Lange, P. F. & Overall, C. M. Ensembles of protein termini and specific proteolytic signatures as candidate biomarkers of disease. *Proteomics Clin Appl* **8,** 338–350 (2014).

254. Marino, G., Eckhard, U. & Overall, C. M. Protein Termini and Their Modifications Revealed by Positional Proteomics. *ACS Chem. Biol.* **10,** 1754–1764 (2015).

255. Alves, S., Neiri, L., Chaves, S. R., Vieira, S., Trindade, D., Manon, S., Dominguez, V., Pintado, B., Jonckheere, V., Van Damme, P., Silva, R. D., Aldabe, R. & Côrte-Real, M. N-terminal acetylation modulates Bax targeting to mitochondria. *Int. J. Biochem. Cell Biol.* **95,** 35–42 (2018).

256. Slee, E. A., Zhu, H., Chow, S. C., MacFarlane, M., Nicholson, D. W. & Cohen, G. M. Benzyloxycarbonyl-Val-Ala-Asp (OMe) fluoromethylketone (Z-VAD.FMK) inhibits apoptosis by blocking the processing of CPP32. *Biochem. J.* **315 (Pt 1,** 21–24 (1996).

257. Mukhopadhyay, A., Ni, L. & Weiner, H. A co-translational model to explain the in vivo import of proteins into HeLa cell mitochondria. *Biochem. J.* **382,** 385–392 (2004).

258. Bayot, A., Gareil, M., Chavatte, L., Hamon, M.-P., L'Hermitte-Stead, C., Beaumatin, F., Priault, M., Rustin, P., Lombès, A., Friguet, B. & Bulteau, A.-L. Effect of Lon protease knockdown on mitochondrial function in HeLa cells. *Biochimie* **100,** 38–47 (2014).

259. Murray, J., Gilkerson, R. & Capaldi, R. A. Quantitative proteomics: the copy number of pyruvate dehydrogenase is more than 10(2)-fold lower than that of complex III in human mitochondria. *FEBS Lett.* **529,** 173–178 (2002).

260. Sacoman, J. L., Dagda, R. Y., Burnham-Marusich, A. R., Dagda, R. K. & Berninsone, P. M. MitochondrialO-GlcNAc Transferase (mOGT) Regulates Mitochondrial Structure, Function, and Survival in HeLa Cells. *J. Biol. Chem.* **292,** 4499–4518 (2017).

261. Feng, Y., Wang, Y., Jiang, C., Fang, Z., Zhang, Z., Lin, X., Sun, L. & Jiang, W. Nicotinamide induces mitochondrial-mediated apoptosis through oxidative stress in human cervical cancer HeLa cells. *Life Sci.* **181,** 62–69 (2017).

262. Rehm, M., Huber, H. J., Hellwig, C. T., Anguissola, S., Dussmann, H. & Prehn, J. H. M. Dynamics of outer mitochondrial membrane permeabilization during apoptosis. *Cell Death Differ.* **16,** 613–623 (2009).

263. Li, H.-N., Nie, F.-F., Liu, W., Dai, Q.-S., Lu, N., Qi, Q., Li, Z.-Y., You, Q.-D. & Guo, Q.-L. Apoptosis induction of oroxylin A in human cervical cancer HeLa cell line in vitro and in vivo. *Toxicology* **257,** 80–85 (2009).

264. Lu, Y., Jiao, R., Chen, X., Zhong, J., Ji, J. & Shen, P. Methylene blue-mediated photodynamic therapy induces mitochondria-dependent apoptosis in HeLa cell. *J. Cell. Biochem.* **105,** 1451–1460 (2008).

265. Canonico, B., Campana, R., Luchetti, F., Arcangeletti, M., Betti, M., Cesarini, E., Ciacci, C., Vittoria, E., Galli, L., Papa, S. & Baffone, W. Campylobacter jejuni cell lysates

differently target mitochondria and lysosomes on HeLa cells. *Apoptosis An Int. J. Program. Cell Death* **19,** 1225–1242 (2014).

266. Reynolds, L. A., Redpath, S. A., Yurist-Doutsch, S., Gill, N., Brown, E. M., van der Heijden, J., Brosschot, T. P., Han, J., Marshall, N. C., Woodward, S. E., Valdez, Y., Borchers, C. H., Perona-Wright, G. & Finlay, B. B. Enteric helminths promote Salmonella co-infection by altering the intestinal metabolome. *J. Infect. Dis.* (2017). doi:10.1093/infdis/jix141

267. Monetti, M., Nagaraj, N., Sharma, K. & Mann, M. Large-scale phosphosite quantification in tissues by a spike-in SILAC method. *Nat. Methods* **8,** 655–658 (2011).

268. Montaldo, C., Mattei, S., Baiocchini, A., Rotiroti, N., Del Nonno, F., Pucillo, L. P., Cozzolino, A. M., Battistelli, C., Amicone, L., Ippolito, G., van Noort, V., Conigliaro, A., Alonzi, T., Tripodi, M. & Mancone, C. Spike-in SILAC proteomic approach reveals the vitronectin as an early molecular signature of liver fibrosis in hepatitis C infections with hepatic iron overload. *Proteomics* **14,** 1107–1115 (2014).